Hydrological processes in volcanic ash soils - Measuring, modelling and understanding runoff generation in an undisturbed catchment

Theresa Blume

A dissertation submitted to the Faculty of Mathematics and Natural Sciences at the University of Potsdam, Germany
for the degree of Doctor of Natural Sciences (Dr. rer. nat.) in Hydrology

Submitted	8. October 2007
Defended	18. December 2007
Published	January 2008

Referees

Prof. Axel Bronstert	University of Potsdam, Institute for Geoecology
Prof. Hubert Savenije	TU Delft, Civil Engineering and Geosciences
Prof. Markus Casper	University of Trier, Institute for Physical Geography

Contents

Abstract

Streamflow dynamics in mountainous environments are controlled by the runoff generation processes in the basin upstream. Runoff generation processes are thus a major control of the terrestrial part of the water cycle, influencing both, water quality and water quantity as well as their dynamics. The understanding of these processes becomes especially important for the prediction of floods, erosion, and dangerous mass movements, in particular as hydrological systems often show threshold behavior. In case of extensive environmental changes, be it in climate or in landuse, the understanding of runoff generation processes will allow us to better anticipate the consequences and can thus lead to a more responsible management of resources as well as risks.

In this study the runoff generation processes in a small undisturbed catchment in the Chilean Andes were investigated. The research area is characterized by steep hillslopes, highly porous volcanic ash soils, undisturbed old growth forest and high rainfall amounts. The investigation of runoff generation processes in this data scarce area is of special interest as a) little is known on the hydrological functioning of the young volcanic ash soils, which are characterized by extremely high porosities and hydraulic conductivities, b) no process studies have been carried out in this area at either slope or catchment scale, and c) understanding the hydrological processes in undisturbed catchments will provide a basis to improve our understanding of disturbed systems, the shift in processes that followed the disturbance and maybe also future process evolution necessary for the achievement of a new steady state. The here studied catchment has thus the potential to serve as a reference catchment for future investigations.

As no long term data of rainfall and runoff exists, it was necessary to replace long time series of data with a multitude of experimental methods, using the so called "multi-method approach". These methods cover as many aspects of runoff generation as possible and include not only the measurement of time series such as discharge, rainfall, soil water dynamics and groundwater dynamics, but also various short term measurements and experiments such as determination of throughfall amounts and variability, water chemistry, soil physical parameters, soil mineralogy, geo-electrical soundings and tracer techniques. Assembling the results like pieces of a puzzle produces a maybe not complete but nevertheless useful picture of the dynamic ensemble of runoff generation processes in this catchment. The employed methods were then evaluated for their usefulness vs. expenditures (labour and financial costs). Finally, the hypotheses - the perceptual model of runoff generation generated from the experimental findings - were tested with the physically based model Catflow. Additionally the process-based model Wasim-ETH was used to investigate the influence of landuse on runoff generation at the catchment scale.

An initial assessment of hydrologic response of the catchment was achieved with a linear statistical model for the prediction of event runoff coefficients. The parameters identified as best predictors give a first indication of important processes. Various results acquired with the "multi-method approach"show that response to rainfall is generally fast. Preferential vertical flow is of major importance and is reinforced by hydrophobicity during the summer months. Rapid lateral water transport is necessary in order to produce the fast response signal, however, while lateral subsurface flow was observed at several profiles in the soil moisture study, the location and type of structures causing fast lateral flow on the hillslope scale is still not clear and needs to be investigated in more detail. Surface runoff is unlikely due to the high hydraulic conductivities of the volcanic ash soils and could not be observed in the catchment. Additionally, a large subsurface storage exists, retaining most of the incident rainfall during events ($>$90%, often even $>$95%) and producing streamflow even after several weeks of drought. Several findings

suggest a shift in processes from summer to winter causing changes in flow patterns, changes in response of stream chemistry to rainfall events and also changes in groundwater-surface water interactions. The results of the modelling study confirm the importance of rapid and preferential flow processes. However, due to the limited knowledge on subsurface structures the model still does not fully capture runoff response. Investigating the importance of landuse on runoff generation showed that while peak runoff generally increased with deforested area, the location of these areas also had an effect.

Overall, the "multi-method approach"of replacing long time series with a multitude of experimental methods was successful in the identification of dominant hydrological processes and thus proved its applicability for data scarce catchments under the constraint of limited resources.

Kurzfassung

Die Abflussdynamik in Mittel- und Hochgebirgen wird durch die Abflussbildungsprozesse im Einzugsgebiet bestimmt. Abflussbildungsprozesse kontrollieren damit zu großen Teilen den terrestrischen Teil des Wasserkreislaufs und beeinflussen sowohl Wasserqualität als auch -quantität. Das Verständnis von Abflussbildungsprozessen ist besonders wichtig für Vorhersagen von Hochwasser, Erosion und Massenbewegungen wie z.B. Erdrutschen oder Schlammlawinen, da hydrologische Systeme oft Schwellenwertverhalten aufweisen. Im Falle weit reichender Umweltveränderungen, wie z.B. Klima- oder Landnutzungsänderungen kann das Verständnis der Abflussbildungsprozesse ein verantwortungsvolleres Management sowohl der Ressourcen als auch der Risiken ermöglichen.

In dieser Studie wurden die Abflussbildungsprozesse in einem kleinen, anthropogen unbeeinflussten Einzugsgebiet in den Chilenischen Anden untersucht. Das Untersuchungsgebiet ist durch steile Hänge, hochporöse vulkanische Ascheböden, ungestörten Naturwald und hohe Niederschlagsmengen charakterisiert. Die Untersuchung von Abflussbildungsprozessen ist hier von besonderem Interesse, da a) wenig über das hydrologische Verhalten der hochporösen und hochleitfähigen jungen Ascheböden bekannt ist, b) in dieser Region bisher keine Prozessstudien auf Hang- oder Einzugsgebietsskala durchgeführt wurden, und c) das Prozessverständnis in ungestörten Einzugsgebieten als Basis zum besseren Verständnis bereits anthropogen beeinflusster Gebiete dienen kann. Dies umfasst die Veränderung der Prozesse als Folge des Eingriffs und möglicherweise auch weitergehende Entwicklungen bis zur Einstellung eines neuen Gleichgewichts. Das hier untersuchte Gebiet hat daher das Potential zum Referenzgebiet für zukünftige Studien und Forschungsprojekte.

Bedingt durch die Kürze der vorliegenden Abfluss- und Niederschlagszeitreihen war es nötig, den bestehenden Datenmangel durch eine Vielzahl von experimentellen Methoden und Ansätzen auszugleichen. Dieser Ansatz wird im Folgenden der "Multi-Methoden-Ansatz"genannt. Die ausgewählten Methoden sollten dabei so viele Aspekte der Abflussbildung abdecken wie möglich. Es wurden daher nicht nur Zeitreihen von Abfluss, Niederschlag, Bodenfeuchtedynamik und Grundwasserdynamik gemessen, sondern auch eine große Zahl an Kurzzeitmessungen und Experimenten durchgeführt. Diese beinhalteten unter anderem Messung des Bestandesniederschlags, Bestimmung der Wasserchemie, Bestimmung bodenphysikalischer Parameter und der Bodenmineralogie, sowie geophysikalische Messungen und die Verwendung von Tracermethoden. Die Synthese der Resultate gleicht dem Zusammensetzen eines Puzzles. Das so entstandene Bild des dynamischen Prozess-Ensembles ist trotz möglicher fehlender Puzzlestücke hochinformativ. In einem nächsten Schritt wurden die ausgewählten Methoden im Hinblick auf Erkenntnisgewinn und Kosten (d.h. finanzielle Kosten und Arbeitszeit) evaluiert. Das durch die experimentellen Ergebnisse gewonnene Bild der Abflussbildung wurde anschließend mit Hilfe des physikalisch basierten Modells Catflow überprüft. Weiterhin wurde mit dem prozessbasierten Modell Wasim-ETH der Einfluss der Landnutzung auf die Abflussbildung auf Einzugsgebietsskala untersucht.

Ein lineares statistisches Modell zur Vorhersage von ereignisbasierten Abflussbeiwerten erwies sich als hilfreich zur hydrologischen Einordnung des Untersuchungsgebiets. Durch die Identifizierung der besten Prädiktoren lassen sich bereits erste Rückschlüsse auf wichtige Faktoren der Abflussbildung ziehen. Die Ergebnisse des "Multi-Methoden-Ansatzesßeigen, dass die Abflussreaktion in diesem Gebiet sehr schnell erfolgt. Vertikales präferenzielles Fliessen ist hier von großer Bedeutung und wird in den Sommermonaten noch durch Hydrophobizitätseffekte verstärkt. Schneller lateraler Fluss im Untergrund ist eine weitere Voraussetzung für die schnelle Reaktion des Abflusses (Oberflächenabfluss ist in diesem Gebiet aufgrund der hohen hydraulischen Leitfähigkeiten un-

wahrscheinlich und konnte nicht beobachtet werden). Obwohl bei der Untersuchung der Bodenfeuchtedynamik in einigen Profilen laterale Fließmuster beobachtet wurden, ist die Tiefe und Art der Untergrundstrukturen, die auf der Hangskala schnellen lateralen Fluss ermöglichen, noch unklar und sollte in Zukunft genauer untersucht werden. Die Tatsache, dass bei Niederschlagsereignissen der Großteil der Niederschlagsmenge nicht zum Abfluss kommt (>90%, oft auch >95%), sowie der kontinuierliche Abfluss selbst nach mehreren Wochen Trockenheit, lassen auf einen großen unterirdischen Speicher schließen. Der Wechsel von Winter (nass) zu Sommer (trocken) scheint eine Veränderung im Prozess-Ensemble hervorzurufen, die sich in der änderung von Fließmustern, der änderung von Grundwasser-Oberflächenwasser-Interaktionen, sowie veränderter Reaktion der Wasserchemie auf Niederschlagsereignisse beobachten ließ. Die Modellstudie bestätigte die große Bedeutung der schnellen Fließwege. Als Folge von Informationsdefiziten über die Strukturen des Untergrunds ließsich jedoch die Abflussbildung noch nicht vollständig reproduzieren. Die Untersuchung zur Bedeutung der Landnutzung auf die Abflussbildung mit Hilfe eines Einzugsgebietsmodells zeigte die Zunahme der maximalen Abflüsse mit zunehmender Entwaldung. Weiterhin erwies sich auch die Lage der abgeholzten Flächen als ein wichtiger Faktor für die Abflussreaktion.

Der "Multi-Methoden-Ansatz"lieferte wichtige Erkenntnisse zum Verständnis der Abflussbildungspozesse in den Anden Südchiles und zeigte sich als adäquates Mittel für hydrologische Prozess-Studien in datenarmen Gebieten.

Chapter 1

Introduction

The dynamics of streamflow in mountainous environments is controlled by the characteristics and the runoff generation processes of the basin upstream. These processes determine the movement or retention of the incident rainfall once it reaches the ground. The amount and dynamics of water reaching the stream is thus the integrated result of all flow processes in the catchment (Brutsaert, 2005). The investigation of these runoff generation processes is an important but also very challenging endeavor.

1.1 The importance of investigating runoff generation processes

The investigation of these processes is important as runoff generation processes are a major control over the terrestrial part of the hydrological cycle: They can influence water quality and quantity as well as the dynamics of both. Runoff generation processes are thus controlling important aspects of water as a resource but also as a risk. Both water quality and quantity are important aspects of water resource management and understanding the runoff generation processes will help to minimize risks to water quality and irresponsible depletion of water quantity. Understanding runoff generation processes and their threshold behavior is also helpful for a better prediction of floods and for the delineation of risk-prone areas. Furthermore, understanding of runoff generation processes and their threshold behavior can also help in the prediction of erosion and thus soil conservation but also in the prediction of dangerous mass movements, such as land slides and debris flows. Especially in the context of fast man-made land use changes, it becomes more and more important to anticipate the consequences of these actions in order to manage our resources responsibly. Land use changes and also climatic changes can lead to dramatic consequences as a result of the often non-linear behavior of natural systems and can thus be the cause of decrease in water quality or quantity, increased flooding, increased erosion, increased number of landslides... In a changing environment, where the systems are not at steady state, simple statistical methods or models calibrated to the status quo can no longer serve for prediction and it becomes especially important to understand the details of the processes underlying the observed phenomena. Understanding runoff generation processes can thus lead to a more responsible management of our resources as well as risks.

1.2 The challenge of investigating runoff generation processes

Why is the task of investigating these runoff generation processes so challenging? It is challenging because even the input to a catchment is difficult to determine in its amount and variability: rainfall

can be highly variable even over short distances. It is also challenging because these processes depend on many factors, including climate, vegetation, topography, geology and soil characteristics. It is challenging because processes in one catchment can differ greatly from the next, even in the direct neighborhood. It is challenging because most of these processes take place in the subsurface, a terrain/zone which is also highly heterogeneous, invisible to the eye and difficult to characterize in its multi-scale heterogeneity and effective structures. It is challenging because we will never have enough data to determine and characterize our system completely, so that generalizations and simplifications are inevitable. It is challenging because runoff generation processes are not mutually exclusive, but can be active at the same time, while shifting in their relative importance (Brutsaert, 2005). It is challenging because this process interaction as well as the processes themselves can show strong threshold behavior and the attempt of their investigation can be as difficult as "'unscrambling an omelet,"(Brutsaert (2005) p. 441). While all this is true even for well gauged catchments with long time series of data, the investigation of runoff generation processes is especially difficult in those many areas of the world where only little readily available data exists, making it necessary to start investigations from zero.

1.3 Data scarcity

How can we improve process understanding in these so called data scarce or ungauged catchments? Usually we also have to deal with the constraints of limited resources, such as time, money, and manpower. Under time constraint it is impossible to measure rainfall and discharge for several decades in order to perform meaningful statistical analyses on these data and understand catchment response in its statistical characteristics. In 2003 the International Association of Hydrological Sciences launched the so-called PUB-Initiative, which stands for "Predictions in Ungauged Basins"with the aim of improving and developing methodologies for this purpose. The improvement of process understanding is of no little importance in this process, as stated by Sivapalan et al. 2003: "If the level of understanding of hydrological systems at-a-place was much better than it is, then the status quo might be acceptable. However, the understanding of the basic processes of where water goes during rainfall and snowmelt, its flow paths to surface water bodies and the residence times of this water, is still so limited that one is often forced into unrealistic black-box approaches. In other words, even in the case of highly gauged basins, one cannot often, based on the current level of process understanding, say much about the functioning of even a neighboring site! Thus, PUB is as much about improved process understanding as it is about prediction, where the increased focus on process is seen as the pathway to better model estimates for the future.". Several approaches to overcome the problem of data scarcity have been suggested, such as the use of remote sensing/satellite data, the extrapolation of data, i.e transferring data from gauged catchments to ungauged catchments, or the application of process-based hydrological models (Sivapalan et al., 2003b).

However, even with present day technology, satellite data can only give us the "big picture", i.e the large scale patterns and coarse (weekly or monthly) temporal resolution. Possible examples for such data sets are soil moisture data for the top 5cm from scatterometer data which have a higher temporal resolution (daily to weekly) but lower spatial resolution (50 km) than for example the Envisat ASAR ScanSAR data with weekly acquisitions and a spatial resolution of $>$ 100 m (Wagner et al., 2007; Ceballos et al., 2005). However, most of the soil moisture estimations from satellite data are strongly influenced by vegetation and correction for these effects is often difficult (Wagner et al., 2007). River stages can be obtained from satellite radar altimetry, but only for sufficiently wide rivers (>250m) (Frappart et al.,

2005) and with a low temporal resolution of 10 days (Topex Poseidon, Jason) to 35 days (ERS, Envisat) (ESA, 2007). Vertical stage resolution is about 10-50 cm (Alsdorf et al., 2007). Only rainfall radar seems to be a bit more promising for process studies as both temporal and spatial resolution can be sufficiently high (Lange et al., 1999; Tetzlaff & Uhlenbrook, 2005). However, distortions can be caused by hail, mountains and density stratification of the atmosphere and are difficult to correct for (Terblanche et al., 2001). Transferring data from other catchments on the other hand, can introduce high uncertainties, especially when geology/topography/rainfall characteristics differ, while the use of process-based models implies that we already have some understanding of the dominating processes of the catchment under investigation. Thus none of these suggested approaches seemed feasible for the study of runoff generation processes in the Malalcahuello Catchment.

1.4 Research area: Southern Chile and the Malalcahuello Catchment

The focus of this study lies on a small catchment in the Andes of Southern Chile. During the last decades extensive land use changes have taken place in Central and Southern Chile, leading to conversion of vast areas of farm land and native forest to forest plantations of exotic species such as Eucalyptus and Pinus radiata (Monterey Pine). Governmental support through subsidies caused an increase in area under plantation from 330000 ha in 1974 to 1.5 million ha in 1992 (Donoso & Lara, 1995) to 2.1 million ha in 2006 (CORMA, 2007). Land use changes at this extent cannot remain without consequences and are likely to affect biodiversity (Ramirez G. et al., 1994; Frank & Finckh, 1997), water and nutrient budgets (Iroumé et al., 2005, 2006; Huber & Trecaman, 2000; Dillon & Kirchner, 1975; Oyarzun et al., 1997) as well as sediment transport (Oyarzun, 1995). In recent years tourism and recreational land use (such as hiking and winter sports) are gaining more importance and thus a new kind of pressure is exerted especially on protected areas such as national parks.

On the other hand, Southern Chile offers the rare possibility to study hydrological and ecological systems that have not experienced anthropogenic intervention. Understanding undisturbed systems becomes increasingly important nowadays, where many areas of the world are subject to fast changes, either in landuse or in climate or even both. In contrast to systems with rapidly changing land use or climate, the anthropogenically undisturbed systems of southern Chile are much more likely to be either close to or at steady state. Understanding the processes and process-interactions of this steady state will also help us to improve our understanding of disturbed systems, the shift in processes that followed the disturbance and maybe also future process evolution necessary until a new steady state can be achieved.

Southern Chile combines an interesting constellation of geo-ecological factors: native old growth forest, young volcanic ash soils, steep topography, and very high annual rainfall amounts. Of special interest is the so far little-understood hydrology of young volcanic ash soils. These soils are characterised by extremely high porosities and high hydraulic conductivities.

The Malalcahuello Catchment was selected for this investigation as it combines all the geo-ecological factors mentioned above, while it is also anthropogenically undisturbed. Geology, geomorphology and soils of this landscape are dominated by active volcanism in this area. The research catchment is situated in the Reserva Forestal Malalcahuello, on the southern slope of Volcán Lonquimay whose last eruption occurred in the years 1988-1989 and generated a flank pyroclastic cone (Crater Navidad). The catchment of the stream Tres Arroyos (called the "Malalcahuello Catchment") covers an area of 6.26 km^2. Figure 1.1 gives an impression of the landscape characteristics of this area. A detailed description of the

study area can be found in Chapter 3. While it is a rare privilege to study an undisturbed or pristine catchment it does come with a number of drawbacks, such as limited/difficult accessibility and data scarcity.

Prior studies carried out in this catchment and in the neighboring pine plantations included two MS theses, one estimating the volume of a debris flow, which occurred in 1992 (Barrientos, 2001) and the other investigating infiltrabilities by carrying out a number of double ring infiltrometer measurements in the undisturbed catchment as well as in close by forest plantations (Schäfer, 1999). At the same time sediment transport was also investigated (Iroumé, 2003). Two additional studies were carried out during the same period as the here described investigation of runoff generation processes and focused on bedload transport (Mao et al., in press; Uyttendaele, 2006) and the transport of large woody debris (Andreoli et al., in pressa,i). A study comparing the interception characteristics of pine plantations with native forest had been carried out in the Reserva Forestal Malalcahuello in 1998-2000 (Iroumé & Huber, 2002; Huber & Iroumé, 2001). However, for this interception study not the undisturbed catchment but managed woodland closer to the village of Malalcahuello was chosen.

1.5 Aims and objectives

The aim of this study is the improvement of process understanding in the undisturbed Malalcahuello Catchment by experimental investigation with the here proposed "multi-method approach". Physically based modelling at the hillslope scale supports this endeavor by serving as a tool for the testing of process hypotheses while process oriented modelling at the catchment scale makes it possible to investigate the effect and influence of land use on catchment response.

1.6 Approach

As none of the suggested strategies for the investigation of data scarce catchments described in 1.3 seemed feasible for the Malalcahuello Catchment an alternative experimental approach requiring intensive field campaigns was taken. However, in contrast to many other hillslope studies were runoff generation processes can be investigated with the help of trenched hillslopes (Buttle & McDonald, 2002; Freer et al., 2002; Tromp-van Meerveld & McDonnell, 2006a,b; Tromp-van Meerveld et al., 2007; McGlynn et al., 2002; Peters et al., 1995; Kienzler & Naef, in press), this approach cannot be used in the Malalcahuello catchments as a) soils are deep, making manual excavation of such a trench unfeasible b) it is impossible to bring in the heavy machinery necessary for the construction of a sufficiently deep trench. Therefore, the following alternative approach was chosen for the Malalacahuello Catchment: Not only the classical data sets rainfall and discharge but also additional other time series were measured: groundwater levels and soil moisture, water temperatures in both stream and groundwater and electric conductivities in the stream. These time series combined with a number of small scale experiments and point measurements of various parameters, such as dye tracer experiments, soil physical parameters, water chemistry or geophysical measurements might give us a sufficient number of pieces of the puzzle to gain a maybe not complete, but nevertheless useful picture of the dynamic process ensemble. However, due to the constraints in time, money and man-power mentioned above, this approach implies the selection of representative focus areas at different scales, i.e. experimental plots, hillslopes, stream reaches or subcatchments. High temporal resolution of the measured time series allows for the investigation of fast processes, while seasonal patterns can be determined by sampling or experiments during different seasons. An overview over the aspects of catchment hydrology investigated in this study is

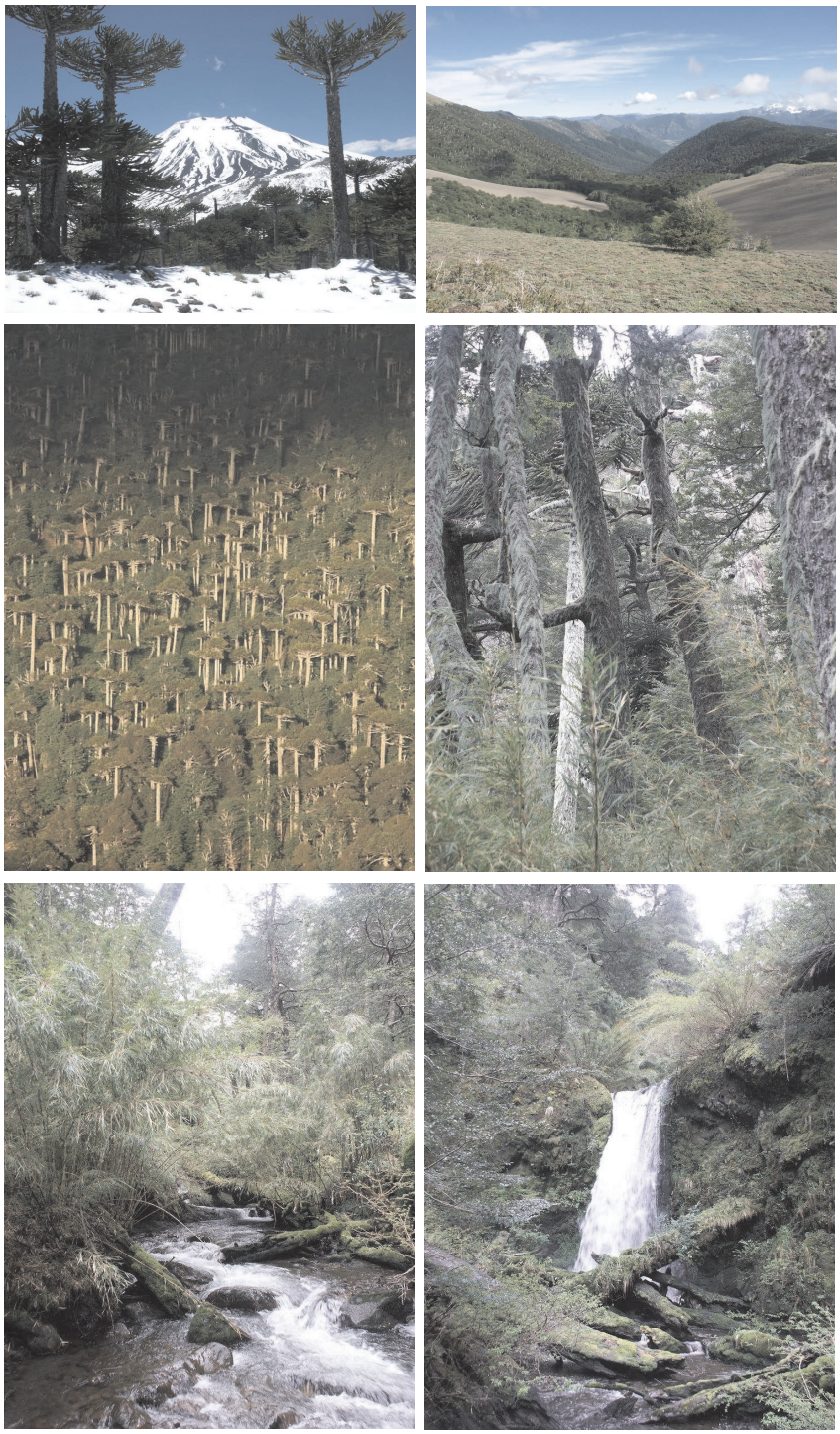

Figure 1.1: An impression of the Malalcahuello Catchment: a) view of Volcano Lonquimay from the catchment rim b) view into the catchment c) Araucaria forest d) old growth forest e),f) the stream Tres Arroyos

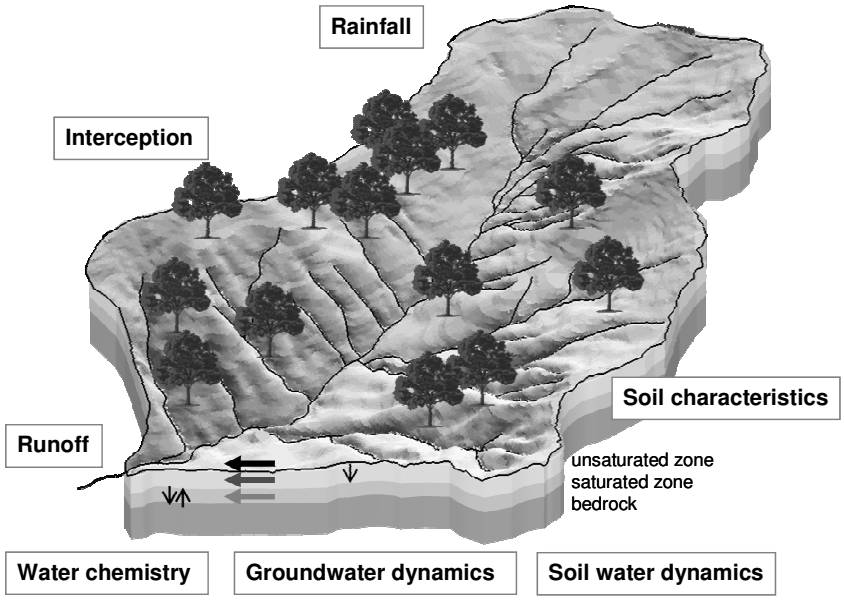

Figure 1.2: The different aspects of catchment hydrology covered in this investigation

given in Figure 1.2. Next to the traditional hydrological time series rainfall and discharge, data sets such as for example soil moisture, water temperatures and geochemical or isotopic tracers are sometimes called "orthogonal data"(Winsemius et al., 2006; Westhoff et al., 2007). However, this term should be used with care, as in its mathematical meaning it implies complete independence of two processes (or vectors), where change in one process has no influence on the other. If this was indeed the case, the measurement of this "orthogonal data"would contribute no additional information concerning runoff generation. However, while the processes governing for example soil moisture or water temperature dynamics are not independent of the processes governing streamflow dynamics, the sampling/measurement of these parameters is independent of the discharge measurement (and is often carried out at a different location or spatio-temporal scale). These "orthogonal measurements"and the resulting data sets are thus a source of highly valuable additional information on flow generation dynamics and processes.

While many of the methods used in the approach suggested here have already been used in other studies for the investigation of runoff generation processes, such as for example soil moisture dynamics (Kienzler & Naef, in press; Meyles et al., 2003; McNamara et al., 2005; Frisbee et al., in press; Zhou et al., 2002), tracers for hydrograph separation (Bazemore et al., 1994; Burns et al., 2001; Uhlenbrook et al., 2002; Hoeg et al., 2000; Rice & Hornberger, 1998) and dye tracer experiments (Zehe & Flühler, 2001b; Weiler & Naef, 2003), the novelty of this study lies in the combination of these methods into a multi-method approach. An overview over the experimental methods and their temporal and spatial scale of application is given in Table 1.1.

Time series of rainfall and discharge can be used to construct linear statistical models for the prediction of event runoff coefficients. The set of best predictors contains first and very basic information on mechanisms of runoff generation and can thus serve for catchment characterization (and possibly even catchment classification). Once we have developed a hypothesis of catchment functioning based on the collected data, physically based

Table 1.1: Experimental methods used in the Malalcahuello Catchment study.

parameter	temporal scale	spatial scale	method
rainfall	event logger	4 rain gauges	tipping bucket
water level	3-10 min intervals	5 stream gauges	capacitive
discharge	point	point (stream gauges)	velocity area meth.
groundwater level	10 min intervals	6 observation wells	capacitive
stream temperature	3-10 min intervals	5 stream gauges	thermister
stream electric cond.	3-5 min intervals	point (stream gauge)	EC electrode
groundwater temperature	3-10 min intervals	5 stream gauges	thermister
soil moisture dynamics	10 min intervals	3 point transect	FDR
soil moisture dynamics	irregular intervals	11 points/2 transects	FDR
snow height	30 min interval	point	ultrasonic
throughfall	event scale	3 plots	accumulators
nutrient export	events/irreg. interv.	main stream gauge	lab analysis
geochemical tracers	events/irreg. interv.	main stream gauge	lab analysis
isotopic tracers	events	main stream gauge	lab analysis
soil water sampling	events	point	suction sampler
subsurface flow paths	hours-1 day	plot	dye tracer exp.
soil stratigraphy	-	points	manual augering
soil phys.charact.	-	point (soil cores)	lab analysis
permeability	point	point	Guelph permeameter
soil minerals	-	point	X-ray diffraction
hydrophobicity	-	point	WDPT test
depth to bedrock/gw table	point	point	electric resistivity

models such as Catflow (Zehe et al., 2001; Zehe & Bloeschl, 2004; Zehe et al., 2005) are a valuable tool for the testing of these newly gained perceptions and hypotheses. While Catflow is used for hypothesis testing at the hillslope scale, the process oriented model Wasim-ETH (Niehoff et al., 2002) is used to investigate the effect of land use on the hydrological response of the catchment. The modelling approaches used in this study are presented in Table 1.2.

1.7 Overview

The general layout of the dissertation is given in Figure 1.3.

The chapters are titled as follows:

- Chapter 1: *Introduction*

  Chapter 1 gives a general overview over the topic of this dissertation and puts it into context. It also presents overall aims and objectives as well as a short presentation of the research area and the experimental approach.

- Chapter 2: *Rainfall Runoff Response, Event-based Runoff Coefficients and Hydrograph Separation*

  Chapter 2 describes the simple approach of event based runoff coefficients. While this approach only uses time series of rainfall and streamflow it can nevertheless give a first impression of response mechanisms. This chapter also covers methods for the determination of event runoff coefficients as well as the development of a linear statistical model for the prediction of event runoff coefficients.

- Chapter 3: *Investigation of runoff generation in a pristine, poorly gauged catchment in the Chilean Andes I: A multi-method experimental study*

- Chapter 4: *Investigation of runoff generation in a pristine, poorly gauged catchment in the Chilean Andes II: Qualitative and quantitative use of tracers at three spatial scales*

- Chapter 5: *Use of soil moisture dynamics and patterns for the investigation of runoff generation processes with emphasis on preferential flow*

  Chapters 3-5 are strongly tied together: Chapter 3 gives an overview over the research area and the experimental approach with its multitude of experimental methods as well as presenting the mosaic of results. An evaluation of the experimental methods with respect to gains in process understanding versus expenditure of time, labor and cost is also attempted. Chapter 4 presents three types of tracer studies covering different spatial scales and chapter 5 gives the details of the soil moisture study. These three chapters thus cover the experimental methods and results.

- Chapter 6: *Different models for different purposes - Physically based modelling at the hillslope scale for hypothesis testing and process-based modelling for the analysis of land use change scenarios at the catchment scale*

  Chapter 6 then acts as a synthesis as here the hypotheses of runoff generation based on the experimental results are tested on the slope scale with the physically based hydrological model Catflow. Additionally, the distributed process-based model Wasim-ETH is used to investigate the effect of land use on runoff dynamics.

- Chapter 7: *Summary and Conclusions*

  Chapter 7 contains the overall summary and conclusions as well as an overview of future work.

Table 1.2: Modelling approaches used in the Malalcahuello Catchment study.

type of model	aim	spatial scale	temporal scale
linear statistical model	prediction of runoff coefficients, catchment characterisation	catchment, no spatial discretization	event, integral values
physically based model (Catflow)	testing of process hypotheses	hillslope, 5-500 cm discretization	1 year, 20 min resolution
process-oriented model (Wasim-ETH)	investigating influence of land use	catchment, 25m grid	3 years, 60 min resolution

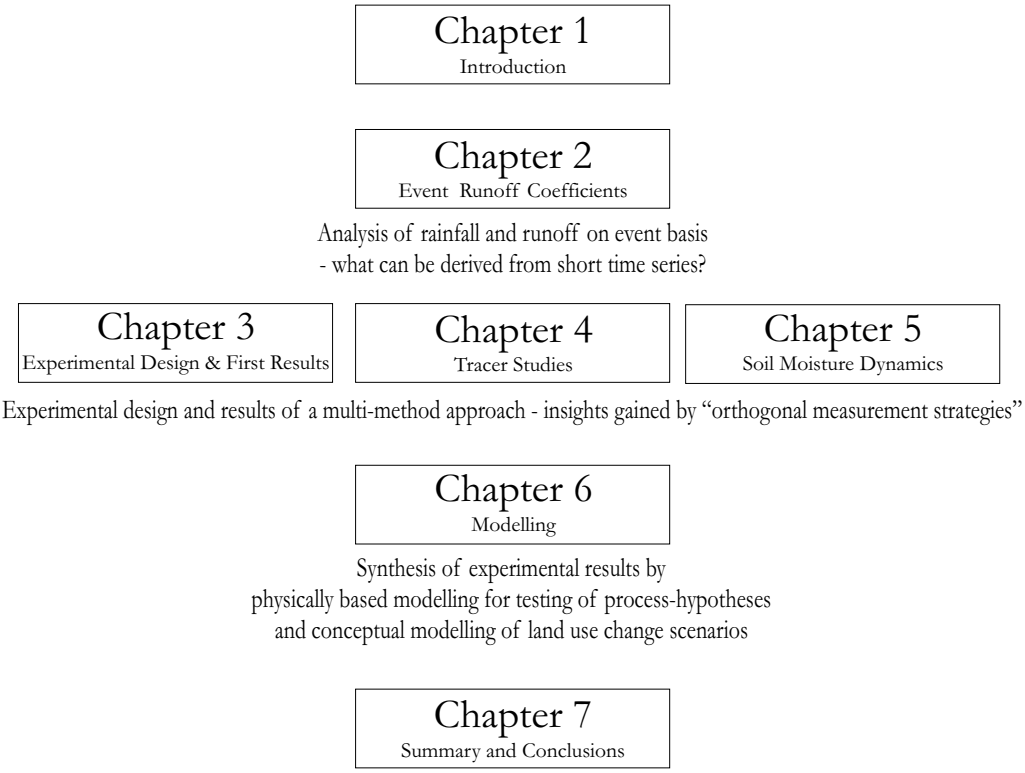

Figure 1.3: Structure and coherence: how the chapters link up

Chapter 2

Rainfall Runoff Response, Event-based Runoff Coefficients and Hydrograph Separation *

Abstract

Event-based runoff coefficients can provide information on watershed response. They are useful for catchment comparison to understand how different landscapes „filter" rainfall into event-based runoff and to explain the observed differences with catchment characteristics and related runoff mechanisms. The big drawback of this important parameter, however, is the lack of a standard hydrograph separation method preceding its calculation. In this study, event runoff coefficients determined with four well-established as well as a newly developed separation method are compared and are shown to differ considerably. This signifies that runoff coefficients reported in the literature often convey less information than could be wished for and possibly not enough to allow for catchment classification. The new separation technique (Constant-k-Method) is based on the theory of a linear storage. Its advantages are that it is theoretically based in determining the endpoint of an event and that it can also be applied to events with multiple peaks. We show furthermore, that event runoff coefficients in combination with simple statistical models improve our understanding of rainfall-runoff response of catchments with sparse data sets.

*Theresa Blume, Erwin Zehe, Axel Bronstert (2007), *Hydrologcial Sciences Journal*, 52 (5), 843-862

2.1 Introduction

Only few catchments throughout the world have been studied intensively concerning hydrological processes and mechanisms (e.g. van Lanen & Dijksma, 1999; McGlynn et al., 2002; Uhlenbrook et al., 2002; McGuire et al., 2005; Tromp-van Meerveld & McDonnell, 2006a). However, many catchments where this knowledge would be crucial for either risk assessment, water management or the assessment of consequences of landuse change, are lacking extensive data sets, making predictions highly uncertain. This is especially the case in developing countries. The PUB initiative (PUB standing for 'Predicition in Ungauged Basins'), launched by the IAHS in 2003 has targeted this problem (Sivapalan et al., 2003a, 2005; Bonell et al., 2006; Sivapalan et al., 2006). The aims of the PUB initiative are to improve and develop models for catchments with little or no data so that predictive uncertainty is reduced. Such models have to be based rather on understanding the hydrological functioning of different landscapes in different climates, than on calibration. Basin inter-comparison and maximization of the scientific value of available data sets in addition to targeted field campaigns are thus important aspects of this endeavour.

Measuring rainfall and discharge for short time spans is relatively simple and inexpensive. But how much information can we gain about the system just by studying rainfall and runoff data from a series of rainfall events? If time series of a length of at least one year exist, it is possible to get a rough estimate of the yearly water budget in most hydro-climatic regions. One can then calculate yearly runoff coefficients, describing either the water budget (using total flow) or the general reaction of the catchment to rainfall (using event flow), depending on the method used. It is also possible to get a first impression of the relevant processes by extracting different parameters describing the hydrograph and its relation to input rainfall (e.g. peak flow rates, lag times, response times). The calculation of runoff coefficients for single events (event-based runoff coefficients) adds additional information on watershed response. Of special interest are changes from event to event or from season to season which can give a first idea of the hydrological functioning of the catchment under different pre-conditions/in different seasons. Depending on the method employed, these runoff coefficients are determined using total flow or direct/event flow. Runoff coefficients are useful for comparisons with other catchments in order to understand how different landscapes „filter" rainfall into event-based runoff. The next step is then the attempt to explain the observed differences by catchment characteristics and related runoff mechanisms. Comparison of these runoff coefficients with coefficients determined for well understood catchments can also give additional insights. Often the calculation of runoff coefficients is preceded by the separation of the event hydrograph into the two components baseflow and direct/event flow. Runoff coefficients are determined and reported based on a variety of separation techniques. Among these separation methods tracer based methods (Hoeg et al., 2000; Ladouche et al., 2001) probably yield the most realistic results, however, they are laborious and expensive and thus restricted to a small number of events and catchments. The number of events is thus likely to be too small for statistical analysis. Other techniques such as graphical methods and digital filters are faced with the difficulties of determining the endpoint of event flow and the interpolation of the baseflow hydrograph during the event.

The present study is part of a research project investigating the hydrological functioning of a small catchment in the foothills of the Chilean Andes. The region is characterised by very high rainfall amounts and highly porous young volcanic ash soils and is little investigated with respect to hydrological processes. On the long term this study has the potential to contribute to a database for basin inter-comparison.

In this study we originally intended to determine

event runoff coefficients for the investigation of rainfall-runoff response as well as for comparison with other catchments and other climates. However, we were confronted with the ambiguity of the terminology on the one hand and the multitude of methods that can be used to determine runoff coefficients on the other hand.

The objective of the present study is therefore threefold: firstly to propose a robust hydrograph separation technique. This method should a) allow for the objective and possibly automated determination of the endpoint of event flow, b) be able to treat events with multiple peaks and c) be, as much as possible, based on a sound hydrological concept i.e. the theory of the linear storage (often used for simulating baseflow in conceptual hydrological models). The second objective is to show how different methods of hydrograph separation do indeed produce differing event runoff coefficients. And thirdly, we want to demonstrate how event runoff coefficients in combination with simple statistical models can help us to understand rainfall-runoff response in this region, even after a relatively short observation period of only 15 months.

2.2 Theory and definitions

2.2.1 Runoff coefficients

The runoff coefficient is a widely used and often reported parameter describing basin response, either on annual or on event basis. Annual runoff coefficients can either be total runoff over total precipitation (percentage of precipitation that is not lost to evapotranspiration, assuming storage as negligible on an annual basis and groundwater outflow out of the catchment as non-existent) (Savenije, 1996; McNamara et al., 1998) or total quick flow over total precipitation (percentage of fast response) (Hewlett & Hibbert, 1967; Woodruff & Hewlett, 1970; van Dijk et al., 2005). However, terminology is not consistent throughout the scientific literature. In the study of Hewlett & Hibbert (1967), the parameter is called „response factor", while in Woodruff & Hewlett (1970) it is called hydrologic response, in McNamara et al. (1998) runoff ratio, Savenije (1996) and van Dijk et al. (2005) called it annual runoff coefficient.

Event runoff coefficients are determined using either the ratio of total flow over total rainfall (Burch et al., 1987; Iroumé et al., 2005) or, after hydrograph separation, the ratio of event-flow volume over total rainfall, i.e. the percentage of the rainfall amount that appears as runoff during or directly following a rainfall event (McNamara et al., 1997, 1998; Sidle et al., 2000; Bowden et al., 2001; Schellekens et al., 2004). Using total flow in the numerator will generally result in higher runoff coefficients, especially during high baseflow conditions. Other terms used in the scientific literature for the same parameter are „water yield" (Sidle et al., 2000), „response factor" (Hewlett & Hibbert, 1967), or „NWCP", which stands for „New water contributing portion of a watershed" (McNamara et al., 1997). In another study the ratio of total runoff to precipitation was called „conversion efficiency" (Burch et al., 1987). As can be seen from the compilation above, many different names for the same parameter exist. This is likely to cause confusion and make inter-comparison of different studies difficult. However, to even increase this confusion, the term 'runoff coefficient' apart from referring either to total flow or quick flow as a fraction of precipitation, often also describes different parameters: In one study ratios termed runoff coefficients were reported where throughfall was in the denominator instead of total precipitation (Brown et al., 1999). Values for runoff coefficients depending on soil and land use have also been tabulated for the rational method, a simple rainfall-runoff model claiming that peak discharge is proportional to rainfall intensity for a given catchment (equation 2.1). These values are loosely defined as ratio of runoff to rainfall (Pilgrim & Cordery, 1992). However, when looking at the rational method formula (equation 2.1), it becomes clear that C is equal to the ratio of peak runoff (mm/h) to rainfall intensity (mm/h). In this case, no hydrograph

separation precedes the calculation.

$$Q_P = F * C * i * A \tag{2.1}$$

with Q_P = peak discharge (m^3/s), F = unit conversion factor, C = runoff coefficient, i = rainfall intensity (mm/h) and A = catchment area (km^2).

In the study at hand event runoff coefficients are determined as the ratio of event flow over total precipitation. Using event flow instead of total flow allows us to investigate rainfall runoff response for a single event, while using total flow would combine the response of the single event with the pre-event flow conditions, be it high flow in the wet season or low flow during summer.

The current state of inconsistency in both terminology as well as methodology is summarized in Figure 2.1. The first part of this figure summarizes the fact that generally event runoff coefficients are determined using either a) total flow or b) event flow as a fraction of total precipitation. In case b), the necessary prior determination of event flow by hydrograph separation additionally increases the ambiguity of this term, as different methods of hydrograph separation will result in different amounts of event flow. The confusion stemming from the many different methods of baseflow separation, has been the target of criticism before: Dunne (1978) compiled runoff coefficients for a number of plot and catchment studies, for overland flow dominated systems, as well as for subsurface stormflow dominated systems and systems where both mechanisms are important. In his chapter on variable-source hydrographs he states that „In areas generating runoff as subsurface stormflow and saturation overland flow, it is difficult to decide upon a definition of storm runoff, and various workers have used different definitions." Along the same lines Hewlett & Hibbert (1967) can be quoted with: „The simplest response factor is R_P, expressing the fraction of rainfall and snowmelt which flows off as quick flow. Such comparisons are not new; direct runoff, separated from baseflow by various methods, has often been reported as a fraction of individual storm rainfalls. But because of the lack of a universal hydrograph separation method, there appears to have been no effort to extend this simple concept to a watershed rating system." Despite the fact that nearly 4 decades have passed since then, we still suffer from the lack of a standard hydrograph separation method. Runoff coefficients are still determined, reported and compared based on a variety of separation techniques.

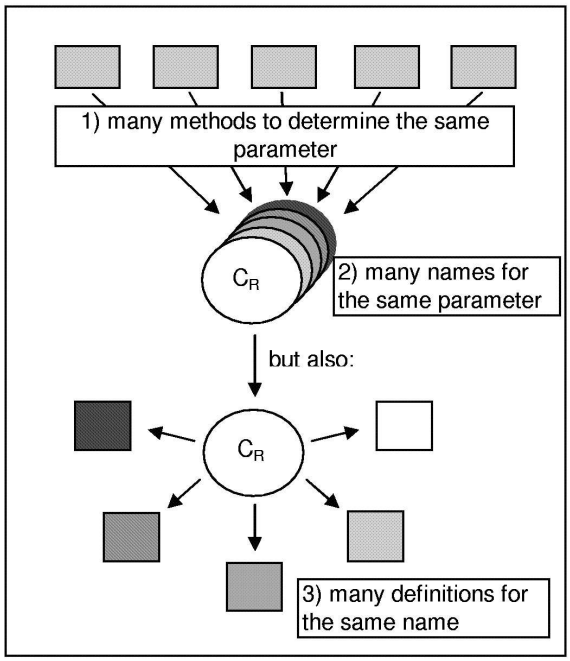

Figure 2.1: Runoff coefficients (C_R) - the current state of inconsistency concerning both terminology as well as methodology.

2.2.2 Hydrograph Separation

In order to determine runoff coefficients for specific events we separated event flow from baseflow. As in the case of the term „runoff coefficient", the term „baseflow" is an ambiguous term. Baseflow can be defined as groundwater exfiltration from shallow aquifers (Wittenberg, 2003), which is higher in dynamics and variation than „the slow flow components considered as base-

flow in traditional flood hydrology" (Wittenberg, 2003). While in the first case direct or event flow consists only of rainwater of the particular event (Wittenberg, 2003), event flow also contains fast subsurface reactions in the second case and therefore is a mixture of „old" and „new" water. Chapman (1999) differentiates between the engineering approach baseflow as „underlying dry weather runoff" as a result of groundwater discharge, the systems analysis „slow flow" and the scientific hydrologists's „old flow" which is based on tracer analysis. Peters & van Lanen (2005) also mention two different definitions.

In this study we use the definition of Dingman (2002) insofar as we will call flow that can be associated with a specific event „event flow" and flow that can not be associated with a specific event „baseflow" as it corresponds to the „base line" of flow. Event flow in this case does not have to originate directly from rainfall input of this specific event but is more likely a mixture of components (surface runoff, interflow, fast groundwater response), which appear as runoff as a direct reaction to rainfall input during the storm event.

As mentioned before, a large variety of separation methods is currently in use:

a) graphical methods (as described in Dingman (2002) or other hydrological textbooks and used in many studies such as, for example Hewlett & Hibbert, 1967; Anderson & Burt, 1980; Bates & Davies, 1988; McNamara et al., 1997; Szilagyi, 1999; Sidle et al., 2000; Sujono et al., 2004; Guillemette et al., 2005)

b) algorithms/digital filters (Arnold & Allen, 1999; Chapman, 1999; Wittenberg, 1999; Furey & Gupta, 2001; Wittenberg, 2003; Sujono et al., 2004; Eckhart, 2005)

c) analytical solutions to baseflow recession (Szilagyi & Parlange, 1998)

All of these methods are faced with two major difficulties: a) identifying the point in time where event flow ends and streamflow consists entirely of baseflow and b) the progression or interpolation of the baseflow hydrograph during the storm event.

Most hydrograph separations (apart from tracer based separations) lack physical basis: Furey & Gupta (2001) state „Only few graphical and filter approaches have been given a physical basis and only during streamflow recession.". Therefore choosing one method or the other introduces an undesirable element of uncertainty and randomness into the analysis and comparison of runoff coefficients.

In the present study we will not focus on the time intensive and expensive separation of event hydrographs by natural tracers such as environmental isotopes and geochemical constituents (Bazemore et al., 1994; Rice & Hornberger, 1998; Hoeg et al., 2000; Ladouche et al., 2001; McGlynn et al., 2002) despite the fact that this is probably the only method to realistically determine runoff components. We will focus on the methods summarized under point (a) which are most likely to be applied by researchers involved in catchment studies for whom hydrograph separation is not the target of the investigation but solely a means to determine runoff coefficients as a parameter descriptive of the respective catchment.

2.2.3 The recession curve

Two extensive reviews on baseflow recession analysis were carried out first by Hall in 1968 (Hall, 1968), commented by Appleby in 1970 (Appleby, 1970) and then by Tallaksen in 1995 (Tallaksen, 1995). Dewandel et al. (2003) also give a brief overview of methods used for hydrograph analysis.

One of the difficult points of baseflow separation is determining the end of storm runoff: at what point on the declining limb of the hydrograph (on the recession curve) does quickflow end and baseflow start to dominate? Is it possible to determine this point just by analyzing the recession curve? The shape of the recession curve is influenced by the hydrodynamic properties of the aquifer, ge-

ological and geomorphologic characteristics, climate and also the characteristics of the soil horizons (e.g. thickness, saturation) (Tallaksen, 1995; Dewandel et al., 2003). Tallaksen (1995) states that: „The recession curve has traditionally been separated into the linear components of surface, unsaturated and saturated flow. The components are thought to represent different flow paths in the catchment, each characterized by different residence times, the outflow rate of groundwater flow from a catchment being lower than the recession rate of the other flow components."

Boussinesq presented the basic nonlinear differential equation governing transient flow from an unconfined aquifer to a stream in 1877 (Hall, 1968). The linearized version of this equation, assuming that vertical flow components and capillary effects above the water table are negligible, is also called the Dupuit-Boussinesq equation (sometimes also Maillet equation) and takes the following form:

$$Q(t) = Q_0 * exp(-kt) \tag{2.2}$$

with $Q(t)$ = discharge at time t (m^3/s), Q_0 = discharge at start of recession (m^3/s), k = recession coefficient (l/s).

Boussinesq also introduced a non-linear solution in 1904, but the overall more convenient mathematical properties of the exponential equation result in a much more widespread use of equation 2.2 for the description of baseflow recessions (Dewandel et al., 2003).

2.3 Methods

2.3.1 Baseflow Separation and Runoff Coefficients

Runoff coefficients were determined by

$$C_R = \frac{\text{eventrunoff}(mm)}{\text{areal precipitation}(mm)} \tag{2.3}$$

Three widely used graphical separation techniques (e.g. Dingman, 2002), as well as the simple „straight line" separation and a newly developed method were used to determine event runoff. The graphical separation methods as well as the „straight line" separation and the new method are shown in Figure 2.2.

1) For the first method (RC), the recession prior to the event is continued under the peak and then connected to a point on the hydrograph N days after time of peak with $N(days) = 0.827 * A^{0.2}$ and A as the drainage area in km^2 (Dingman, 2002).

2) For the second method ($SLog$) the hydrograph is plotted semi-logarithmically, a straight line is fitted to the end of the recession curve, transferred back to the arithmetic plot and then used to project the recession backwards under the peak. This point is then connected with the starting point of the rising limb (Dingman, 2002).

3) The third method (CS) uses a line with a constant slope of $0.05 ft^3 s^{-1} * A(mi^2)$ per hour which is equal to $1.415 * 10^{-3} m^3 s^{-1} * 2.59^{-1} * A(km^2)$ per hour, connecting the first point of rise with the point at which it intersects the recession curve (Dingman, 2002).

4) The straight line method (SL) simply connects the point at which discharge first increases with the point on the recession curve of equal discharge.

5) The newly developed method (CK) is described in the following section.

2.3.1.1 New Method of Baseflow Separation: The Constant-k-Method

The graphical separation methods described above lack physical basis in interpolating the baseflow hydrograph, as well as in determining the end

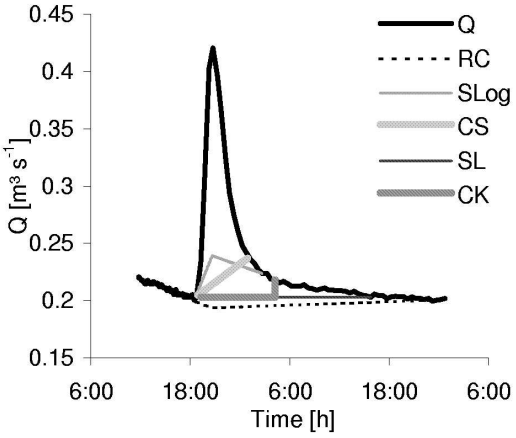

Figure 2.2: Methods of hydrograph separation including new CK method (RC = Recession Continued, $SLog$ = Semi-logarithmic plot, CS = Constant Slope, SL = Straight Line, CK = Constant k Method))

of event runoff. The semi-logarithmic method ($SLog$) has a physical basis for the endpoint determination but at the same time introduces a certain degree of subjectivity. Our newly developed method is theoretically based and objective in the determination of the endpoint, but non-physically based in the interpolation of the baseflow hydrograph.

Based on the assumption that the groundwater/baseflow storage is a linear storage, the baseflow recession curve is expected to decline exponentially. In determining the recession coefficient k of the exponential function in equation 2.2 for all points on the hydrograph it is possible to identify the point in time (t_e) after which k is approximately constant. t_e is therefore defined as the end of event runoff. k (min^{-1}) is calculated for each point by differentiating equation 2.2:

$$\frac{dQ}{dt} = -k * Q(t) \tag{2.4}$$

and then dividing by $Q(t)$:

$$k = -\frac{dQ}{dt} * \frac{1}{Q(t)} \tag{2.5}$$

In case that Q approaches zero in low flow conditions k becomes highly sensitive to very small changes in Q. To decrease this sensitivity of k with respect to the baseline of Q, all events are standardized concerning pre-event Q and thus their baseline. This modified baseline is chosen to be the yearly mean of discharge (in this study 0.4 m^3/s). However, using equation 2.5 with this modified time series of discharge results not in the calculation of k (the real recession coefficient) but of k^* (the stabilized recession coefficient). This modification is viable as not the exact value of k is of interest here, but rather its progression over time. The hydrograph for one event as well as values for k^* and the 2 h moving average of k^* are shown in Figure 2.3. In a next step the gradient of a regression line of k^* is determined for each data point over the period of the following five hours. The end point of event flow (t_e) is defined as the point where the gradient of k^* becomes approximately zero ($\pm 10^{-7}$ min^{-2}), i.e. the point where k^* becomes constant (Figure 2.4). It was not possible to choose the exact value of zero for this criteria as k^* tends to oscillate slightly even at late times. The cut-off value of 10^{-7} min^{-2} is generally 2-3 orders of magnitude smaller than maximum gradients.

The interpolation of the baseflow hydrograph between the beginning of the event and the determined end point of event flow is arbitrary and unlikely to come close to reality (tracer based hydrograph separations often result in hydrographs of pre-event water which are in shape similar to the storm hydrograph). However, as reproducing the „real" baseflow (or pre-event water) hydrograph is impossible, a simple, objective method of interpolation seems appropriate. Therefore, the simplest method - the straight line, assuming constant baseflow with the rate of the pre-event discharge - is used. The resulting separation (CK) in compar-

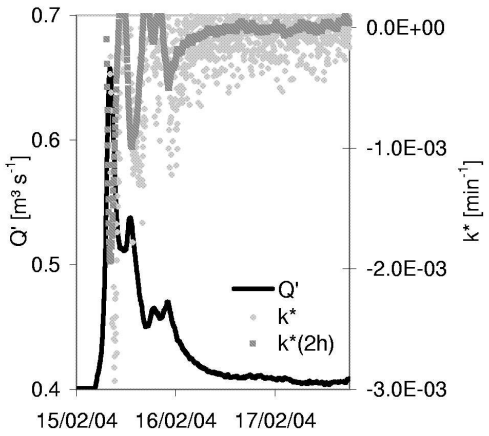

Figure 2.3: Constant-k-Method: Determination of k^* and its 2 h moving average for each data point; Q' = discharge with modified baseline (0.4 m^3/s for all events)

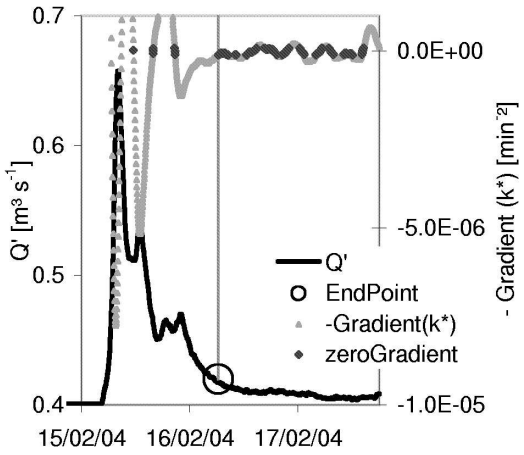

Figure 2.4: Constant-k-Method: Determination of the gradient of k^* (here shown as negative values for better visualization), points of zero gradient and the resulting end point of event runoff; Q' = discharge with modified baseline (0.4 m^3/s for all events)

ison to the other graphical separation methods is shown in Figure 2.2.

2.3.2 Linear Statistical Model

To investigate runoff processes without further field campaigns and detailed modeling, interrelationships between event runoff coefficients and various parameters describing input rainfall and hydrograph characteristics were analyzed. This can either be done by correlation matrices (McNamara et al., 1998) or by statistical models such as Hewlett et al. (1977, 1984) used for predicting storm flows. Linear statistical models in our study were determined with the logit-transformed C_R (equation 2.6) being the response variable and various parameters describing the input rainfall or hydrograph characteristics as possible predictor variables. The logit transformation of C_R is necessary as its values are bounded between 0 and 1, while the transformed values lie between $-\infty$ and ∞. Without this transformation a linear statistical model might predict nonsensical event runoff coefficients smaller than 0 or larger than 1. The logit transformation is described be the following equation:

$$C_R trans = ln(\frac{C_R}{1 - C_R}) \tag{2.6}$$

Possible predictor variables were total precipitation, pre-event discharge, amount of precipitation during the first two hours of the event, maximum hourly rainfall intensity, average hourly rainfall intensity, duration of rainfall, response lag, lag times between rainfall and runoff centroids as well as endpoints. According to the significance of predictor variables and the model‘s goodness of fit described by R^2 the best model was chosen and its performance judged by „Jackknifing”. Jackknifing allows you to refit the model while in turn dropping one input value after the other. The result of this procedure is n models (n being the size of the sample used to build the model). Each of these

models can then each be used to predict the single value left out during the model's calibration. It is thus possible to validate a model without the need for additional data. Model performance was then determined by its Nash-Sutcliffe efficiency:

$$NS = 1 - \frac{\sum(C_R obs_i - C_R mod_i)^2}{\sum(C_R obs_i - \overline{C_R} obs)^2} \quad (2.7)$$

($C_R$obs = observed runoff coefficients, $C_R$mod = modeled runoff coefficients, $\overline{C_R} obs$ = mean observed runoff coefficients) as well as by its mean absolute error (MAE) and its mean absolute error (in percent) ($MAEP$):

$$MAE = \frac{1}{n} \sum |C_R obs_i - C_R mod_i| \quad (2.8)$$

$$MAEP = \frac{1}{n} \sum |\frac{C_R obs_i - C_R mod_i}{C_R obs_i}| * 100\% \quad (2.9)$$

2.3.3 Research Area

The research area is situated in the Reserva Forestal Malalcahuello, in the Precordillera of the Andes, IX. Region (Región de la Araucanía), Southern Chile. The catchment of the Tres Arroyos is located on the southern slope of Volcán Lonquimay (38°25.5'-38°27'S; 71°32.5'-71°35'E). The catchment covers an area† of 5.93 km^2. Elevations range from 1080 m to 1856 m above sea level, with average slopes of 40% (Figure 2.5). 80% of the catchment is covered with forest of the type Araucaria and Roble-Raulí-Coigue (native forest, without anthropogenic intervention). The soils are young, little developed volcanic ash soils with corresponding high porosities and high hydraulic conductivities (Iroumé, 2003). No information on the hydrogeology of this catchment exists. Yearly rainfall amounts range from 2000 to over 3000 mm/a. Snowfall is likely in the upper parts of the catchment from June until November.

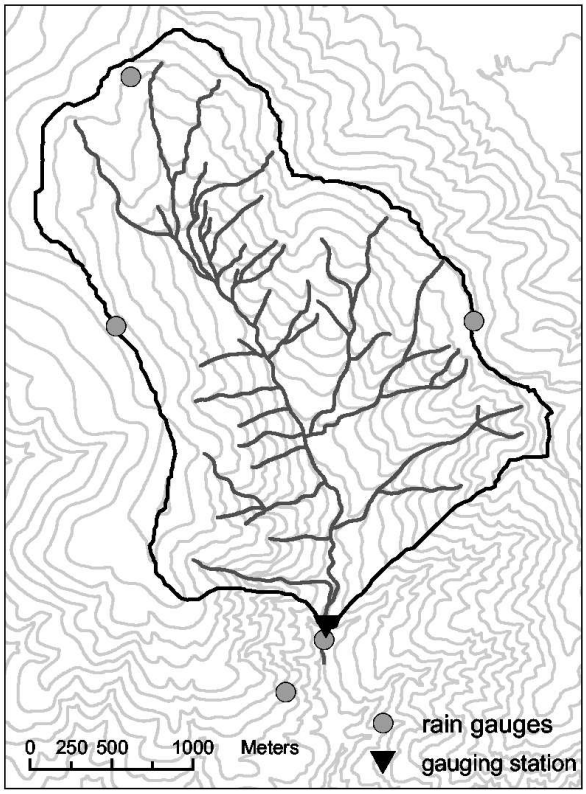

Figure 2.5: The research area with positions of rain gauges and stream gauging station. The vertical resolution of the contour lines is 50 m.

Starting 2004, rainfall was measured with 4 tipping bucket raingauges (3 near the upper catchment boundary at approx. 1700-1800 m, one in the valley at 1080 m.a.s.l.) with a resolution of 0.27 mm. As it was not possible to establish a clear correlation between rainfall amounts and elevation areal precipitation was calculated with Thiessen polygons. Also starting in 2004, water levels at the stream gauging station (natural cross-section) were measured with capacitance water level sensors (Trutrack WT-HR) and a time resolution of 3 - 10 minutes. Water levels were converted to dis-

†GIS analysis for this publication was carried out on the basis of a DEM with 50 m vertical resolution. Topographical analyses for all following chapters/publications were based on a higher resolution DEM and thus slightly different results were obtained.

charge with the help of a rating curve which was determined with current meter measurements and the velocity-area method (Dingman, 2002).

This catchment is considered data scarce as high temporal resolution streamflow and higher spatial resolution rainfall data only exists since January 2004. (Hourly data from a water level sensor and a climate station was collected since 1999.) For this study a time series of a length of 15 months was used: January 2004-March 2005.

2.4 Results

2.4.1 Baseflow separation

The new method of baseflow separation was applied to 19 events during the period 2004-2005. This corresponds to 80% of the events which occurred during the snow-free period. The advantage of this new method over the semi-logarithmic method is that it is more objective in identifying the endpoint of event runoff on the one hand and also works for events with multiple peaks on the other hand. In Figure 2.3 and 2.4 can be seen that the recession coefficient k^* is not constant until very late. Most of the recession in this catchment is thus non-linear. The separation of 4 of the events using the five methods described above is shown in Figure 2.6. It can be seen that endpoints as well as amount of separated event flow differ greatly from method to method. The figure also shows that endpoints defined by the different methods do not follow the same succession for each event. Figure 2.6(c) illustrates the problem arising from multiple peaks when using the $SLog$ separation method. In this case, event flow above the separation line was summarized, neglecting the apparently „negative" event flow where the separation line exceeds measured flow. However, with certain events (February 16^{th} and March 1^{st}) separation with this method was impossible as practically all flow was declared as baseflow.

2.4.2 Runoff coefficients

Runoff coefficients based on the 5 different separation methods for the 19 events are listed in Table 2.1 together with the corresponding total areal precipitation in mm. Overall runoff coefficients are surprisingly low with less than 3% for most events and only 20% for an event with a total precipitation of 280 mm (April 11^{th}-14^{th}). It can also be seen that while the absolute values of the small runoff coefficients determined with the different methods seem to be quite similar, values for the bigger events can vary from 11 to 22% or 4 to 22%. Runoff coefficients standardized by the runoff coefficient determined with the Straight Line Method (SL) are plotted in Figure 2.7. The SL values were chosen as reference as this method is a) the simplest of all and b) results in the longest periods of baseflow as its endpoint is always the latest of all methods. While most of the smallest fractions are produced by the $SLog$ Method (down to 20%), values of more than 100% are often produced by the method where prior recession is continued under the peak (RC Method). It is furthermore impossible to identify a systematic ranking or interdependence of the different hydrograph separation methods.

2.4.3 Linear Statistical Model

It was attempted to construct a linear statistical model predicting runoff coefficients from the parameters shown in Table 2.2. Runoff coefficients were determined with the CK Method. The input data originates from 19 events during the period from January 2004 to March 2005, two of which were later excluded: the event of April 7^{th} 2004 was excluded because the end point was not clearly identifiable due to additional rainfall during the recession and the event of April 11^{th} 2004 was excluded because it was the only extreme event with more than 280 mm of precipitation and thus was identified as outlier (it would be disproportionately influential in the statistical model). Events

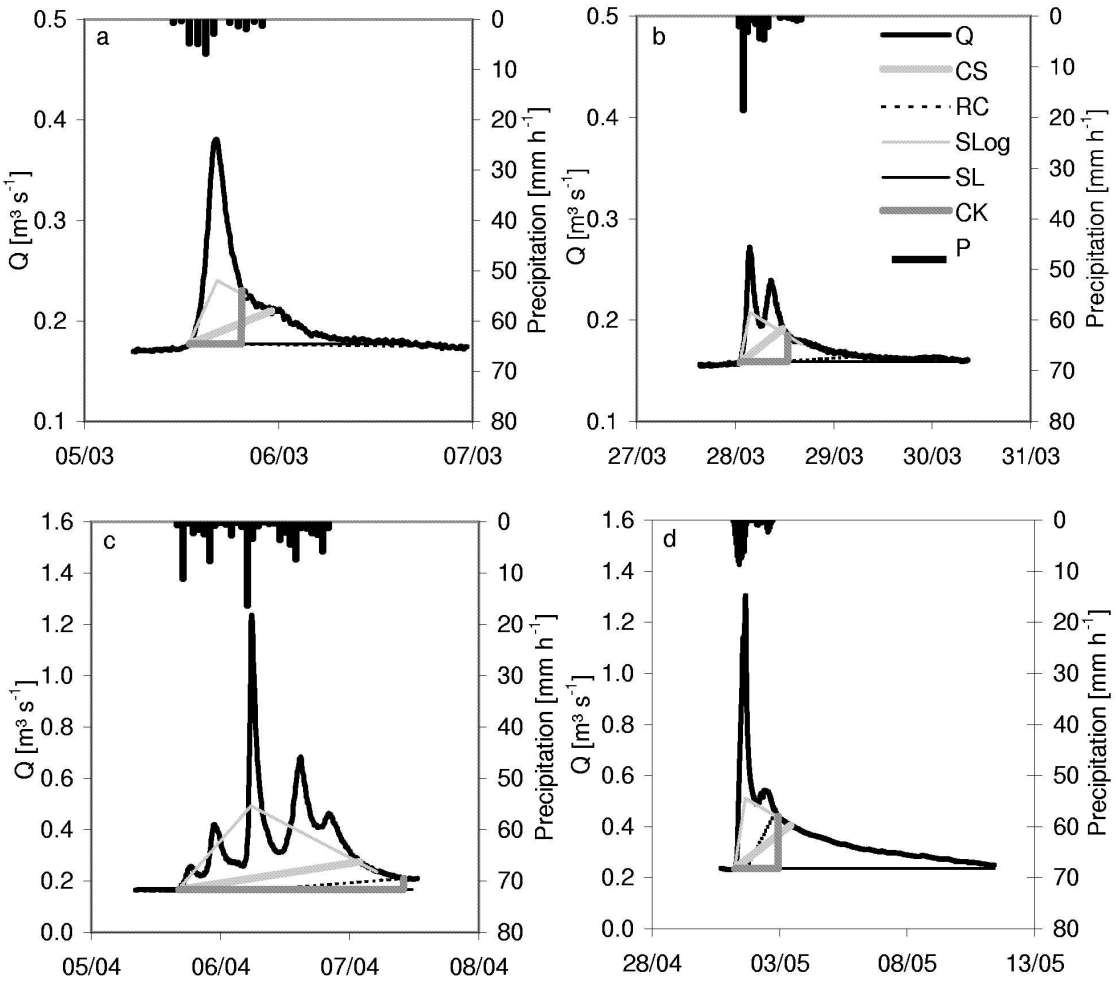

Figure 2.6: Examples of hydrograph separation for 4 events in 2004 - comparison of different methods (CS = Constant Slope, RC = Recession Continued, $SLog$ = Semi-logarithmic plot, SL = Straight Line, CK = Constant k Method, Q = discharge, P = precipication)

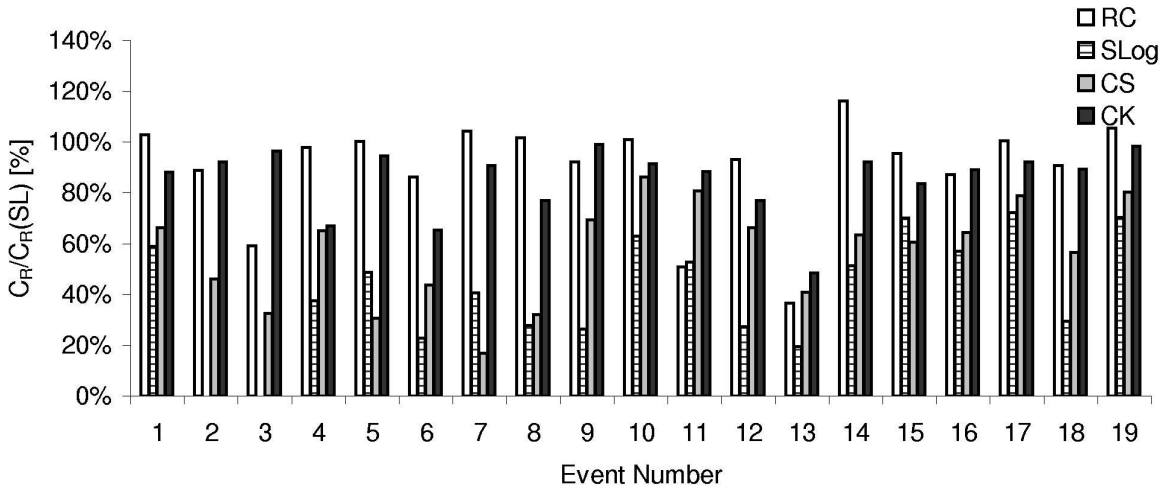

Figure 2.7: Comparison of Runoff Coefficients (C_R) determined with different hydrograph separation methods standardized by C_R (SL). (RC = Recession Continued, $SLog$ = Semi-logarithmic plot, CS = Constant Slope, CK = Constant k Method, SL = Straight Line)

Table 2.1: Runoff coefficients (in%) and total precipitation (P_{tot} in mm) for 19 events

Date	P_{tot}	RC	$SLog$	CS	SL	CK
28/01/04	27	1.95	1.12	1.26	1.90	1.67
15/02/04	58	1.92	-	1.00	2.16	2.00
01/03/04	44	1.56	-	0.86	2.64	2.55
05/03/04	25	2.34	0.90	1.56	2.39	1.60
16/03/04	13	1.59	0.77	0.49	1.59	1.50
28/03/04	39	1.26	0.34	0.64	1.47	0.96
30/03/04	53	2.99	1.16	0.48	2.86	2.60
03/04/04	28	2.23	0.61	0.70	2.19	1.69
05/04/04	81	5.61	1.60	4.23	6.08	6.03
07/04/04	106	9.92	6.18	8.49	9.83	8.99
11/04/04	280	11.38	11.81	18.05	22.35	19.44
17/04/04	24	7.93	2.32	5.65	8.50	6.55
01/05/04	85	7.90	4.21	8.82	21.59	10.44
03/12/04	26	5.46	2.41	2.98	4.70	4.33
14/12/04	41	3.20	2.34	2.02	3.34	2.80
23/12/04	56	4.98	3.25	3.67	5.71	5.08
21/01/05	35	2.90	2.09	2.28	2.89	2.66
28/01/05	41	3.51	1.14	2.19	3.87	3.46
03/03/05	52	2.15	1.43	1.64	2.04	2.01

RC: Recession Continued, Slog: Semi-logarithmic plot, CS: Constant Slope, SL: Straight Line, CK: Constant k Method

from mid-May to end of November were not included as snow fall is likely to occur during these months. The event of May 1^{st} probably included some snow (10-15 mm) in the upper part of the catchment, most of which apparently melted a few hours later. However, the event was not excluded as the snow fall was assumed to have little effect on the hydrograph due to the large amount of overall areal precipitation (85 mm total) during this event. A model with P_{tot} (total areal precipitation in mm), Q_pE (pre-event runoff in m^3/s) and $PInt_{Max}$ (maximum hourly rainfall intensity at one station in mm/h) as predictor variables proved to be the best choice and results in the following equation, where $C_R$trans is the logit-transformed runoff coefficient (see equation 2.6) and C_R is the dimensionless runoff coefficient:

$$C_Rtrans = -5.45 + 0.0267 * P_{tot} + 6.43 * Q_pE - 0.0393 * PInt_{Max} \quad (2.10)$$

Table 2.2: Runoff coefficients and various parameters describing rainfall and hydrograph, which were used to identify the linear statistical model.

Date	Event#	C_R (%)	P_{tot} (mm)	Q_{Ev} (mm)	Q_pE (m^3/s)	$PInt_{Max}$ (mm/h)	$PInt_{Av}$ (mm/h)	PDur (min)	Resp.Lag (min)	Cent.Lag (min)	LagCP (min)	EndLag (min)
28/01/04	1	1.67	27.37	0.46	0.20	19.3	5.9	280	10	161	80	303
15/02/04	2	2.00	57.55	1.15	0.17	18.2	3.0	1160	40	271	-80	416
01/03/04	3	2.45	43.93	1.07	0.17	8.8	1.4	1890	57	287	-404	262
05/03/04	4	1.60	24.70	0.40	0.17	8.5	3.8	390	167	107	96	167
16/03/04	5	1.50	12.82	0.19	0.16	5.4	1.3	610	22	257	191	382
28/03/04	6	0.96	38.79	0.37	0.16	27.8	5.0	470	52	192	-4	277
30/03/04	7	2.60	52.56	1.37	0.16	9.1	1.4	2230	136	552	336	632
03/04/04	8	1.69	28.36	0.48	0.17	12.6	1.6	1090	132	582	-4	132
05/04/04	9	6.03	81.39	4.91	0.17	21.1	2.9	1710	17	432	36	822
17/04/04	10	6.55	23.82	1.56	0.37	9.0	2.1	680	227	342	117	487
01/05/04	11	10.44	85.16	8.89	0.23	12.8	2.9	1770	142	522	57	812
03/12/04	12	4.33	26.20	1.14	0.30	6.4	1.6	1010	250	270	95	430
14/12/04	13	2.80	40.73	1.14	0.24	9.5	2.9	840	8	268	38	248
23/12/04	14	5.08	56.01	2.85	0.22	10.5	2.9	1160	58	518	258	998
21/01/05	15	2.66	35.37	0.94	0.17	9.7	7.6	280	58	198	178	518
28/01/05	16	3.46	40.77	1.41	0.16	6.2	2.7	920	18	238	-82	488
03/03/05	17	2.01	52.38	1.05	0.13	21.9	9.5	330	18	198	88	718

C_R: runoff coefficient, P_{tot}: total precipitation, Q_{Ev}: event runoff, Q_pE: pre-event runoff, $PInt_{Max}$: maximum hourly rainfall intensity measured at a station, $PInt_{Av}$: average hourly areal precipitation, PDur: rainfall duration, Resp.Lag: response lag, Cent.Lag: centroid lag, LagCP: lag time between centroid rainfall to peak discharge, EndLag: lag between end of rainfall and end of event runoff

$$C_R = \frac{1}{1 + (exp(C_R trans))^{-1}} \tag{2.11}$$

The squared Pearson correlation coefficient R^2 of the calibrated model is 0.94. However, squared Pearson correlation coefficients are not sensitive to constant additive or proportional differences and can thus be misleading (feigning a better fit than is actually achieved by the model). Examining mean values and standard deviations for the observed and modeled data as well as Nash-Sutcliffe efficiencies (equation 2.7) provide a better measure of model performance. Mean values of observed and modelled dimensionless runoff coefficients are 0.034 and 0.033 and standard deviations are 0.024 and 0.022 respectively (difference is not significant - p-value of the Mann-Whitney-U-Test is equal to 0.579). The Nash-Sutcliffe efficiency of the calibrated model is 0.93. The small differences in means and standard deviations as well as the high NS suggest that model calibration was successful.

Total amount of areal precipitation as well as pre-event discharge are driving catchment runoff response. A model including only these two parameters results in a Nash-Sutcliffe efficiency of 0.90. Including the maximum hourly rainfall intensity measured at the rainfall gauges (equation 2.11) further improves model performance (NS = 0.93 s.a.). Surprisingly this predictor variable has a negative coefficient (it seems more intuitive to assume higher runoff coefficients with increasing rainfall intensity). Maximum station rainfall seems thus to be a proxy for certain rainfall characteristics not captured otherwise in our list of possible predictor variables.

In order to investigate the model's robustness and its ability for prediction a jackknifing routine was carried out. This method was preferred over a split sampling approach because of the small sample size. Each of the resulting n models was used to predict the value left out during its calibration. These predicted values in comparison to the „observed" C_R and the values returned by the calibrated model are shown in Figure 2.8. „Observed" in this case meaning calculated from measured data. The Nash-Sutcliffe efficiency of the jackknifed model is 0.87. The mean absolute error (in percent) ($MAEP$ – equation 2.9) and the mean absolute error (MAE – equation 2.8) are 16% / 0.0048 for the dimensionless runoff coefficients of the calibrated model and 21% / 0.0065 for the validated model (jackknifed data) respectively. Observed vs. modelled values of C_R are plotted in Figure 2.9. Perfect fit would fall on the diagonal line. The results are surprisingly good, given the simplicity of the model and the limited number of data points.

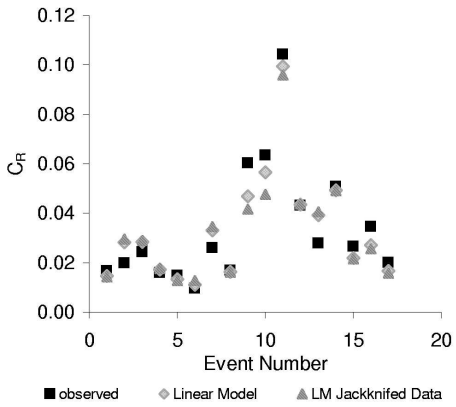

Figure 2.8: Linear statistical model - observed, modeled and jackknifed data (dimensionless runoff coefficients).

2.5 Discussion and conclusions

Even though the comparison of runoff coefficients of different catchments is a rather simple and standard approach to assess the differences in rainfall-runoff responses, this proves to be difficult due to inconsistencies in both terminology and methodology. The determination of event runoff coefficients is often preceded by hydrograph separation, in order to separate the event response from „background flow". In this study 4 different graphical separation methods were compared with a newly

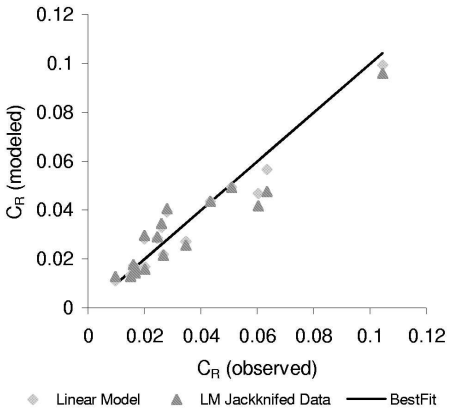

Figure 2.9: Linear statistical model - modeled vs. observed data (dimensionless runoff coefficients).

developed method.

The recession coefficient k for the events studied in the Malalcahuello catchment is not constant until very late. Nevertheless, as it indeed becomes a constant at late times, it seems possible to consider late-time recession as outflow from a linear storage, a common conceptualization used by many meso-scale hydrological models (Zhao, 1992; Bergström, 1995; Leavesley & Stannard, 1995; Lohmann et al., 1998). It also seems a viable interpretation of the data to define the point were k becomes constant (t_e) as the point where event flow ends and baseflow takes over. Our newly developed method has three main advantages over the other methods used in this study: it is at least partly theoretically based, it does not suffer from a more or less subjective determination the endpoint of event flow as for example the $SLog$ method and it can also be used with multiple peak events. Furthermore it does not claim to offer information on the progression of baseflow between beginning and end of event flow. The routine could easily be automated allowing for faster data processing in case of larger data sets.

Runoff coefficients obtained with the 5 different methods differ considerably. The relative difference of runoff coefficients determined with different separation methods depends mainly on hydrograph shape. Acknowledging the big variety of separation methods in use, the appropriateness of intercomparison of runoff coefficients seems doubtful, as they are likely to be determined with different methods.

Overall, event runoff coefficients ascertained for the Malalcahuello catchment are very low (a third of the events has a $C_R < 2\%$) which is probably due to the extremely high porosities of volcanic ash soil, interception (ca. 80% of the catchment are covered with forest), and the lack of anthropogenic influences such as soil compaction.

The linear statistical model developed here shows that simple interrelationships can be used to predict runoff coefficients with surprisingly good results. However, the model should not be used outside of the range of precipitation and discharge it was calibrated for, i.e. for extrapolation. The predictor variables rendering the best model performance improve our understanding of the catchment and its reaction to rainfall. Total precipitation and pre-event discharge are the most important parameters in our study. Runoff coefficients increase with total precipitation. The more rainfall, the higher the fraction of event flow during the event. This does not necessarily mean that it is the precipitation water itself which is being routed to the stream, as would be the case during overland flow. Possible reasons could be rising groundwater tables, groundwater mounding (increasing hydraulic gradients), pipe flow, but also saturation overland flow. However, due to the extremely high porosities as well as hydraulic conductivities of the volcanic ash soil, overland flow is not likely and has so far not been observed in this catchment. The positive correlation of pre-event discharge indicates that this parameter seems to be a good indicator of catchment state prior to rainfall. Pre-event discharge could be describing groundwater and soil water storage and associated momentarily active runoff processes. Hewlett et al. (1977, 1984) did not find that rainfall intensity had an effect on storm runoff, while our linear statistical model for runoff coefficients showed that it was possible to improve model performance by adding

the $PInt_{Max}$ parameter. However, as mentioned before, the estimated coefficient for this parameter is negative. Maximum station rainfall therefore seems to serve as proxy for one or several rainfall characteristics.

The objective and consistent determination of runoff coefficients might be even more important in data-scarce catchments than elsewhere, as rainfall and runoff are generally the first parameters to be measured in previously ungauged catchments. Having collected data for a few events, the natural question to ask oneself is: „How does the catchment respond to rainfall?" Event runoff coefficients are thus one of the first parameters to be extracted from these short time series and thus contain the first information on rainfall runoff response of a data-scarce catchment. The method of employing a linear statistical model for runoff coefficients to infer runoff processes and thus using the model as an additional catchment descriptor is useful in data scarce catchments. However, at least several months of higher resolution discharge and precipitation data are needed in order to accumulate a sufficient number of rainfall events. The more additional data (e.g. on soil physics, hydrogeology or soft data such as observations of local residents) is gathered on targeted field campaigns the better the results of the statistical analysis (i.e. the statistical model) can be interpreted.

However, event runoff coefficients cannot be compared if their determination is based on different methods of hydrograph separation. Furthermore, it is impossible to identify a systematic ranking or interdependence of the runoff coefficients determined with different hydrograph separation methods. Thus, we are not dealing with a simple bias that could be corrected for retrospectively. Overall must be said, that a standard procedure of baseflow separation and determination of runoff coefficients would considerably improve possibilities of catchment intercomparison concerning their rainfall response. A standard procedure should be objective and allow for rapid and easily automated separation and it should also be applicable to events with multiple peaks. Event runoff coefficients based on a standard procedure might allow for classification of catchments with respect to runoff response and for inference of runoff processes. This is an important point within the PUB initiative as catchment classification can help in the selection of appropriate models for predictions in ungauged catchments (Bonell et al., 2006). In the common case of data scarce catchments this possibility of catchment intercomparison (also with data-rich catchments) will improve our understanding of runoff generation in the catchment at hand, as well as our understanding of hydrological similarity as a function of both the rainfall conditions and the bio-physiographic setting of the landscape, such as morphology, soils and vegetation cover.

Acknowledgements

The authors would like to thank Dominik Reusser, Andreas Bauer and Hardin Palacios for extensive help in the field, Andres Iroumé and Anton Huber for logistic and technical assistance and Boris Schröder for statistical support. We thank two anonymous reviewers for their very valuable comments which helped us to improve the manuscript considerably. This work was partially funded by the International Office of the BMBF (German Ministry for Education and Research) and Conicyt (Comisión Nacional de Investigación Científica y Tecnológica de Chile) and the „Potsdam Graduate School of Earth Surface Processes", funded by the State of Brandenburg.

Chapter 3

Investigation of runoff generation in a pristine, poorly gauged catchment in the Chilean Andes
I: A multi-method experimental study *

Abstract

Catchment scale hydrological process studies in Southern Chile are of special interest as little research at this scale has been carried out in this region. Especially the young volcanic ash soils, which are typical for this area, are not well understood in their hydrologic behaviour. In addition, extensive land use changes require detailed knowledge of hydrological processes in disturbed as well as undisturbed catchments in order to estimate resulting risks of erosion, eutrophication, floods and droughts.

This study focuses on data collection and experimental determination of relevant processes in an undisturbed forested catchment in the Andes of Southern Chile. The here gained understanding of runoff generation can serve as a reference for purposes of comparison with sites subject to human intervention, improving the estimation of the effects of land use change.

Due to the lack of long term data for this catchment it was necessary to replace long time series by a multitude of experimental methods covering as many aspects of the runoff generation process as possible. The methods used in this investigation include: measurements of streamflow, rainfall, throughfall, water chemistry, soil water dynamics, groundwater dynamics, soil physics, soil mineralogy, geo-electrical sounding, and tracer techniques. Methods and equipment used during field campaigns are described and evaluated for usefulness vs. expenditures (labour and findancial costs). Selected results and the hypotheses developed from these findings are presented. The results suggest the importance of fast processes for rainfall runoff response on the one hand as well as considerable dampening effects of a large subsurface storage on the other hand.

*Theresa Blume, Erwin Zehe, Dominik E. Reusser, Andrés Iroumé, Axel Bronstert (in press), *Hydrological Processes*

3.1 Introduction

Southern Chile offers the rare possibility to study hydrological and ecological systems that have not suffered anthropogenic intervention. The region features an interesting, if not unique constellation of geo-ecological factors: native old growth forest, young volcanic ash soils, steep slopes, and very high annual rainfall amounts. Of special interest is the so far little-understood hydrology of young volcanic ash soils. These soils are characterised by extremely high porosities and high hydraulic conductivities.

On the other hand extensive land use changes have taken place in Central and Southern Chile during the last decades, leading to conversion of vast areas of farm land and native forest to forest plantations of exotic species such as Eucalyptus and Pinus radiata (Monterey Pine). Governmental support through subsidies caused an increase in area under plantation from 330000 ha in 1974 to 1500000 ha in 1992 (Donoso & Lara, 1995) to 2.1 million ha in 2006 (CORMA, 2007). Land use changes at this extent cannot remain without consequences. Not only biodiversity but presumably also water and nutrient budgets as well as sediment transport will be severely affected. In recent years tourism and recreational land use (e.g. hiking and winter sports) are gaining more importance and thus a new kind of pressure is exerted especially on protected areas such as national parks.

Several studies on water/nutrient budget and sediment transport in forest plantations in Chile have been carried out in recent years (Ellies, 2000; Frank & Finckh, 1997; Gayoso & Iroumé, 1991; Huber & Iroumé, 2001; Iroumé, 1990, 2003; Iroumé et al., 2005, 2006; Oyarzun et al., 1998; Salmon et al., 2001; Uyttendaele & Iroumé, 2002), but only two of these studies focus on areas with young volcanic ash soils and of these two one focuses on soil chemistry (Frank & Finckh, 1997) and the other on sediment transport (Iroumé, 2003). There is thus a general lack of studies of hydrological processes at both the hillslope and the catchment scale in this area of Chile. This is especially true for areas dominated by young volcanic ash soils. In contrast to most studies on the effect of land use change (e.g. Bradshaw et al., 2006; Buytaert et al., 2005) it is here possible to study the landscape in its „original", undisturbed state. The knowledge of landscape functioning in this undisturbed state can then be used a) as a reference for future studies of land use change comparing it to other (disturbed) sites and b) as a basis for the simulation of land use change scenarios for this specific area itself.

In this study we are investigating a small catchment in Southern Chile, in the foothills of the Andes; trying to achieve an understanding of how this undisturbed landscape translates rainfall into runoff at the event and the seasonal time scale. However, the rare opportunity of studying an undisturbed catchment comes with a number of drawbacks. Accessibility of the study area is very limited due to the dense vegetation and steep hillslopes. No roads or paths exist. Prior data is also limited: no soil maps or hydro-geological maps of this area exist. And, as in most studies, financial resources, manpower and time are also limited. Starting an investigation under these circumstances is difficult. Experimental design cannot be an iterative process under time constraint. And, in order to understand the catchment in its hydrological response many different aspects need to be covered. Data scarcity in space is a widely known problem in hydrology. Nevertheless, in case of a previously ungauged catchment that is sought to be understood in its hydrological processes, we also have to deal with data scarcity in time. Thus, long data records have to be replaced with results from a multitude of methods and experiments all carried out within a short time frame. From short time series of data we need to extract as much knowledge and understanding as possible.

Within a time frame of 2-3 years a large variety of experimental methods were used to investigate as many aspects of the relevant hydrological processes as possible. These methods include the

measurement of catchment precipitation, throughfall and runoff to determine input and output of the system, the characterisation of the subsurface in order to understand the water movement through the volcanic ash soil and the determination of event response as well as the seasonal dynamics of the system. While some data was measured continuously over the years (rainfall, water level, ground water level and soil moisture), all other measurements as well as the experiments were carried out during field campaigns: December 2003 – February 2004, October 2004 – December 2004 and November 2005 – December 2005.

After introducing the research area in section 3.2, section 3.3 presents the approach of the study including the derivation of research questions from limited prior knowledge as well as the description of the experimental methods that were chosen to answer these questions. The discussion of results in section 3.4 is followed by a synthesis , integrating the results presented here and in the tracer study (chapter 4) and resulting in first hypotheses on runoff generation. This is followed by a critical evaluation of the applied experimental methods.

3.2 Research Area

Field investigations concentrate on the Malalcahuello Catchment with its undisturbed old growth forest and the stream Tres Arroyos. There is no anthropogenic intervention in this area. The research area is situated in the Reserva Forestal Malalcahuello, in the Precordillera of the Andes, Southern Chile, (Región de la Araucanía). The catchment is located on the southern slope of Volcán Lonquimay (38°25.5'-38°27'S; 71°32.5'-71°35'E). It covers an area of 6.26 km^2 (Figure 3.1). Elevations range from 1120 m to 1856 m above sea level, with average slopes of 27° (51%). 10 percent of the area has slopes of more than 43°. The length of the main channel is 4 km and the total length of the stream network is 23 km. The drainage density is 3.67 km/km^2. The terrain analysis is based on a digital elevation model (produced by the Instituto Geografico Militar de Chile) at a scale of 1:10 000 and 10 m resolution in elevation. The subcatchments defined by the stream gauging stations S2, S3, S4 and S5 have catchment areas of 0.34 km^2, 0.64 km^2, 4.95 km^2 and 0.38 km^2, respectively. More details on the topography of the subcatchments can be found in Table 3.1.

The Lonquimay volcano (38.4°S; 71.6°W, 2865 m) is a stratovolcano that has been active in the late-Pleistocene and Holocene. The last eruption of the Volcano Lonquimay (1988-1989) generated a flank pyroclastic cone (Crater Navidad) and resulted in a 20 cm thick layer of ash in the village of Malalcahuello (Moreno & Gardeweg, 1989).

The volcano is predominantly andesitic, with some basaltic and dacitic rocks (Smithsonian-Institution, 2007).

The soils are young, little developed volcanic ash soils (Andosols, in Chile known as Trumaos) with corresponding high infiltration rates (Iroumé, 2003). Bulk densities of ash soils are usually low (0.4-0.8 g/cm^3), porosities usually range between 60% and 80%. High water permeabilities (saturated and unsaturated) are typical for these soils. They are also known for strongly hysteretic moisture retention curves (Shoji et al., 1993).

80% of the catchment is covered with forest of the type Araucaria and Roble-Raulí-Coigue (native forest, without anthropogenic intervention) with a dense understorey of bamboo. The remaining 20% are bare volcanic ashes above the tree line up on the catchment rim.

The climate of this area can be described as temperate/humid with large altitudinal effects. Yearly rainfall amounts range from 2000 to over 3000 mm/a, depending on elevation. The mean annual precipitation for the period 1989-2002 is 2264 mm/a, of which 71% fall between April and September. However, this is data from the lower climate station, situated at 960 m above msl, ca. 150 m lower than the catchment outlet and thus probably underestimates the precipitation for the

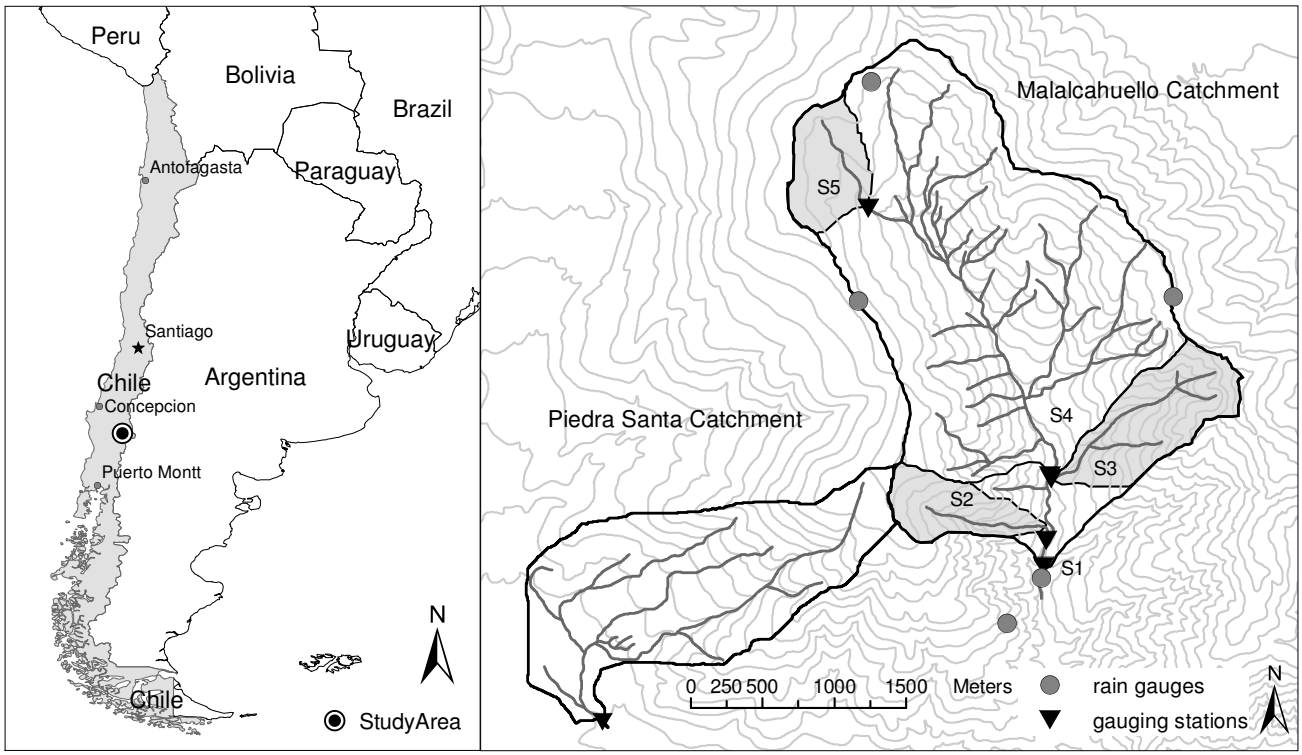

Figure 3.1: Location of the study area and a map of the Malalcahuello and Piedra Santa Catchments showing the positions of rain gauges and gauging stations. The vertical resolution of the contour lines is 50 m.

Table 3.1: Topographic characteristics of the Malalcahuello catchment (S1) and its subcatchments (S2-S5). For the location of the subcatchments see Figure 3.1.

Subcatchment	Area [km^2]	Mean slope [°]	Length of main channel [km]	Slope of main channel [°]
S1	6.26	26.9	4.2	9.4
S2	0.34	33.1	1.2	23.1
S3	0.64	34.5	1.6	21.1
S4	4.95	25.3	3.5	10.1
S5	0.38	14.0	0.8	10.1

study area. Daily data from this station is available since 1989. While snow at the altitude of this climate station is rare, it is common during the winter months at higher elevations. The wettest month is June with >400 mm, the driest is February with 60 mm on average. Temperatures in January and July average at 14 °C and 3 °C respectively.

The focus of this study lies on the Malalcahuello catchment, but data was also collected in a catchment with mixed land use (Piedra Santa Catchment) located just to the west of the Malalcahuello catchment (Figure 3.1). This catchment has an area of 2.9 km^2 and average slopes of 18.5° (25% of the area has slopes > 27°). Soils, climate and geology are similar to the Malalcahuello catchment. Land use, however, includes small farm houses, gravel roads and pasture farming (44%) in the valley, managed woodlands with diminished forest cover (22%), as well as old growth forest on the steeper slopes (34%).

3.3 Study approach and methodology

Even with limited prior knowledge it is possible to develop first perceptual models of how the catchment translates the large annual precipitation input into runoff. The high porosities and hydraulic conductivities typical for volcanic ash soils suggest that surface runoff due to infiltration excess is probably of little importance and that the dominating flow processes are likely to happen in the subsurface. Due to the steep topography subsurface stormflow is likely to be important (McGlynn et al., 2002; Sidle et al., 2001) if near-surface impermeable layers or pipes exist or if there is a fast connection to the soil-bedrock interface where a temporary perched water table could lead to threshold processes such as the „fill and spill" mechanism described by Tromp-van Meerveld & McDonnell (2006a). To investigate these processes it is necessary to a) have information on hydraulic conductivities for various depths and layers, b) study the flow paths in the unsaturated zone and c) explore subsurface structures such as layering and depth to bedrock. Suitable methods for these questions are a) field and/or laboratory measurements of conductivity, b) tracer methods such as dye tracers and c) manual augering and electric resistivity tomography. The large porosity of volcanic ash soil could also lead to a strongly dampened reaction of catchment response to rainfall, as most of the input water is stored instead of being routed directly to the stream, resulting in low event runoff coefficients and a strong baseflow contribution to streamflow. We therefore need to know more about the components of the storm hydrograph, the dynamics of soil moisture at different depths and the response of groundwater levels. These issues can be studied with the help of isotopic and geochemical tracers, high temporal resolution measurement of soil moisture at as many locations and depths as possible and continuously recording water level sensors in a number of observation wells. A nested design of stream gauges can tell us if catchment responses differ between subcatchments, possibly depending on their size or other topographical characteristics.

3.3.1 Investigating rainfall, throughfall and runoff

As rainfall can be highly variable even over small catchments, it is necessary to measure precipitation at different locations within the catchment. In our case the fact that most of the catchment is covered with forest complicates the installation of rain gauges. As a consequence, three of the installed rain gauges are situated near the catchment boundary at or above the tree line (1700-1800 m.a.s.l.) and one at the large confluence at the catchment outlet at an elevation of 1100 m.a.s.l.. All rain gauges are tipping bucket rain gauges (Davis®) measuring rainfall with a resolution of 0.27 mm (according to our own calibration, 0.2 mm according to the product information) and were equipped with Hobo® event loggers.

The measurement of snow heights and water equivalents was not possible due to problems of accessibility during the winter months, caused by high flows or snow cover. The rain gauges could not be equipped with a heating system as it was impossible to supply them with sufficient electric power.

As mentioned before, native forest covers most of the catchment, so interception of rainfall plays an important role. Amounts and spatial variability of throughfall were determined with 3 fields of accumulative precipitation gauges (52 gauges in total). The dense understorey of the native forest and one of the accumulators is shown in Figure 3.2. The position of interception fields 1 and 3 can be found in Figure 3.3. Interception field 2 is located close the stream gauging station of subcatchment S2 (for location of subcatchment S2 and its stream gauging station see Figure 3.1). Accumulators were constructed from PVC sanitary pipes which were cut into 30 cm pieces and closed at one end with a lid. The accumulators had a diameter of 10.5 cm and were positioned in a 5 m grid at fields 1 and 2 and in a 4 m grid at field 3 where space was limited due to difficult topography. All three accumulator fields are located close to the stream for easier accessibility. The accumulators were weighed and emptied after rainfall events during the periods December 2003 - February 2004, October 2004 - December 2004 and November 2005- December 2005. Throughfall data was compared to rainfall amounts measured at the rain gauge close to the catchment outlet.

Located in the vicinity of the Malalcahuello catchment are two climate stations. The first one, located at an elevation of 960 m, is maintained by the CONAF (Corporacion National Forestal de Chile). From this station daily data is available since 1989. The second one, maintained by the Universidad Austral de Chile, is located in a nearby forest plantation at 1270 m elevation. This climate station measures rainfall, temperature, relative humidity, wind direction and velocity as well as global radiation at hourly intervals since 1999.

Figure 3.2: Throughfall accumulator #16 (interception field 1). The dense thicket of bamboo is the typical understorey for most of the catchment.

During the winter of 2005 an ultra-sonic snow height sensor was also connected to this climate station.

Water levels at 5 stream gauging stations were measured with capacitance water level sensors (Trutrack WT-HR®) at a time resolution of 3 - 10 minutes. As bedload transport is too high for the use of weirs, natural cross-sections had to be used. Rating curves were determined with the help of a current meter or by dilution gauging with a salt tracer at low flows during summer. A pressure transducer has been measuring water levels in hourly intervals at S1 since 1998, while the other sensors were installed in December 2003. The stream gauging station at S5, at a first order stream close to the source area, was installed in November 2005. The other stream gauging stations are located in the lower reaches of the catchment as a result of the inaccessibility of most of the research area.

3.3.2 Investigating the subsurface

3.3.2.1 Soils and soil stratigraphy

Soil type was determined in several soil pits in the Malalcahuello catchment. Furthermore about

30 holes were drilled with a manual auger with depths ranging from 2 to 7 meters. Changes in substratum were documented along with their depth.

Soil minerals of three soil samples were analyzed with a Siemens D5005® X-ray Diffractometer. Soil mineral composition, especially the secondary minerals, is a good indicator of soil age and stage in soil evolution.

3.3.2.2 Soil sampling and soil physical laboratory measurements

90 soil cores were taken in different horizons and locations for the determination of hydraulic conductivity and pF curves in the lab. pF curves were determined with a pressure chamber at pressures of 0.06, 0.33 and 15 bar. Bulk densities and particle densities were also determined. Saturated hydraulic conductivities were measured with the constant head method. The soil was tested for potential hydrophobicity (chapter 5) with the Water Drop Penetration Time (WDPT) test (Dekker & Ritsema, 1994).

3.3.2.3 Soil permeability

Soil permeability was measured in situ with a Guelph Permeameter® (Elrick et al., 1989; Munoz-Carpena et al., 2002; Reynolds & Elrick, 1987) in 5 different sites: 3 in native forest, one in conifer plantation and one on forest road. At each site permeabilities were measured at two depths in 4 to 6 locations. The Guelph Permeameter uses the principle of the Mariott bottle to maintain a constant water level within a borehole while measuring the rate of water outflow. Measurements were limited to only three sites for the native forest due to the steep slopes and dense vegetation.

3.3.2.4 Resistivity measurements as a tool for subsurface characterisation

Electric resistivity tomography (ERT) is increasingly used in hydrologic studies to determine either subsurface structures or depth to groundwater (Schellekens et al., 2004; Uhlenbrook et al., 2005). An electric resistivity sounding device (4-point light, LGM®) was used to get information on subsurface characteristics, such as depth to bedrock or groundwater. Point measurements were obtained with measuring transects of 80 to 100 m length using the Schlumberger array (Knödel et al., 1997). In this array 4 electrodes are aligned along a straight horizontal transect (perpendicular to the slope) with as little changes in elevation as possible. An electric current is injected at the two outer electrodes and the voltage is measured at the two center-electrodes. From the voltage the apparent resistivity of the underground is computed. The two outer electrodes are moved stepwise further and further apart, repeating the measurement for each set-up. The larger the spacing of the electrodes the deeper the current penetrates into the ground, thus producing a profile of apparent resistivities at the midpoint of the transect. Data inversion was carried out with RES2DINV® (Geotomo Software) in order to obtain estimates of resistivity changes along this profile and the corresponding depths. As resistivities differ for different geologic materials and also depending on water content, it is often possible to identify bedrock, clay layers or groundwater (Knödel et al., 1997). Due to the steep slopes, pronounced micro topography and dense vegetation the installation of the transects proved difficult and only 25 measurements were achieved, 17 of which on slopes close to the stream (10 near the catchment outlet and 7 close to S5 (Figure 3.1)) and 8 up on the rim of the catchment (bare ash soil, no vegetation).

3.3.3 Investigating seasonal dynamics and event response

The investigation of seaonal and event dynamics included measurement of water chemistry and isotopic tracers as an integrated measure of catchment state and runoff components/dynamics, and groundwater level and soil moisture dynamics for

the subsurface processes at the slope scale. At the local reach scale temperature was employed as tracer for exchange processes between stream and groundwater, and at the plot scale dye tracer experiments were used for the determination of flow paths in the unsaturated zone.

3.3.3.1 Water chemistry, nutrient export and hydrograph separation

Samples were taken from stream water, rain water, throughfall, snow, soil water, and groundwater. Sampling was carried out at irregular intervals during the field campaigns in order to get an impression of typical composition of the different compartments as well as the variability of concentrations. The number of samples taken from these different sources is given in section 3.4.3.1. Analysis of the major cations and anions as well as nitrogen and phosphorous can give us an estimation of nutrient export and geochemical interactions along the subsurface flow paths.

During five rainfall events stream water samples were taken in half hour to hour intervals with an automatic sampler. Natural tracers such as environmental isotopes and geochemical constituents can be used to study runoff generation processes on event basis. This is done by hydrograph separation into event water and pre-event water or by multi-component separation (including for example soil water or shallow groundwater) (Bazemore et al., 1994; Hangen et al., 2001; Hoeg et al., 2000; Ladouche et al., 2001; McGlynn et al., 2002; Rice & Hornberger, 1998; Wenninger et al., 2004). Thus source areas or runoff components can be determined (Uhlenbrook et al., 2002). Environmental stable isotopes such as Deuterium or Oxygen-18 are present in varying concentrations in rainwater as well as groundwater and can even vary highly from one rainstorm to the other at a given site. If the difference in isotopic composition of the so called event and pre-event water is sufficiently high, this difference can be used to separate between fractions of old and new water present in the stream during an event and thus be used for a two-component hydrograph separation.

Samples taken during the rainfall event of February 16^{th} 2004 (rainfall and discharge) as well as the baseflow sample taken a few days prior to the rainfall event were analysed only for Deuterium, while samples taken during the event of December 3^{rd} 2004 were analysed for both Deuterium and Oxygen-18 by mass spectroscopy. Rainfall amounts (and intensities) for the February event were higher than for the December event (58 mm and 26 mm, respectively).

Electric conductivity of stream water as an indicator of total ion concentration was measured continuously during field campaigns, while all other parameters such as the major cations and anions as well as nitrate and phosphate were analyzed in the laboratory. Na and Ca were analyzed with atomic emission- and Ca and Mg with atomic absorption spectrometry. NO_3-N, PO_4-P and SiO_2 were analyzed with spectrophotometric methods, Cl and SO_4 were determined by ion chromatrography.

3.3.3.2 Groundwater and soil moisture dynamics

Groundwater observation wells were installed in two locations, in close proximity of the stream gauging stations S1 (well W1, see Figure 3.3) and S2 in the beginning of 2003. Three additional wells were drilled with a manual auger in November 2004 (wells W3, W4 and W5, see Figure 3.3). A sixth well was installed close to one of the first order streams not far from the source area (S5 Figure 3.1) in November 2005. All wells were equipped with capacitance water level sensors (Trutrack WT-HR®) measuring with a time resolution of 10 minutes.

Soil moisture was measured along two transects with FDR (frequency domain reflectometry) profile probes (Delta-T®) in 10, 20, 30, 40, 60 and 100 cm depth. Both transects are located on the slope close to the main stream gauging station S1 (Figure 3.3). 3 profile probes were connected to a

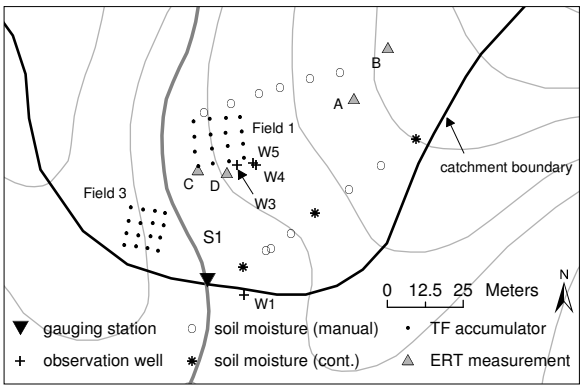

Figure 3.3: Details of the Malalcahuello Catchment near the catchment outlet. Shown are the main stream gauging station (S1), as well as the position of the interception fields including the arrangement of the throughfall (TF) accumulators, the soil moisture transects, the observation wells and the location of the electric resistivity (ERT) measurements. The contour lines have a resolution of 20 m.

data-logger and were measuring continuously. The first of these three probes was installed in March 2003 and the two others in December 2004. A fourth probe was used for manual measurements (irregular time intervals) at 11 points along the transects. As a result of the special characteristics of the volcanic ash soil (e.g. extremely high porosity) the built-in standard calibrations were not applicable and it was necessary to calibrate the probe specifically for this type of soil.

3.3.3.3 Investigating groundwater-surface water exchange with temperature as a tracer

Water temperatures of stream and groundwater were measured continuously at all stream gauging stations and observation wells. Temperature dynamics can be used as tracers to determine locations and amounts of groundwater inflow or outflow if the temperature gradients between stream and groundwater are sufficiently pronounced (Constantz, 1998; Constantz et al., 2003a; Selker et al., 2006).

3.3.3.4 Investigation of flow paths in the unsaturated zone: dye tracer experiments

Applied dye tracers can be used to investigate small-scale flow processes in the subsurface (Kim et al., 2006; Weiler & Flühler, 2004; Weiler et al., 2003; Zehe et al., 2001; Zehe & Flühler, 2001a). In order to get an impression of the infiltration/percolation characteristics of the catchment 13 tracer experiments were carried out (12 under forest, one on bare volcanic ashes). For all experiments the food colorant Brilliant Blue was used with a concentration of 4 g/l. 30 liters of the dye were applied to an area of 1.2 m^2 over a period of 3-4 hours. This corresponds to a total of 25 mm at application rates between 6 and 8 mm/h. The dye was applied with a hand pressurized pesticide sprayer in order to simulate rainfall. For one experiment two directly neighbouring plots were sprayed with the dye, the second plot with twice the amount (60 l) and double the application rate. Soil profiles were excavated the following day and photographs of the dye pattern were taken with a digital camera. Images were rectified with ArcGIS and enhanced further with Corel Photopaint by splitting it into the channels HSB (Hue, saturation and brightness). After adjusting the tone curve of the hue channel image the blue stains appear as white and the unstained areas as dark grey. A detailed description of these experiments and their results can be found in chapter 4.

3.4 Results and discussion

In this section the observed characteristics of rainfall, throughfall and runoff are described. In order to understand how rainfall is transformed into runoff, the characteristics of the subsurface need to be investigated: its structures and characteristic

parameters and the processes that are transporting the water from the soil surface into the stream. As it is often impossible to measure these processes directly, we sometimes have to content ourselves with the „footprints" of these processes and infer them. This could be for example the changing of stream water chemistry during the course of an event. It could also be the temperature dynamics of groundwater or the dynamics of soil moisture at certain profiles along the slope (data scarcity in space does not allow us to measure water movement directly but forces us to infer patterns of movement from the very narrow view of single sensors along a hillslope).

3.4.1 Rainfall, throughfall and runoff

Mean and maximum annual discharges in the Malalcahuello catchment for the years 2004 and 2005 are listed in Table 3.2. These mean annual discharges have a probability of exceedence of 42% and 33%, respectively (with flow duration curves of daily data calculated for each of these years separately). Measurement intervals were 5-10 minutes, depending on the observation period.

Yearly runoff coefficients of the Malalcahuello catchment amount to 63% for the year 2004 and 77% for 2005 (Table 3.2), with rainfall amounts of 3640 mm/a and 3040 mm/a, respectively (measured at the catchment outlet). The runoff coefficient for 2005 is probably overestimated due to unusually high amounts of snow even at lower altitudes and the resulting underestimation of precipitation with unheated rain gauges. Altitudinal effects may also cause underestimation of areal precipitation and thus overestimation of runoff coefficients. However, no clear altitudinal gradient could be derived from the 5 rain gauges. The baseflow index (BFI) calculated with the 5 day smoothed minima technique (Institute of Hydrology, 1980; Post & Jones, 2001) is also high and amounts to 82% for 2004 and 77% for 2005.

Pan evaporation measured at the lower climate station (Table 3.2) is equivalent to 21% of precipitation in 2004 and 24% of precipitation in 2005 (again: precipitation probably underestimated in 2005). Long term mean annual pan evaporation is 796 mm/a. This leaves us with 16% of the water budget unaccounted for in 2004 and an extra 1% in 2005 (where we are underestimating precipitation). However, as we are using pan evaporation as estimate for actual evapotranspiration and are neglecting interception losses, such discrepancies are to be expected.

Event runoff coefficients are low and lie between 1 and 10% for the 17 events analyzed in 2004/2005, of which a third are smaller than 2% (see chapter 2). Precipitation amounts for these events range from 13 to 85 mm, whith maximum hourly intensities between 5 and 28 mm/h. For the analysis of event runoff, baseflow was separated with a simple straight horizontal line until the endpoint of event runoff. The determination of the endpoint of an event is described in chapter 2. Response to rainfall is generally fast ($<$ 1 h for 65% and $<$ 0.5 h for 35% of 17 events) and recessions are steep with lag times between end of rainfall and end of event response of rarely more than a few hours. Maximum hourly rainfall intensities are $>$ 20 mm/h for 3 out of 17 events (see chapter 2).

The variability of throughfall amounts was determined for 15 rainfall events. Results are shown in Table 3.3. Overall 601 measurements were taken, 2 of which were discarded as outliers. The outliers were due to the fact that the accumulator was positioned directly below the „drip point" of a fallen tree. The water was channelled along the tree trunk into the accumulator, resulting in an overfilling of the container and consequent loss of sample. The remaining sample (i.e. the total volume of the accumulator) amounted to 6.3 and 7.6 times the precipitation measured at the rain gauge. The accumulator was moved after these two events.

On average 80% of total precipitation reaches the forest floor as throughfall. On average (over all events and all fields) 18% of the measurements

Table 3.2: Streamflow, rainfall and climate characteristics of the Malalcahuello catchment.

year	mean Q $[m^3/s]$	max. Q $[m^3/s]$	Q_95 $[m^3/s]$	precip $[mm/a]$	C_R [%]	BFI [%]	E_{pot} $[mm/a]$
2004	0.43	3.75	0.17	3640	63	82	770
2005	0.46	4.16	0.13	3040	77	77	742

Table 3.3: Results of throughfall (TF) measurements for the three interception fields. Throughfall data is given as fraction of total precipitation (P_{tot}). The last two lines show the average (over all events) and the maximum (for a single event) percentage of measurements that are higher than total precipitation.

	Field 1	Field 2	Field 3	Total
# of accumulators	16	20	16	52
# of measurements	235	255	109	599
# of events	15	13	7	15
Average TF/P_{tot}	0.79	0.82	0.78	0.80
Median TF/P_{tot}	0.76	0.82	0.78	0.79
Standard Dev.	0.34	0.24	0.34	0.30
% $>P_{tot}$ (avg.)	16	17	20	18
% $> P_{tot}$ (max.)	38	42	31	38

are higher than total precipitation. The maximum percentage of measurements exceeding total precipitation (P_{tot}) for a single event is 38% for field 1, 42% for field 2, 31% for field 3 and 38% over all accumulators of all fields.

Statistical tests were carried out to compare mean values and variances of the different fields of throughfall accumulators. Sample means were compared with Wilcoxon rank sum test (Crawley, 2005) and were not significantly different from one field to another. Comparing the variances using Fisher's F test (Crawley, 2005) showed that Fields 1 and 3, both located at the catchment outlet, do not have a significantly different variance, while the variance of Field 2 is significantly different from both Fields 1 and 3. The reason for this difference in variance is probably due to differences in vegetation cover. Furthermore, the terrain at Field 2 is relatively level compared to the other two locations. The boxplot in Figure 3.4 shows median values and interquartile ranges of the ratio TF/P as well as the distribution of values outside the interquartile range.

In an interception study carried out in 1998 in close vicinity of the catchment, stemflow measurements had been included into the analysis, thus giving a better estimation of how much of the precipitation is actually reaching the soil. Over the hydrologic year 1998 the interception losses in the native forest plot amounted to 26% of total precipitation. Of the precipitation reaching the forest floor, 8% were stemflow. More details of this study can be found in Huber & Iroumé (2001). Over the period Feb. 1998 - March 2000 throughfall was 79% of total precipitation (Iroumé & Huber, 2002) (stemflow 7%), which is close to our total average of 80%.

However, while these spatial average values are needed for an estimation of the yearly water budgets, for the question of runoff generation it is more the variability than the average values which are of interest. The fact that throughfall can amount to 3 times the total precipitation in some places (or even > 6 times as in the situation where a fallen

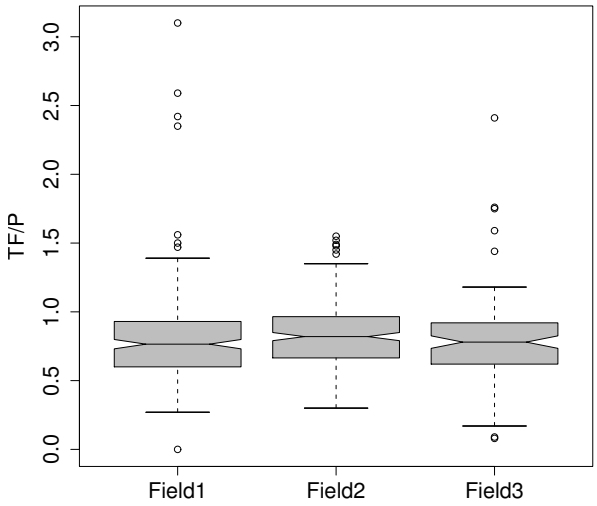

Figure 3.4: Boxplot of throughfall measurements for the three interception fields as fraction of total precipitation. The horizontal bar in the middle of the boxes shows the median values, upper and lower edge of the boxes the interquartile range. The whiskers of the boxes extend to the last data point within a distance of 1.5*interquartile range from the box. Values outside these limits are drawn as circles (Crawley, 2005)

tree acted as „rain water funnel"), suggests the occurrence of variable infiltration. In these locations antecedent soil moisture is likely to be higher than average, leading to higher soil hydraulic conductivities and therefore likely preferential flow. Additionally, the locally higher intensity of rainwater input further enhances preferential flow.

3.4.2 The subsurface

3.4.2.1 Soils and soil stratigraphy

Soils in the catchment are young, little developed volcanic ash soils with a silty sand texture in the upper layers (60% sand, 30% silt). Grain size distribution can be highly variable below a depth of about 1 m, ranging from layers of almost exclusively fine gravel (4-6 mm diameter), to layers with silt, sand and gravel fractions. Single stones can be several cm in diameter. The fine gravel layers were found in varying depths from 100 cm to 290 cm. In one soil pit a layer of pumice (gravel grain size) was found at a depth of 55 cm. Layer thickness is also highly heterogeneous, from 2-4 cm to several meters. 19 out of 30 auger holes extended to a depth of 200 cm and 8 out of these 30 holes were deeper than 300 cm. Drilling at most points could not be continued due to the presence of impeding stones. Unfortunately it was not possible to establish if these impeding stones were single small stones in the ash soil matrix or weathered bedrock. However, one hole was drilled to a depth of 710 cm (maximum auger length).

Them main mineral component of the upper soil horizons is feldspar (plagioclase) and probably volcanic glass (which is difficult to identify with X-ray diffractometry). Neither quartz nor clay minerals were found. The fact that secondary minerals such as allophane and imogolite, which are typical for weathered Andosols (Besoain & Gonzalez, 1977) were also not found, indicates that at least the upper horizons of the soils in the research area are indeed very young ash soils in their first stage of soil evolution.

3.4.2.2 Soil physical parameters

Soil hydraulic conductivities determined in the lab from undisturbed soil cores range for the top 45 cm from 1.22 * 10^{-5} to 5.53*10^{-3} m/s, with an average of 5.63*10^{-4} m/s (42 samples). For the fine gravel and pumice layers the conductivities range between 1.02*10^{-3} and 2.76*10^{-3} m/s (9 samples). Permeability measurements carried out in situ with the Guelph permeameter, resulted in Ksat values of 5.3*10^{-5} m/s on average for a depth of about 30 cm. Average values for this depth determined in the lab are 4.0*10^{-4} and 8.2*10^{-5} m/s depending on the horizon. The difference could be due to a number of different reasons: a) the fact that the soil was not completely saturated during the field experiments, b) smearing of the bore hole walls/interruption of flow paths during augering, c) spatial variability. Partial hydrophobicity might be another reason for the lower in-situ values, – as the „Water Drop Penetration Time" test showed strong to extreme potential hydrophobicity for the upper horizons (chapter 5) . Hydrophobicity has also been observed in volcanic ash soils in Ecuador (Poulenard et al., 2004) as well as in Southern Chile (Bachmann et al., 2000).

Porosities range from 56.8% to 82.1%. Mean porosity for the top 45 cm is 71.7% (16 samples, with a standard deviation of 6.6%). Water content at the permanent wilting point (at 15 bar pressure) ranges from 8% to >25% for the 87 samples taken in various ash soil horizons. High residual water contents are common in volcanic ash soils due to intra- and inter-particle micropores (Shoji et al., 1993). Grain size distributions for the upper horizons resulted in an average of 66.5% sand, 30.4% silt and 3% clay. In the more gravely layers the fraction of grain size $>$ 2 mm ranges from 38-86%.

3.4.2.3 Geoelectric measurements

Inversion results of the geoelectrical soundings are presented in Figure 3.5. The black line represents the best fit model, the grey lines show inversions of the sounding profile which are also acceptable (lie within the margin of error around the best fit). Profiles A and B show the models for two soundings in the upper part of the slope, while profiles C and D show the models of soundings from the lower end of the slope, close to the stream at S1 (see Figure 3.3). The difference in elevation is about 40 m, while the distance is about 60 m. A prominent feature of all plots is the layer of low resistivity at greater depths. Resistivities between 20 and 200 ohm-m can indicate groundwater. Resistivities of sand lie between 50 ohm-m (saturated) and 10000 ohm-m (dry). The same values apply for gravel (Knödel et al., 1997). While this low resistivity layer which might be groundwater lies at a depth of 7-8 m for the two upper soundings, its upper limit is much closer to the surface at the near-stream profiles (1.5-2 m). The observation well not far from the two lower soundings indicated groundwater level at 2.7 m below the surface (measured 5 days after the sounding). 3 more soundings carried out in the upper part of this slope also show a layer of low resistivities in a depth of $\sim$10 m, while one measurement did not show this type of layer. Another sounding close to the stream located the layer of low resistivities at a depth of 0.6 m. A layer of high resistivities which would correspond to bedrock could not be identified.

3.4.3 Seasonal dynamics and event response

3.4.3.1 Water chemistry, nutrient export and hydrograph separation

Nutrient concentrations were generally very low in the stream with 20 μg/l NO_3-N (median of 30 samples) and 22 μg/l PO_4-P (92 samples). While the median concentrations of sulphate and chloride are also low, 0.13 mg/l (92 samples) and 0.65 mg/l (92 samples), respectively, the concentration of silica is relatively high with 19.3 mg/l (96 samples). The high concentrations of silica as well as the low val-

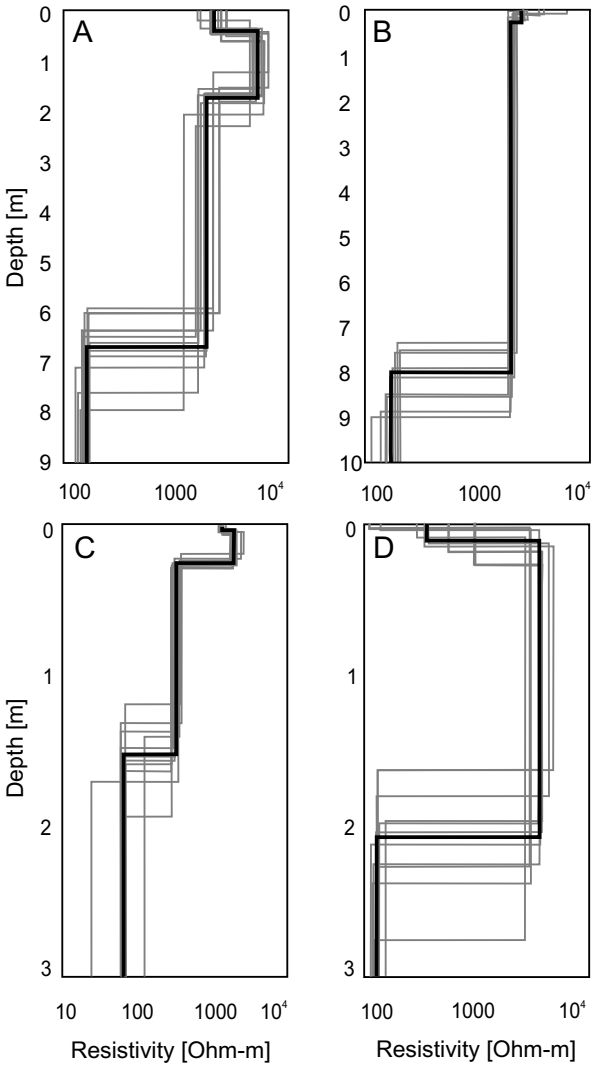

Figure 3.5: Inversion results of the geoelectrical soundings. Profiles A and B were measured in the upper part of the slope, profiles C and D at the lower end of the slope, not far from the stream (see Figure 3.3). The black line represents the best fit model, the grey lines show inversions of the sounding profile which are also acceptable (lie within the margin of error around the best fit). The layer of low resistitvies at greater depth could signify groundwater.

ues for the other compounds result from the nature of the volcanic ash soil. Also the lack of anthropogenic intervention within the catchment is likely a reason for the low concentrations of nitrate, phosphate, sulphate and chloride. Median concentrations of the same constituents in the Piedra Santa Catchment (2-5 samples) are between 15% and 110% higher than in the Malalcahuello Catchment. The analysis of the water chemistry of different runoff components and stream water is shown exemplarily for the major cations in Figure 3.6. It was found that soil water concentrations (85 samples) are generally very low, much lower than in stream (144 samples) and groundwater (3 samples) (Figure 3.6). This is probably due to the short residence time of water in the upper part of the soil column resulting from the high flushing frequency and the high hydraulic conductivities. The fact that soil water concentrations are lower than throughfall concentrations (9 samples) is surprising and possibly due to sorption within the organic layer. Even when comparing samples taken during the same event throughfall concentrations in K and Ca are generally higher than soil water concentrations. This was observed for 5 out of 6 events for K and for 4 out of 6 events for Ca. Throughfall concentrations are enriched in Ca and K. This can be due to leaching, washoff of dry deposition and also evaporation within the canopy and is not unusual for these forests (Godoy et al., 2001; Uyttendaele & Iroumé, 2002). The fact that stream water concentrations are only slightly lower than groundwater concentrations and higher than concentrations of rainfall, throughfall and soil water, indicates that groundwater is the major component of stream flow. However, mean groundwater concentrations are only based on three samples. The high concentrations in groundwater are likely to be due to its longer residence time and deep subsurface flow causing prolonged interaction with the bedrock (i.e. chemical weathering). Overall there is a slight negative correlation of ion concentration with discharge (e.g. R^2 = 0.4 for Na when low flows with their strong variability in concentration

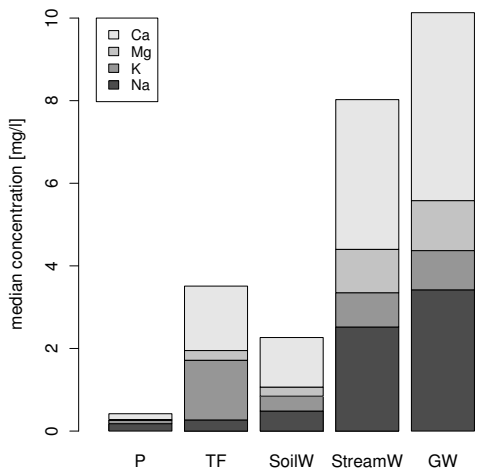

Figure 3.6: Median concentrations of the major cations of 5 different components: precipitation (P), throughfall (TF), soil water (SoilW), stream water (StreamW) and groundwater (GW).

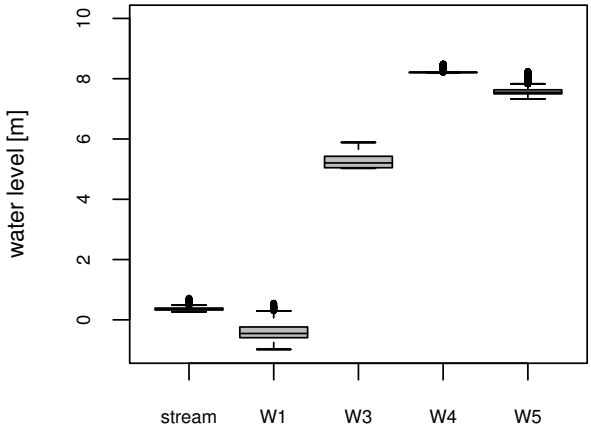

Figure 3.7: Boxplot of stream and groundwater levels from May to December 2005 (all in reference to the datum of the stream gauge). Circles identifying outliers overlap, forming a line extending upward from the end of the upper whisker. For details on boxplots see Figure 3.4.

are excluded), which becomes more obvious during some events (e.g. R^2 = 0.8 for Na for an event in December 2004). Hydrograph separations determined with different constituents, electric conductivity and stable isotopes indicate a high fraction of old water even during events (chapter 4). However, while hydrograph separation worked well for an event in early December 2004, separation into pre-event and event water showed mixed results for an event in February 2004 (summer, after several weeks of drought). This suggests a shift in flowpaths from early spring to late summer.

3.4.3.2 Groundwater and soil moisture dynamics

Groundwater dynamics were compared to stream water level dynamics for four wells (W1, W3, W4 and W5). While water levels at W1 are below the stream bed, water levels in the other wells are between 5 and 8.5 m above the stream bed (Figure 3.7). Well W3 dries out during certain periods and W4 only connects to the groundwater at times of peaks. Water level fluctuations are strongest in the wells closest to the stream. For the positions of the wells in relation to the stream see Figure 3.3.

A comparison of water level dynamics in stream and groundwater (well W5) is shown in Figure 3.8. Both time series are referenced to the datum of the stream gauge. The Pearson correlation coefficient for correlation between the time series of stream and groundwater level is R=0.69. The smoothed time series of stream water level (96 hour moving average), however, leads to a stronger correlation of the two time series with a coefficient of R=0.79, as the fast responses are smoothed out and the slow flow component of stream water is likely dependent on groundwater levels. In a next step lag times between the time series of stream and groundwater level were analyzed. Streamflow shows fast and short response, while groundwater response is delayed and prolonged. The analysis for the original time series lead to correlation coefficients of R=0.75 for W3 at a lag time of 99 h and R=0.8 for W5 at 40 h. The same analysis was carried

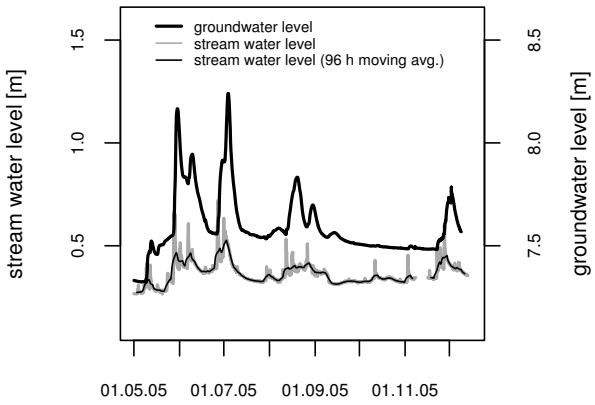

Figure 3.8: Comparison of stream water and groundwater hydrographs (well W5).

out with the differentiated time series in order to remove serial dependencies. The most prominent peaks in correlation can be found at time lags of 11 h (R=0.20) and 125 h (R=0.14) for well W3 and at 37 h (R=0.10) and 73 h (R=0.08) at W5. Generally the first of these two maxima seems to coincide with the rising limb and the second with the falling limb of the hydrographs. While correlation coefficients seem low with values between 0.1 and 0.2, one has to keep in mind that these analyses were carried out for the differentiated time series and are significant within the 95% confidence interval. Due to the large gaps of data within the time series of W4 the analysis was not carried out for this well. The poor quality of the time series at well W7, close to the first order stream at S5 (Figure 3.1) prevented a statistical lag time analyses, however, groundwater level at this well also lagged behind surface water response.

Yearly soil moisture dynamics for the three sensors measuring at 10 min resolution show that spatial variations are generally larger than temporal variations (Figure 3.9). This is due to the large spatial heterogeneity of the soil layers and their corresponding grain size distributions. Moisture content at field capacity for these soils lies between 20 and 57 Vol%, depending on the soil layer. This corresponds quite well with median and maximum soil moisture contents observed in the field.

The fact that soil moisture contents rarely exceed these values of field capacity suggests that water transport in these soils is fast, preventing saturation and overland flow. Soil moistures at 10 cm depth decrease with elevation (sensor 1 is lowest on the slope, sensor 3 the highest, see Figure 3.3). This is probably due to differences in incident solar radiation: the deeper in the valley the more shading as a result from the steep topography. Event response dynamics also suggest temporary hydrophobicity in the top layer during summer and lateral water transport at certain depths (chapter 5).

3.4.3.3 Groundwater-surface water interactions and flow paths in the unsaturated zone

Analysis of groundwater levels and temperature dynamics in the stream and at well W1 showed that at this location groundwater levels are below the stream bed, leading to water exfiltration from the stream. During high flows flow reversal is observed (chapter 4). However, these interactions are likely to be highly variable in space, i.e. groundwater-surface water interactions might be different from one stream reach to the next, depending on the geology and topography of the stream bed.

Dye tracer experiments indicate that flow paths differ significantly in summer and winter, i.e. during wet and dry periods, as well as from forested to unvegetated areas. While flow patterns show preferential flow under forest, the dye infiltrated as a straight front in the unvegetated soil on the catchment rim. The difference in flow patterns from dry (narrow flow paths) to wet season (wider flow paths) is probably due to hydrophobicity in the top soil layer (chapter 4). Lateral flow in the duff layer was observed during a high intensity (20 mm/h) sprinkling experiment (chapter 4).

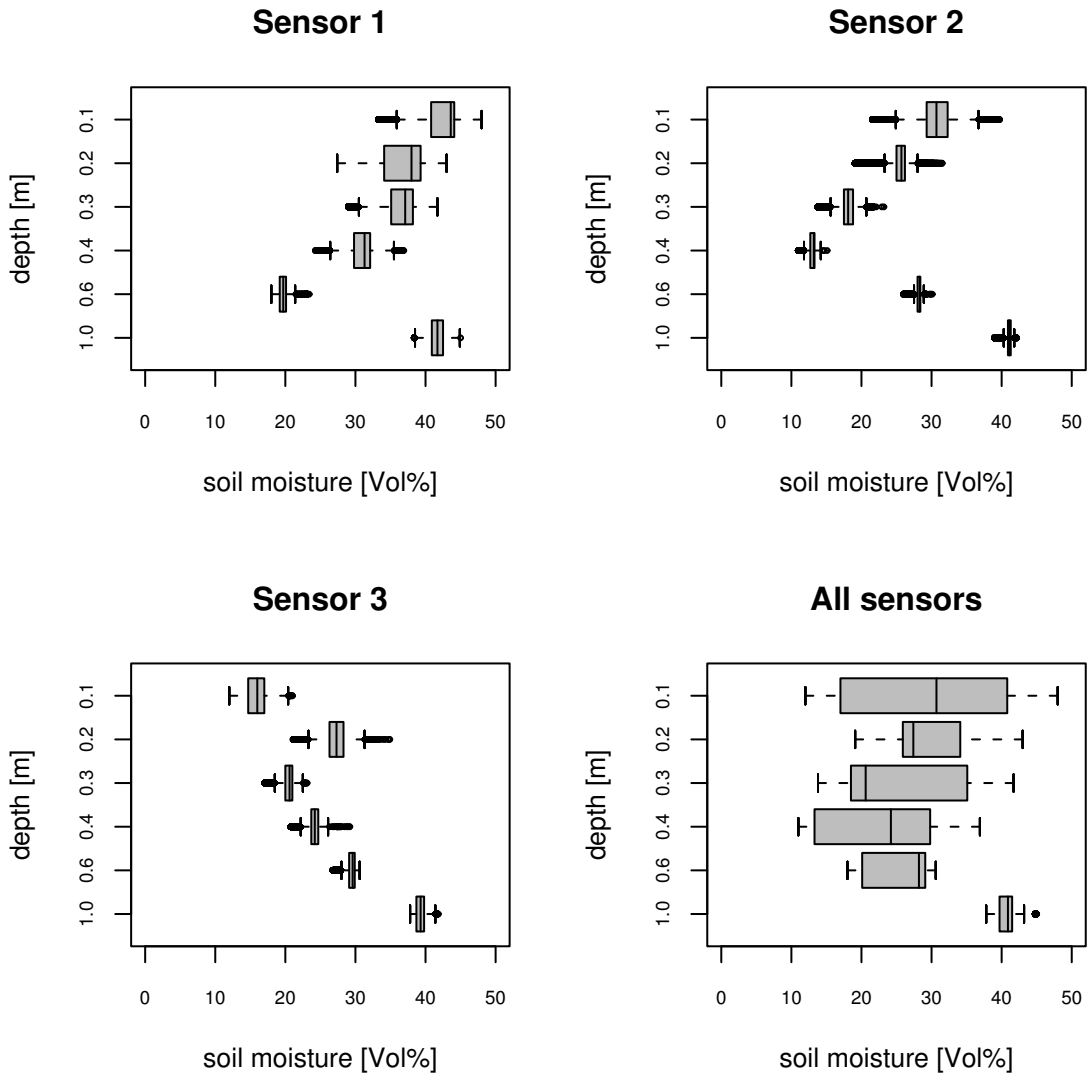

Figure 3.9: Soil moisture variations for the three continuously measuring probes (October 2004 to October 2005). The sensors are numbered according to their position on the slope, with sensor 1 being the lowest and sensor 3 the highest in elevation. For location of the transect see Figure 3.3.

3.5 Summary and conclusions

3.5.1 Runoff generation processes – conclusions and open questions

The „multi-method approach" used in this investigation includes measurements of streamflow, rainfall, throughfall, water chemistry, soil water dynamics, groundwater dynamics, soil physics, soil mineralogy, geo-electrical sounding, and tracer techniques.

A conceptual model of runoff generation processes in the Malalcahuello catchment is produced by using the results of the „multi-method-approach" as pieces of the puzzle (Table 3.4). From discharge data we conclude that in this catchment two main principles are dominant. Firstly we have a *fast response to rainfall* (short response times and quick recessions), which means fast runoff processes (e.g. movement in the unsaturated zone, preferential flow, pressure wave/piston flow, kinematic wave). Several factors suggest vertical preferential flow, e.g. the high variability of throughfall and thus also soil moisture, the soil moisture dynamics and the temporally persistent small scale soil moisture patterns (chapter 5), plus the fact that the catchment is dominated by forests, where preferential flow patterns were observed in all dye tracer experiments (chapter 4). Vertical preferential flow (flow along roots or fingering) is therefore likely the rule and not the exception in this catchment. On the other hand, the fast response of streamflow while groundwater response lags behind suggests rapid lateral flow. This is further supported by the fact that during rainfall events an increase in soil moisture was observed in deeper layers while the horizons above showed no response. Wetting of this deeper layer did thus not result from vertical percolation (chapter 5). The considerable heterogeneity of the volcanic ash soils with strong layering is also likely to enhance fast lateral flow processes.

The layer interfaces resulting from the textural differences between different layers of volcanic ash (from gravel fraction to silty sand) can serve as flow paths. However, connectivity of these gravel layers along the hillslopes is necessary in order to make them hydrologically relevant on hillslope or catchment scale.

Furthermore, a *large soil-/groundwater storage* seems to exist, generating flow even after several weeks of drought. This perception is further supported by the fact that event runoff coefficients are low and yearly runoff coefficients are high, as well as by soil characteristics, such as high porosities (determined in the lab) and the large unsaturated zone as confirmed by augering and geo-electrical sounding (Figure 3.5).

The results of the tracer study presented in chapter 4 show that a shift in processes occurs from winter to summer: changes were observed in flow patterns, groundwater-surface water interactions and in the response of stream chemistry to rainfall events. Hydrophobicity is likely to have an effect after extended dry periods, causing persistent small scale soil moisture patterns and fingering (chapter 5) .

In addition, response times of streamflow, soil moisture and groundwater were shorter for summer events (chapter 5) .

However, several open questions remain. We still do not know, where exactly the fast response of streamflow is generated, as both soil and groundwater often respond slower than the stream (section 3.4.3.2 and chapter 5) . What structures control rapid lateral flow (so far not observed pipes, flow along the bedrock or flow along layer interfaces)? Is there a deep groundwater system? There also seems to be a contradiction between the results of hydrograph separation (high fraction of old water) (chapter 4) and the lag times of at least several hours between surface water and groundwater response at well W3. This might be explained by the replacement of old water with a similar chemical signature as groundwater in zones of rapid lateral flow along layer interfaces.

Torres et al. (1998); Rasmussen et al. (2000) and Williams et al. (2002) describe the phenom-

Table 3.4: Synthesis of the multi-method approach: inferred runoff generation processes and underlying experimental evidence.

Runoff generation process	Evidence
fast vertical flow (matrix and preferential)	high hydraulic conductivities high input variability (throughfall) high variability of soil moisture persistent small scale patterns in soil moisture soil moisture dynamics hydrophobicity flow patterns fast streamflow response
lateral preferential flow	soil layering soil moisture dynamics lateral flow during high intensity sprinkling fast streamflow response
large subsurface storage	high annual runoff coefficient persistant flow during drought low event runoff coefficients high porosities deep unsaturated zone
process shift summer/winter	faster streamflow response in summer change in response of stream chemistry hydrophobicity change in flow patterns change in groundwater surface water interaction

enon of kinematic waves in the unsaturated zone which leads to response velocities much faster than pore water velocities. Modelling these phenomena with the help of a physically based model that also allows for the simulation of transport processes might help to shed light on this interesting question. Another open question is the question of residence time – how long does the water remain in the catchment, how „old" is the water that flows in the stream? Has it entered the system that same year or has it been stored for longer than that? These questions could be answered by determining isotope ratios in rainwater and streamflow over a longer period of time.

3.5.2 Evaluation of experimental methods

As mentioned in the introduction, most experimental studies in poorly gauged catchments are faced with limited time, financial resources and manpower. The experimental methods used in this study were thus evaluated for a) the gain of process understanding and the gain of important model input and validation data and b) the expenditures necessary for their application, such as labor and financial cost. This evaluation is summarized in Table 3.5. Some disadvantages of the selected methods are also listed. However, the evaluation only applies for the study presented here, as for example the installation of groundwater observation wells will be more expensive in situations where manual drilling is not an option.

In an attempt to further minimize time and financial expenditures while keeping the gain of process understanding as high as possible, the experimental methods used in this study were assessed and the most essential methods were selected. These methods are indicated by bold printing in Table 3.5. Expensive and time consuming methods were only selected if the gain in process understanding was rated as high. A short assessment of the selected methods is given in this section. Discharge measurements, for example, are very time consuming but nevertheless crucial. Event hydrograph separation by isotopic tracers is both time consuming and expensive but can deliver high-level integral information about runoff generation in the catchment. Isotopic tracers were preferred over other geo-chemical tracers because of their conservative behaviour. The measurement of water temperatures in wells and in the stream as well as the measurement of electric conductivity have the advantage of producing continuous time series of potential (non-conservative) tracers at relatively low cost. Continuous measurement of soil moisture profile gives valuable insights in flow processes in the unsaturated zone, especially when combined with dye tracers (chapter 5) and are worth the relatively high costs of the sensors. Both, laboratory analysis of soil cores as well as permeability measurements in the field deliver valuable information, however, laboratory analysis of soil cores was preferred. Lab analysis has the advantage that not only hydraulic conductivities can be measured, but also soil moisture characteristic curves. While the measurement of snow cover and snow water equivalent is important in mountainous catchments it is difficult to achieve in densely forested areas with limited accessibility. Snow height measured at one point in the catchment only gives information about increase or decrease of the snow pack: the conversion of snow height to snow water equivalent is impossible without further manual measurement. The input of water to the catchment can thus only be estimated from this data. The use of geophysical techniques, such as electric resistivity soundings, is expensive, time consuming and especially difficult on densely forested steep slopes. Nevertheless, it is the only possible source of information concerning depth to bedrock or groundwater table in this catchment, as soil layer thickness is likely to exceed several meters. While highly variable throughfall amounts are likely to influence runoff generation and this fact should be kept in mind, the actual measurement of this variability is probably of less importance in cases of severe time constraint.

Table 3.5: Evaluation of experimental methods: gain (of process understanding and model input/validation data) vs. expenditure. (Positive ratings (+) correspond to greater gains and lower expenditures.) Experimental methods rated as most crucial are printed in bold. (Abbreviations: EC – electric conductivity, FDR – frequency domain reflectometry, SWE – snow water equivalent, WDPT – water drop penetration time)

parameter	**method**	**gain**		**expenditure**		**problems**
		process	model	labor	cost	
rainfall	tipping bucket	+++	+++	+	+	point data – how representative?
water level	capacitive	+++	+++	+	+	
discharge	velocity-area	+++	+++	- -	+	uncertainty
groundw. level	capacitive	+++	+	+ -	+	installation
water temp.	thermister	++	+	++	++	
stream EC	EC electrode	++	+	++	+	not a conservative tracer
soil moisture (continuous)	FDR	+++	++	+	-	point data – how representative?
soil moisture (manual)	FDR	++	+	-	+	
snow height	ultra-sonic	+	+ -	+	-	point data, not SWE
throughfall	accumulators	++	++	+ -	++	no temporal resolution
nutrient export	lab analysis	+ -	+ -	-	-	
geochemical tracers	lab analysis	++	++	-	-	small number of events
isotopic tracers	lab analysis	+++	++	-	- -	small number of events
flow paths	dye tracers	+++	++	+ -	++	destructive sampling
soil stratigraphy	manual augering	++	++	+ -	++	point data – how representative?
soil physics	lab analysis	++	+++	+ -	-	point data – how representative?
permeability	Guelph permeameter	++	+++	-	+	point data – how representative?
soil minerals	x-ray diffraction	+ -	+ -	+	+	
hydrophobicity	WDPT test	+++	+	+	++	not field conditions
depth to bedrock/gw	electric resistivity	++	++	-	- -	difficult in difficult terrain

3.5.3 Conclusions and outlook

The presented experimental results suggest the importance of fast processes for rainfall runoff response on the one hand as well as considerable dampening effects of a large unsaturated subsurface storage on the other hand. With the help of physically based models it is possible to test the perceptions gained from point data for their importance on the hillslope and catchment scale. In a next step these findings can be used as a basis for the simulation of land use change scenarios for this area.

Overall, the approach of replacing long time series of data with a multitude of experimental methods was successful and delivered important insights into the hydrological functioning of this catchment. The critical evaluation of the applied experimental methods concerning expenditures vs. gain in process understanding will be helpful for future process studies.

Acknowledgements

The authors would like to thank Andreas Bauer (Potsdam University), Hardin Palacios and Luis Opazo (Universidad Austral de Chile) for help in the field, Prof. Anton Huber (Universidad Austral de Chile) for logistic and technical assistance and Erika Lück (Potsdam University) for assistance with the geoelectrical sounding equipment and the corresponding data analysis. Chemical analyses were carried out by laboratories at the University of Potsdam, the Universidad Austral de Chile and at Benthos, Validvia. We also want to thank two anonymous reviewers whose comments significantly improved an earlier version of this manuscript. This work was partially funded by the International Office of the BMBF (German Ministry for Education and Research) and Conicyt (Comisión Nacional de Investigación Científica y Tecnológica de Chile) and the „Potsdam Graduate School of Earth Surface Processes", funded by the State of Brandenburg.

Chapter 4

Investigation of runoff generation in a pristine, poorly gauged catchment in the Chilean Andes
II: Qualitative and quantitative use of tracers at three spatial scales *

Abstract

Understanding runoff generation processes is important for flood prediction, water management, erosion control, water quality, contaminant transport and the evaluation of impacts of land use change on runoff processes. However, little process research has been carried out in Southern Chile and especially the young volcanic ash soils, which are typical for this area, are not well understood in their hydrologic behaviour.

In order to establish a „reference study" which can then be used for comparison with other (disturbed) sites, this study focuses on the investigation of runoff generation processes in an undisturbed, forested catchment in the Chilean Andes. Presented here is the investigation of these processes with different tracer methods at different spatial scales. Hydrograph separation with environmental isotopes and geochemical constituents was used on the catchment scale. Thermal energy was used as a tracer to investigate groundwater-surface water interactions at the local stream reach scale and dye tracers were used to study infiltration and percolation characteristics at the plot scale. It was found that pre-event water dominates the storm hydrograph. In the lower reaches, however, water usually exfiltrates from the stream into the adjacent aquifer. The dye tracer experiments showed that while preferential vertical flow dominates under forest, water infiltrates as a straight horizontal front in the bare volcanic ashes (no vegetation) on the catchment rim. Subsurface flow patterns in the forest differ significantly from summer to winter. All three approaches used in this study suggest an important shift in dominant processes from dry to wet season.

*Theresa Blume, Erwin Zehe, Axel Bronstert (in press), *Hydrological Processes*

4.1 Introduction

Little research on hydrological processes and runoff generation has been done in Southern Chile, especially not in areas with young volcanic ash soils (chapter 3). However, these soils are of special interest as a) they are characterized by unusually high porosities and hydraulic conductivities which are likely to have an effect on runoff generation, and b) they are prevalent in Southern Chile, covering 62% of the area (Tosso, 1985). Furthermore, understanding runoff generation processes is a general pre-requisite to quantifying the hydrologic consequences of land use change.

Runoff generation processes have been studied at the plot and hillslope scale as well as in headwater basins in many areas of the world (e.g. Bonell, 1993), (review); (Buttle & McDonald, 2002), (Ontario, Canada); (Chirico et al., 2003), (North Island, New Zealand); (McGlynn et al., 2002), (South Island, New Zealand); (McNamara et al., 2005), (Idaho, USA); (Schellekens et al., 2004), (north-east Puerto Rico); (Torres et al., 1998), (Oregon, USA); (Tromp-van Meerveld & McDonnell, 2006b), (Georgia, USA); (Wenninger et al., 2004), (south-west Germany); (Zehe & Flühler, 2001a), (south-west Germany); While surface runoff processes on hillslopes are easier to identify, subsurface runoff generation processes are much more difficult to observe, interpret and model. These processes include, depending on subsurface substrates and structures, matrix, macropore-, finger- and bypass flow (flow in macropores within the unsaturated matrix), lateral flow along a perched water table, groundwater mounding, piston flow, etc. Further difficulties arise from the fact that these processes are not mutually exclusive. Some of them can be active simultaneously and interactively. The relative importance of each process is not constant over time but is dependent on antecedent conditions, actual soil moisture and rainfall characteristics (Brutsaert, 2005). As mentioned above, subsurface processes are difficult to investigate and most often impossible to observe directly. We thus often have to content ourselves with the „footprints" of these processes. These „footprints" can be the dynamics of stream water chemistry or groundwater temperature over the course of an event. They can also be the traces left by dye infiltrating into the soil. Tracer methods making use of these footprints can provide a powerful tool for the investigation of subsurface runoff generation processes, on plot, slope as well as catchment scale.

In this study an integrated approach combining several experimental techniques was used in order to improve the understanding of runoff generation in the Malalcahuello Catchment, which is dominated by high rainfall amounts, volcanic ash soil, steep topography and old growth forest:

- Hydrograph separation with stable isotopes and geochemical tracers – is event flow dominated by „old" or „new" water? Do changes occur from dry to wet season?
- Thermal energy as a tracer – what are the characteristics of groundwater - surface water interactions?
- Dye tracer experiments – does preferential flow occur in the unsaturated zone? Which type of preferential flow?

While dye tracers are used on the plot scale, the water temperature study covers the local stream reach and hydrograph separation is based on discharge chemistry as an integrated output signal for the entire catchment. The three scales are strongly linked: understanding the flow paths in the unsaturated zone (even only on plot scale) and the interaction of groundwater and surface water will help us understand the integral measure of stream water chemistry and its dynamics over the course of an event.

A brief introduction to the different tracer methods used in this investigation is given in the next section of this paper. In sections 4.3 and 4.4 the research area and the details of the methodology are

described. The results for the each of the experimental techniques are given in section 4.5, leading to summary and conclusions in section 4.6.

4.2 Theory - The use of tracers at different spatial scales

4.2.1 Hydrograph separation the catchment scale

Natural tracers such as environmental isotopes and geochemical constituents can be used to study runoff generation by determining the source areas of stream water on event basis. It is also possible to determine runoff components and flow paths (e.g. Uhlenbrook et al., 2002). This is typically done by hydrograph separation into event water and pre-event water or by multi-component separation (including for example soil water or shallow groundwater) (Bazemore et al., 1994; Burns et al., 2001; Hoeg et al., 2000; Ladouche et al., 2001; McGlynn et al., 2002; Rice & Hornberger, 1998; Shanley et al., 2002; Wenninger et al., 2004).

Hydrograph separation using tracers is based on the steady-state mass balance equations of water and tracer fluxes and their simultaneous solution (Sklash & Farvolden, 1979).

In case of n runoff components and $n-1$ observed tracers $t_1, t_2, \cdots t_{n-1}$ the following n linear mixing equations can be written

$$Q_T = Q_1 + Q_2 + ... + Q_n \tag{4.1}$$

$$c_T^{ti} Q_T = c_1^{ti} Q_1 + c_2^{ti} Q_2 + ... + c_n^{ti} Q_n \tag{4.2}$$

where Q_T is total runoff, Q_1, Q_2, $\cdots Q_n$ are the runoff components and c_1, c_2,$\cdots c_n$ are the respective concentrations of the tracer t_i (Hoeg et al., 2000). The application of these equations is based on certain assumptions: a) tracer concentrations of the different components differ significantly; b) the tracer concentration of each component is constant throughout the event; c) there are no significant additional components not accounted for; d) conservative mixing of the tracers; e) no collinearity between the tracer concentrations of the different components (Hinton et al., 1994; Hoeg et al., 2000).

The simplest way of using equations 4.1 and 4.2 is to determine the contributions of event water and pre-event water to total runoff. The event component is defined as that part of total runoff that entered the system during the rainfall event, while the pre-event component is defined as present in the catchment before the beginning of the rainfall event. Baseflow concentrations before the event may be used to define this component (Hoeg et al., 2000). According to equations 4.1 and 4.2 the contribution of pre-event water to total runoff can be estimated using

$$\frac{Q_P}{Q_T} = \frac{c_T - c_E}{c_P - c_E} \tag{4.3}$$

where Q_P is pre-event water, Q_T is total runoff, c_T is the concentration in the stream, c_E the concentration in event water (rainfall) and c_P the concentration in pre-event water (base flow).

4.2.2 Thermal energy as a tracer the stream reach scale

Thermal energy carried by flowing water can serve as a tracer for the identification of groundwater – surface water interactions. This method uses the fact that a) temperature dynamics and b) temperature itself can differ significantly between ground- and surface water. Measuring temperatures of stream water and the stream bed or sediment can help to identify gaining and losing reaches in streams (Allander, 2003; Anderson, 2005; Conant, 2004; Constantz et al., 2003b; Constantz & Stonestrom, 2003; Johnson et al., 2005; Selker et al., 2006; Silliman & Booth, 1993; Silliman et al., 1995). It is also possible to make a quantitative

estimate of either groundwater discharge (Becker et al., 2004; Conant, 2004) or surface water loss (Silliman et al., 1995).

While rivers and streams normally show a diurnal variation in temperature, groundwater temperature is expected to be constant at this time scale (Silliman & Booth, 1993; Constantz et al., 2002). Temperatures of groundwater or creek sediments are controlled by both advective/convective heat transport and heat conduction simultaneously, but one process may dominate depending on hydraulic conditions (Silliman & Booth, 1993). The three extreme cases of groundwater – surface water interaction are:

a) strong groundwater discharge into the stream. The temperature of the sediments beneath the river and the water in the hyporheic zone will be controlled by the temperature of the groundwater (advection) and diurnal variations are not to be expected.

b) no interaction between groundwater and surface water and thus no water flux through the sediments. The temperature of the sediments is controlled by heat conduction from surface water and will thus show diurnal variation (depending on the depth and sediment material). Average temperature at shallow depths (8-10 cm) is lower than the average stream temperature for most of the year.

c) strong exfiltration of stream water to the groundwater. The temperature of the sediment is strongly controlled by surface water temperatures (advection). The average temperature at shallow depths is approximately equal to the average temperature of the exfiltrating water (Silliman & Booth, 1993; Silliman et al., 1995). In the third case the diurnal variation of sediment temperature will show a lag compared to stream water as a result of travel time and a reduction in amplitude which is due to heat conduction (Silliman et al., 1995).

For the case of pure heat conduction (which usually dominates in soils but also in case b) – see above) the amplitude of temperature variation at depth z is $e^{-z/d}$ times smaller than the amplitude of surface temperature fluctuation (Hillel, 1998). The damping depth d can be calculated by (Hillel, 1998):

$$d = \left(\frac{2D_h}{\omega}\right)^{0.5} = \left(\frac{2D_h\tau}{\pi}\right)^{0.5} \tag{4.4}$$

where d is the damping depth, D_h is the thermal diffusivity, τ is the period of the oscillation. Thermal diffusivity is the ratio of thermal conductivity to volumetric heat capacity, where both thermal conductivity and volumetric heat capacity depend on water content, bulk density and composition of the substrate.

4.2.3 Dye tracer experiments – the plot scale

Dye tracers are often used to investigate small-scale flow processes such as the occurrence of preferential flow (Flury et al., 1994; Flury & Wai, 2003; Kim et al., 2006; Ohrstrom et al., 2004; Weiler & Flühler, 2004; Weiler et al., 2003; Zehe et al., 2001; Zehe & Flühler, 2001a). Dye tracers are usually applied on the plot scale, mostly by uniform sprinkling application simulating rainfall. The resulting flow pattern can be observed and photographed at excavated soil profiles.

4.3 Research Area

The research area is situated in the Reserva Forestal Malalcahuello, in the Precordillera of the Andes, IX. Region (Región de la Araucanía), Chile. The catchment is located on the southern slope of Volcán Lonquimay. It covers an area of 6.26 km^2 and elevations range from 1120 m to 1856 m above sea level (Figure 4.1). Slopes are steep with an average of 27° (51%) and 10% of the area with slopes

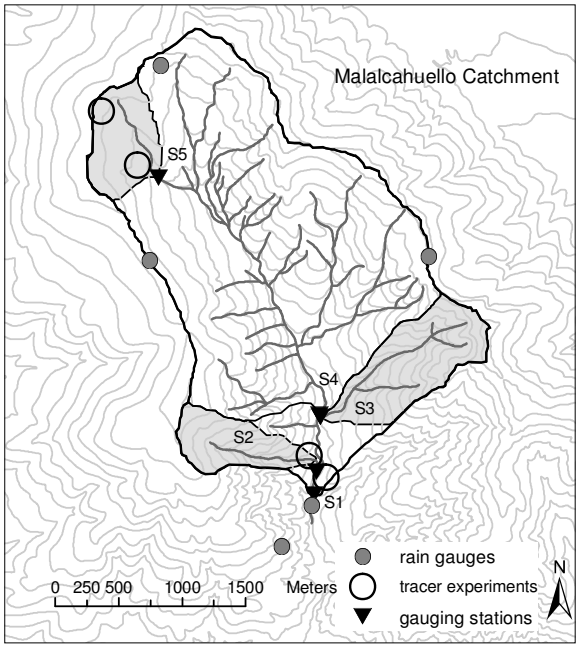

Figure 4.1: The Malalcahuello Catchment including the positions of rain gauges, the location of the dye tracer experiments and the gauging stations. S1 refers to the main gauging station, S2-S5 to the subcatchments. S3 and S4 are separated only by a few meters: S3 on the tributary coming from the east and S4 on the main stream. The vertical resolution of the contour lines is 50 m.

$> 43°$. Drainage density is 3.67 km/km^2. The terrain analysis is based on a digital elevation model (produced by the Instituto Geografico Militar de Chile) at a scale of 1:10 000 and 10 m resolution in elevation.

The soils are young, little developed volcanic ash soils (Andosols, in Chile known as Trumaos) (Iroumé, 2003). High water permeabilities (saturated and unsaturated), high porosities (60-80%) and low bulk densities (0.4-0.8 g/cm^3) are typical for volcanic ash soils. They also usually show a strong hysteresis and irreversible changes (e.g. in water retention) with air-drying (Shoji et al., 1993).

Soil hydraulic conductivities determined in the lab are high with an average of $5.63*10^{-4}$ m/s for the top 45 cm. For the fine gravel and pumice layers the mean conductivity is $1.88*10^{-3}$ m/s. Mean porosity for the top 45 cm is 71.7%. Soil layer thickness is highly heterogeneous, from several centimeters to several meters. Depth to bedrock is unknown but manual augering to depths > 3 m was possible, in one case even > 7 m (for details see chapter 3).

80% of the catchment is covered with forest of the type Araucaria *(Araucaria araucana)* and Roble *(Nothofagus obliqua)* – Raulí*(Nothofagus alpina)* – Coigue *(Nothofagus dombeyi)* with a dense understory of bamboo *(Chusquea culeou)*. This is native forest without any intervention. Above the tree line (20% of the catchment) there is no significant vegetation cover.

The climate of this area can be described as temperate/humid with altitudinal effects and snow at higher elevations during winter. Yearly rainfall amounts range from 2000 to over 3000 mm, depending on elevation. About 70% of the precipitation falls between April and September; June is the wettest month with >400 mm and February usually the driest with an average of 60 mm. Mean temperatures in June and January are 3°C and 14°C, respectively.

For a more detailed description of the catchment and the experimental study see chapter 3.

4.4 Methodology

4.4.1 Measurement of rainfall, discharge, groundwater levels and soil moisture

Climate data is available from a station located in a nearby forest plantation at 1270 m (most southern rain gauge in Figure 4.1). Rainfall, temperature, relative humidity, wind direction and velocity and global radiation have been measured at hourly intervals since 1999. Additionally, four tipping bucket rain gauges (resolution = 0.27 mm) were installed in 2003. Three are situated near the upper catchment boundary at approx. 1700-1800 m, and

one at the catchment outlet at 1100 m.a.s.l. (Figure 4.1).

Water level at the main stream gauging station was measured with a capacitance water level sensor (Trutrack WT-HR®) at a time resolution of 3 - 10 minutes. As bedload transport is too high for the use of weirs, a natural cross-section had to be used. Discharge measurements to establish a rating curve were carried out with a current meter or salt dilution. The same method was used for the other stream gauging stations (Figure 4.1).

The groundwater observation well W1 in close vicinity to the main stream gauging station (12 m distance to the stream) was equipped with the same type of water level sensor. For exact location see chapter 3. Water levels were measured with 10 minute resolution. The well consists of a PVC tube 5 cm in diameter, installed to a depth of 260 cm. The tube is slotted over the lowest 100 cm. A second well was installed in similar fashion close to the stream gauging station at S2 (Figure 4.1).

Soil moisture was measured along two transects with FDR (frequency domain reflectometry) profile probes in 10, 20, 30, 40, 60 and 100 cm depth. Both transects are located close to the main stream gauging station. 3 profile probes were connected to a datalogger and were measuring continuously. A fourth probe was used for manual measurements (irregular time intervals) at 11 points along the transects. More details on the experimental set-up can be found in chapter 3.

4.4.2 Hydrograph separation with isotopes and geochemical tracers

Environmental stable isotopes such as Deuterium or Oxygen-18 are present in varying concentrations in rainwater as well as groundwater and can even vary highly from one rainstorm to the other at a given site. If the difference in isotopic composition of the so called event and pre-event water is sufficiently high, this can be used to separate between fractions of old and new water present in the stream during an event and thus be used for a two-component hydrograph separation. The same applies for other geochemical constituents as long as they essentially behave conservatively.

Samples taken during the rainfall events of February 16^{th} and December 3^{rd} 2004 (rainfall and discharge) as well as baseflow samples taken a few days prior to the rainfall event were analysed for Deuterium.

Electric conductivity of stream water as an indicator of total ion concentration was measured continuously during field campaigns, while all other parameters such as the major cations and anions as well as nitrate, phosphate, and silicate were analyzed in the laboratory. Samples were taken from stream water, rain water, throughfall, snow, soil water, and groundwater at irregular intervals to get an impression of typical composition of the different compartments as well as the variability of concentrations. During five rainfall events stream water samples were taken in half hour to hour intervals with an automatic sampler while soil water, rainfall and throughfall were sampled as bulk samples. However, only 2 of these events could be used for hydrograph separation. The three other events turned out to be too small (water level change of less than 1.5 cm, increase in discharge of only 0.06 m^3/s (16%), 0.03 m^3/s (10%) and 0.04 m^3/s (12%)) to show a significant change in stream chemistry. The data of the two larger events (in Feb. and in Dec. 2004) were used to conduct a simple hydrograph separation (Eq. 4.3). Areal precipitation estimated with the Thiessen polygon method amounted to 57.6 mm for the February event and 26.2 mm for the December event. Thiessen polygons were used because no clear correlation of precipitation with altitude could be established. Event runoff coefficients were 0.02 and 0.04, respectively. These runoff coefficients were determined with a straight line hydrograph separation combined with a cut-off criterion for the endpoint of event flow (chapter 2).

4.4.3 Thermal energy as a tracer

To investigate groundwater-surface water interactions, temperature dynamics of stream and groundwater at the main stream gauging station (S1) were analyzed. Instead of measuring temperatures in the sediment below the stream bed, data from a nearby observation well (well W1) were used for the groundwater component. The distance between well and stream is 12 m. For exact location of the well see chapter 3. The temperature in stream bed sediments was difficult to measure as the stream bed consists mainly of stones and boulders. Using groundwater temperature implies that measuring the effects of cases a) groundwater discharge and b) no interaction (see Section 4.5.3) will not be possible.

The water level sensors installed at the stream gauging station and in the observation well measured water temperature at a time resolution of 3-10 minutes with a thermistor located at the lower end of the probe. The temperature was measured with a precision of 0.3°C. Cross correlation and time lag analysis of groundwater and stream temperatures were then used to investigate the interactions between groundwater and surface water.

4.4.4 Dye tracer experiments

In order to get a visual impression of the infiltration/percolation characteristics of the catchment, 10 tracer experiments were carried out (9 under forest, close to stream gauging stations S1, S2 and S5, one on bare volcanic ashes, see Figure 4.1). For all experiments Brilliant Blue was used with a concentration of 4 g/l. 30 liters of the dye were applied to an area of 1.2 m^2 over a period of 3-4 hours. This corresponds to a total of 25 mm at application rates between 6 and 8 mm/h. The dye was applied with a hand pressurized pesticide sprayer in order to simulate rainfall. For one experiment two directly neighbouring plots were sprayed with dye, the second plot with twice the amount (60 l) and more than twice the application rate (20 mm/h compared to 8.3 mm/h). Soil profiles were excavated the following day and photographs of the dye pattern were taken with a digital camera. Image analysis included the extraction of the hue component of the image (HSB channels) followed by a further increase of contrast by adjusting the tone curve and thus producing a grey shade image with stained areas appearing light grey or white and non stained areas appearing dark. Recitification of the image was possible for photos where the grid scale was included. Percentage of dye coverage for each depth was also determined.

4.5 Results

4.5.1 Rainfall and discharge

Mean annual discharges in the Malalcahuello catchment were 0.43 m^3/s in 2004 and 0.46 m^3/s for 2005. Maximum discharges for these years were 3.76 and 4.17 m^3/s, respectively. Temporal resolution of the measurements was 5 or 10 minutes, depending on the observation period.

The annual runoff coefficient was 63% for the year 2004 and 77% for 2005, with rainfall amounts of 3640 and 3040 mm, respectively (measured at the catchment outlet) (chapter 3). Event runoff coefficients are low and lie between 1 and 10% for the 17 events analyzed in 2004/2005, of which a third are smaller than 2%. Baseflow separation was carried out with a horizontal straight line, for the determination of the endpoint of the event see chapter 2 . Response time (time between onset of rainfall and first response of streamflow) is generally fast: less than an hour for 11 out of 17 events, less than half an hour for 6 out of 17 events. Maximum hourly rainfall intensities were $>$ 20 mm/h for 3 out of 17 events (chapter 2).

4.5.2 Hydrograph separation

The rainfall events in February and December 2004 produced strongly different responses of

stream chemistry and thus also in hydrograph separation. The major cations (Na^+, K^+, Mg^{++}, Ca^{++}) show a clear response to rainfall in December, but not in February (the grey polygons in Figures 4.2 and 4.3 span the fractions of pre-event water calculated with these constituents). For the February event, old water fractions of more than 100% were calculated by using the cations Na, K, Mg and Ca as tracers (Figure 4.2). This suggests that processes not captured by the simple two component approach are of importance during the dry season.

SiO_2 can give an indication as to the contact or residence time of water within the catchment (Uhlenbrook et al., 2002), i.e. the longer the contact time the higher the concentration of SiO_2. High silicate concentrations in baseflow in February thus suggest that relatively „old" water is now leaving the catchment. These high SiO_2 concentrations are strongly diluted during event response, indicating that younger water is now transported into the stream by faster flow paths. The December concentrations in SiO_2 are much lower (20 mg/l instead of 29 mg/l) and no clear response to rainfall could be observed (Figure 4.3).

Deuterium, the only really conservative tracer used in this study, also shows two different responses: in February the minimum of pre-event water is delayed compared to the main peak in discharge, while the minimum coincides with the peak(s) in flow in December.

Electric conductivity (EC), while not being a conservative tracer nevertheless has the advantage that it can be measured continuously and in-situ. Fractions of pre-event water calculated with EC show a distinct but weak response in February with a minimum of 90% (Figure 4.4). Minima of pre-event fractions calculated with both SiO_2 (28%) and deuterium (62%) are much lower (Figure 4.2). In December, the major cations (grey polygon in Figure 4.3), deuterium and EC show a similar response, producing minima of pre-event water of 86% (Na^+) to 94% (Ca^{++}). Note that the scale of the axis for the fractions of old water was adjusted for each of the figures 4.3, 4.4 and 4.2 in order to give a better impression of the dynamics.

4.5.3 Thermal energy as a tracer

Ground water levels at well W1 close to S1, the main stream gauging station, are generally low, about 200 cm below the soil surface and about 100 cm below the stream bed. This well is located at 12 m distance from the stream. Groundwater levels lower than the neighbouring stream were also observed at a second well located next to the lower reach at S2 (Figure 4.1). The direction of the hydraulic gradient thus makes it likely that water exfiltrates from the stream at this point. This hypothesis is further supported by an analysis of stream and groundwater temperature dynamics at the main stream gauging station during a two-month period in the late summer of 2004. During this period, episodes of warm weather alternated with episodes of cool weather. These changes in air temperature clearly influence stream water temperatures (Figure 4.5). While for the stream water temperatures we also see daily oscillations, this cannot be found for groundwater temperature. However, groundwater temperatures also show temporal variability, oscillating not on a daily basis but over a period of several days. Whether these dynamics are correlated to the episodes of warmer and cooler days also visible in the stream water temperatures was tested with cross-correlation and time lag analysis of groundwater and stream temperatures. It was found that the groundwater temperature signal follows the stream temperature signal with a time lag of 55 hours. This correlation is significant with a coefficient of 0.77 (Figure 4.6).

Average flow velocity from the stream to the observation well W1 was calculated using the 55 hour time lag between temperature peaks as travel time and the distance between stream and well as travel length (12 m). The estimated flow velocity amounts to $6*10^{-5}$ m/s. Combining this with the average difference in hydraulic head of

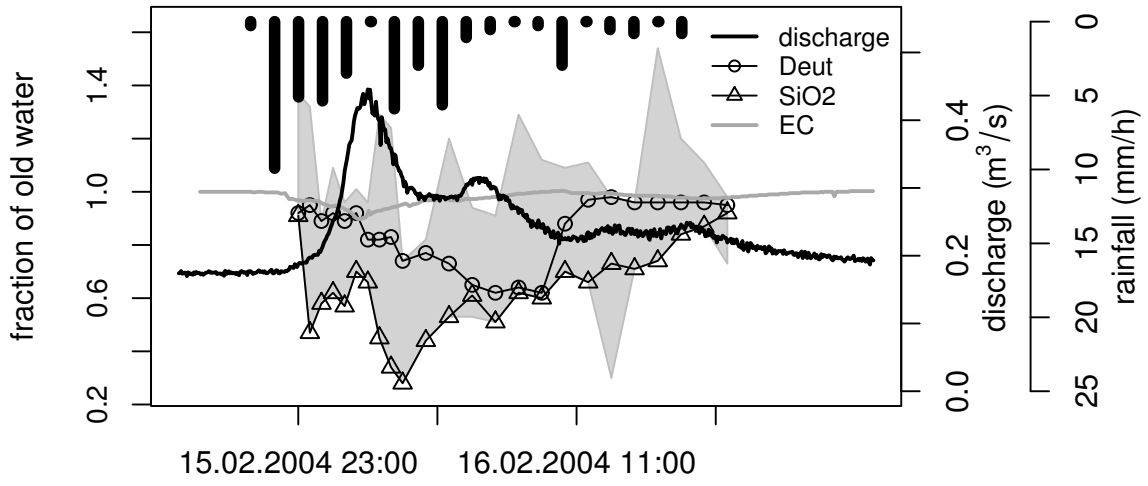

Figure 4.2: Event February 2004. Hydrograph, precipitation and fractions of pre-event water calculated with a variety of different tracers. The grey polygon spans the fractions of pre-event water calculated with Na^{+}, K^{+}, Mg^{++} and Ca^{++}.

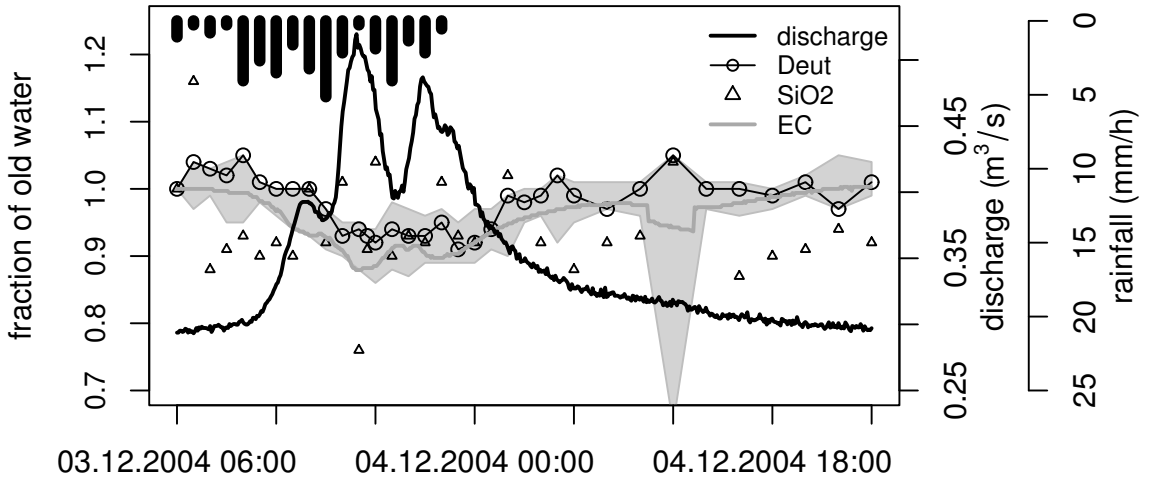

Figure 4.3: Event December 2004. Hydrograph, precipitation and fractions of pre-event water calculated with a variety of different tracers. The grey polygon spans the fractions of pre-event water calculated with Na^+, K^+, Mg^{++} and Ca^{++}. The extremely low value at 12 am on December 4^{th} (K^+) is probably due to measurement problems.

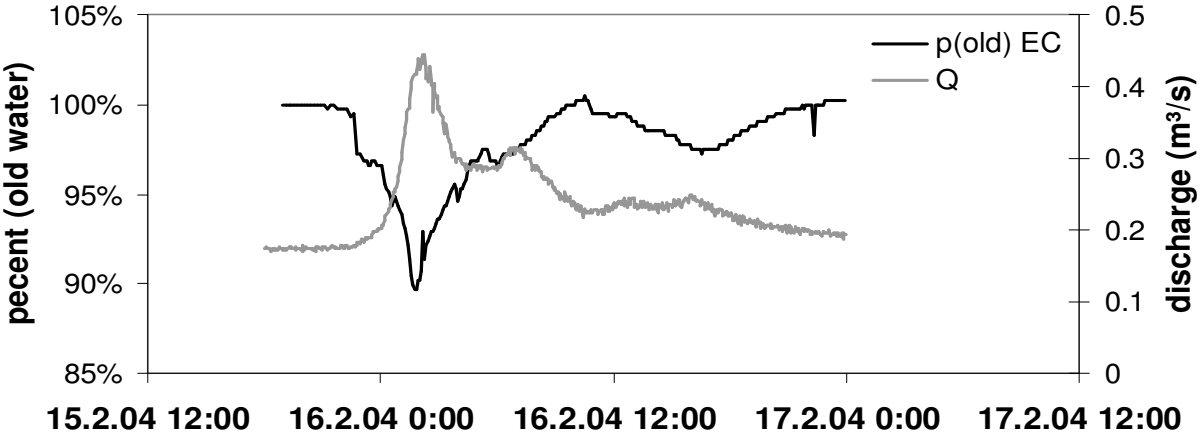

Figure 4.4: Event in February 2004. Hydrograph and fraction of pre-event water calculated using electric conductivity as a tracer (Eq. 4.3).

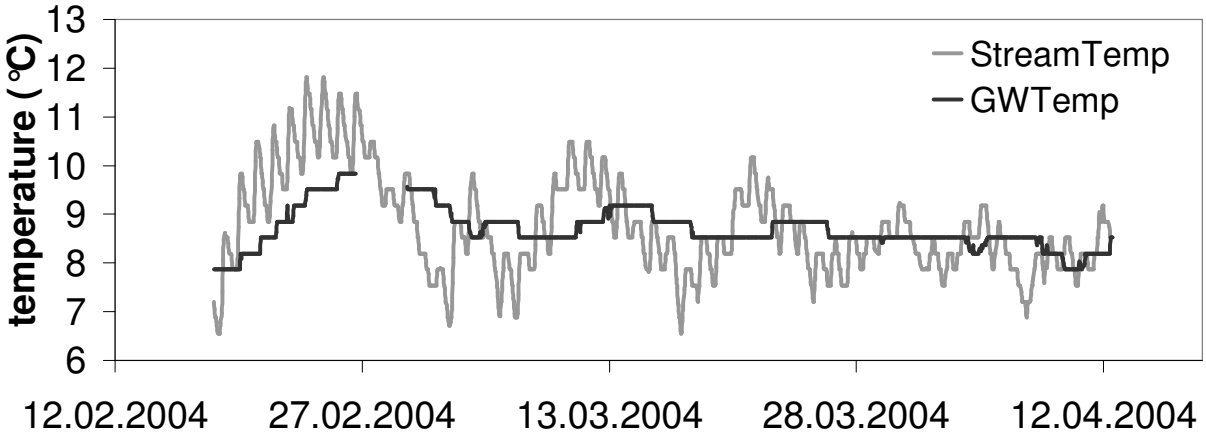

Figure 4.5: Stream water and groundwater temperatures during 8 weeks of fall 2004.

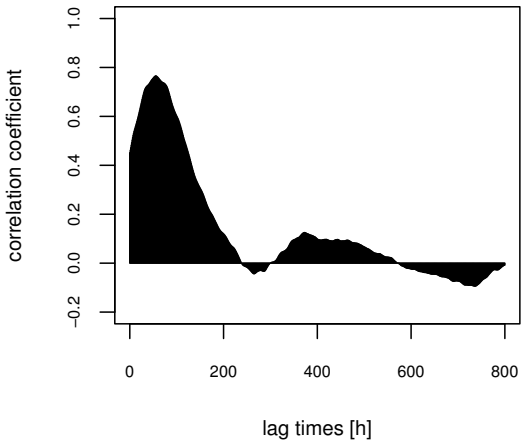

Figure 4.6: Cross-correlation and time lag analysis of groundwater and stream temperatures. The groundwater temperature signal follows the stream temperature signal with a time lag of 55 hours.

1.2 m (estimated from ground and stream water levels) over the distance of 12 m allows us to estimate the hydraulic conductivity. However, we also need to include the porosity of the medium (Eq. 4.5 and 4.6), as we do not need the actual average velocity of the groundwater (U_x) estimated with the tracer, but the Darcy velocity or flux (V_x) in order to calculate hydraulic conductivity (Dingman, 2002).

$$V_x = U_x * n \tag{4.5}$$

$$Ksat_x = V_x * \frac{dx}{dh} \tag{4.6}$$

(V_x is Darcy velocity, $Ksat_x$ is saturated hydraulic conductivity, dh is difference in head, dx is travel length, U_x is actual groundwater flow velocity (pore velocity) and n is porosity). As we do not have measurements of the porosities between stream and observation well, we use the minimum and maximum of porosity determined for soil cores in the laboratory: 56% and 82%. We thus estimate the Darcy velocity with 3.4*10^{-5} – 5*10^{-5} and the hydraulic conductivity with 3.4*10^{-4} – 5*10^{-4} m/s. This is very close to the average hydraulic conductivity measured in the laboratory

for 42 samples of the upper 45 cm of the soil ($5.63*10^{-4}$ m/s).

To ascertain that these temperature effects are not the result of pure thermal conduction within the soil, the damping depth (Eq. 4.4) was calculated. For thermal diffusivity a typical value for fresh sandy soil of $0.24*10^{-6}$ m^2/s was assumed (Arya, 2001). It was found that a temperature oscillation of 20°C (air temperature) would be reduced to an oscillation of 0.1°C at a depth of 1.5 m. As groundwater levels are below 2 m and the groundwater temperature oscillation is almost 2°C, the variation in groundwater temperature is attributed to advective heat transport of water exfiltrating from the stream.

From the time series of discharge, groundwater level, and stream, groundwater and air temperatures (Figure 4.7) three events with unusual temperature dynamics have been extracted. The first event (B), in April 2004, shows a sudden and fast decrease in groundwater temperature (faster than the decrease in stream temperature). At the same time groundwater levels rise above the estimated elevation of the stream bed (Figure 4.8). Events C and D, both in June 2004, exhibit a sudden increase in groundwater temperature without prior increase in stream temperature (Figure 4.8). Groundwater temperatures for all events stabilize at 6.2-6.5°C. All temperature changes are preceded by high peaks in groundwater level (Figure 4.8). This indicates a sudden change in groundwater flow. Groundwater in this well seems no longer dominated by exfiltrating stream water, but by lateral influx of groundwater with a temperature of about 6.5°C. A possible explanation is that during these events the hillslope at this point is now contributing groundwater. This hypothesis is further supported by data from a well further up this slope which was installed in November 2004 (well W5, for exact position see chapter 3). Groundwater levels at this well do not react during smaller events, however, during several events of the same magnitude as events C and D there was a strong, but delayed response, with lag times of about 40 hours (chapter 3). A rising groundwater table at this point coincided with rising groundwater temperatures at well W1, thus also suggesting a connection between slope groundwater and groundwater close to the stream (Figure 4.9). The second, strongly delayed peak in well W5 might also be the reason for the strongly dampened recession in well W1 during this time. For more information on groundwater dynamics at this slope see chapter 3.

4.5.4 Dye tracer experiments

10 dye tracer experiments were carried out between January 2004 and December 2005. 9 of the experimental plots were located in forest. An overview of all experiments is given in table 4.1. It was found that that flow patterns differed significantly between experiments carried out in late summer or fall and experiments carried out in late winter/spring. The late winter/spring experiments showed flow patterns which could be described as an infiltration front down to a depth of 10-15 cm followed by a breaking up of this front into several preferential pathways („comb"-pattern). The flow pattern of the 3 late summer/fall experiments showed narrow flow paths in the top 15 cm which then ended in wider plumes at greater depths („frying pan"-pattern). An example for both types of flow patterns is given in Figure 4.10. Figure 4.10A shows a typical flow pattern of a dye tracer experiment in spring (17.11.04). Maximum infiltration depth is 50 cm. Soil moisture content was relatively high (see Table 4.1). The plot of dye coverage with depth on the right shows that dye coverage is highest in the top layer and decreasing with depth. Figure 4.10B shows a typical flow pattern of a dye tracer experiment in late summer (10.02.04). Maximum infiltration depth is 80 cm. Soil moisture content was relatively low (Table I). The plot of dye coverage is also distinctly different compared to Figure 4.10 A: the zone of highest dye coverage is here found in a depth of approximately 30 cm. Both experiments presented in Figure 4.10 were carried out on the same slope,

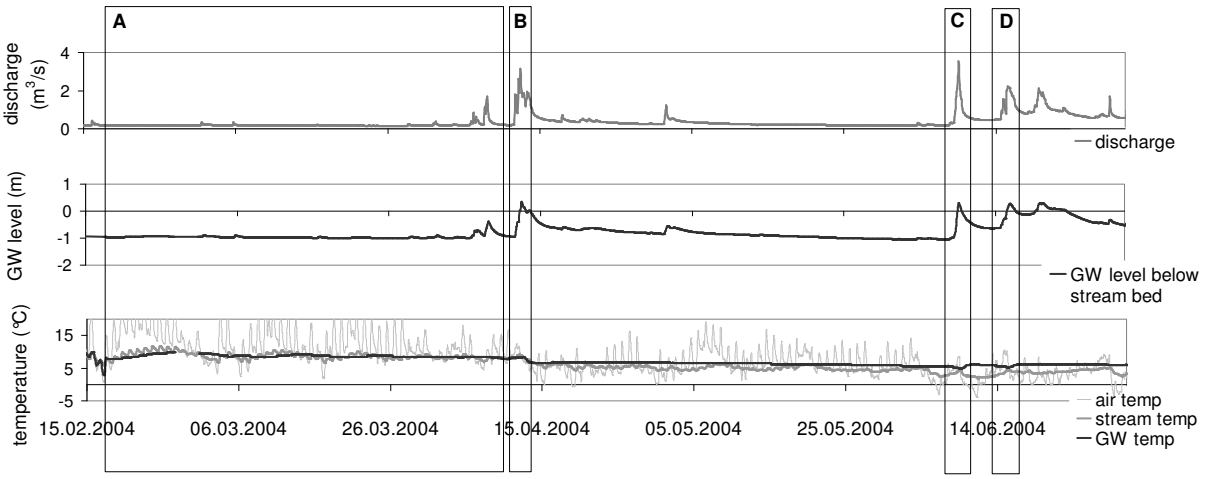

Figure 4.7: Time series of discharge (m^3/s), Groundwater level (well W1) in relation to the stream bed (m), and stream, groundwater and air temperatures. Box A shows the period used for the lag time analysis, box B, C and D are events of sudden changes in groundwater temperature.

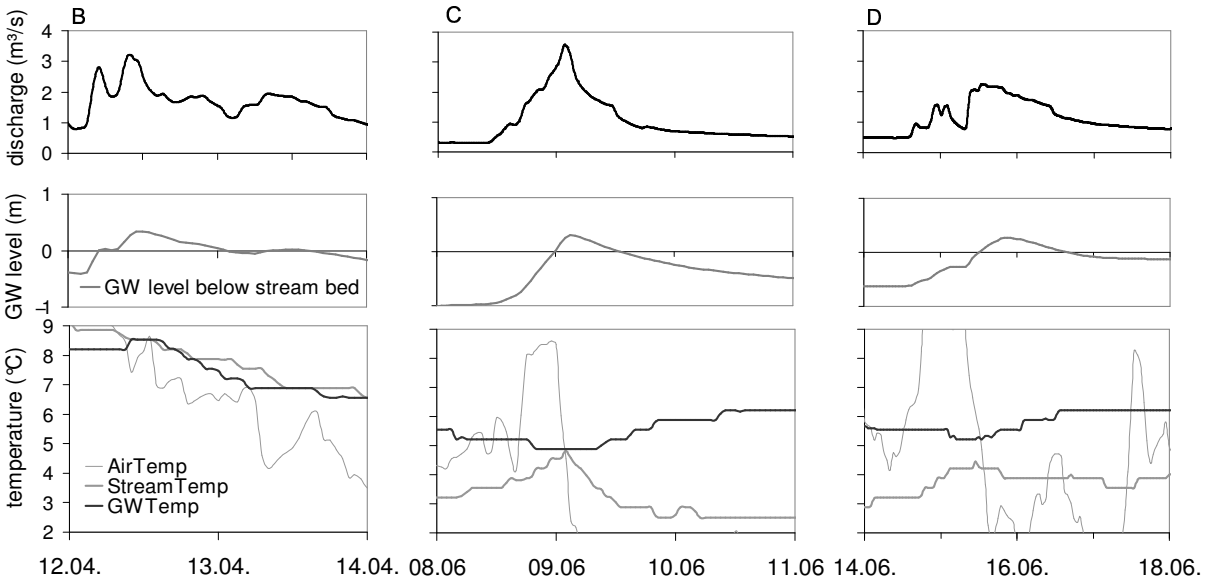

Figure 4.8: Groundwater, stream water and air temperatures as well as groundwater levels (well W1) and stream discharge for three events in April and June 2004. Groundwater temperatures decrease faster than stream water temperatures during event B. For events C and D we observe a sudden increase in groundwater temperature without prior increase in stream temperature. (Temperatures change stepwise due to a measurement resolution of 0.3°C).

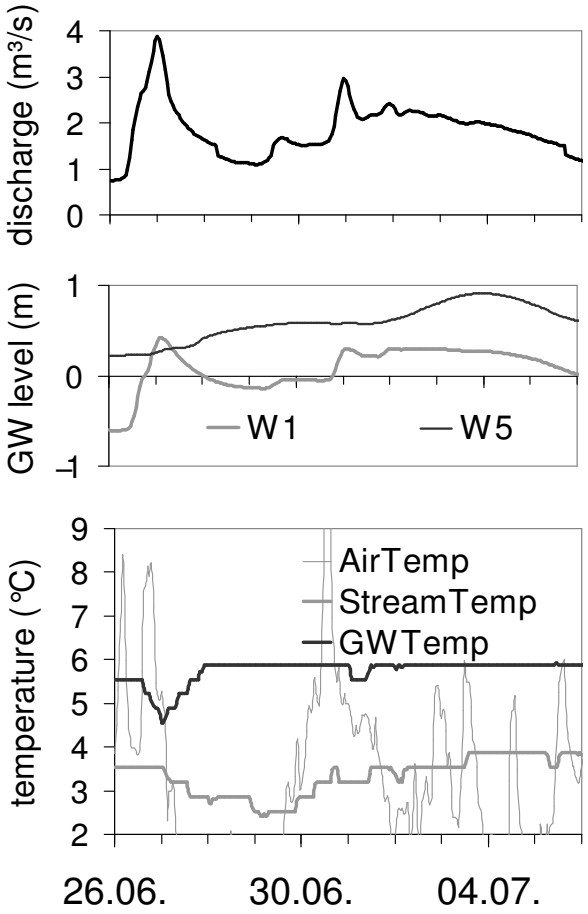

Figure 4.9: Groundwater (well W1), stream water and air temperatures as well as groundwater levels and stream discharge for an event in June/July 2005. With rising groundwater levels there is first a drop and then, as in June 2004, a sudden increase in groundwater temperature of well W1 without prior increase in stream temperature. Groundwater levels are shown for well W1 and well W5 (black line). The response of W5 is delayed and dampened compared to W1.

close to the main stream gauging station (for location see Figure 4.1). As antecedent moisture conditions are likely to have an influence on subsurface flow, soil moisture content was measured manually at irregular intervals at 11 points along the slope and continuously at three locations since November 2004 (details in chapter 3). Comparison of soil moisture for the different experiments is difficult as for some experiments we have only the manual measurements (11 points) and for other experiments we have only the data from the continuously measuring sensors (3 points). Soil moisture for the summer experiments was generally lower (21-22 Vol% at 10 cm depth; average of 11 points), while it is higher (31-32 Vol%; average of 3 points) during the spring experiments.

The dryness of the top layer during the three summer experiments might cause increased water repellency in this layer, which in turn might be the explanation for the narrow flow paths in the upper horizon. Similar flow patterns were described in Ritsema et al. (1993, 1998) and de Rooij GH. (2000), where hydrophobicity of the top layer caused finger flow until these fingers diverged in the wettable subsoil. Ritsema et al. (1998) also argue that fingers are likely to be fixed in place for soils under permanent plant cover and that water repellency is most prominent in dry soils. Hydrophobicity has indeed been observed in air dried samples of the upper forest soil horizons in the Malalcahuello Catchment. Using the „Water Drop Penetration Time" test (Dekker & Ritsema, 1994), potential hydrophobicity in the upper horizons was found to be strong to extreme for the 4 sampled locations (chapter 5) . The fact that few macropores have been found in these upper horizons further supports the theory that fingering as a consequence of water repellency is the main transport mechanism here, sometimes enhanced by flow along roots.

The experiments on 19.11.04, where two directly neighbouring plots were sprayed with different amounts and intensities showed that the maximum infiltration depth was higher for the high in-

Table 4.1: Overview of 10 dye tracer experiments carried out in 2004 and 2005. Soil moisture data marked HH are manual measurements, while the data marked CL is data from the sensors that are logging continuously. Soil moisture is given for 3 depths: 10, 20 and 30 cm. The flow patterns „comb" and „frying pan" are described in the text. Examples can be seen in Figure 4.10. On February 16^{th}, 2004 an additional 45.6 mm of rain water infiltrated after application of the dye and before excavation of the profiles. Maximum distance down-slope signifies the distance the dye travelled downhill measured from the lower boundary of the plot.

date	**05.01.04**	**10.02.04**	**13.02.04**	**16.02.04**	**05.11.04**	**17.11.04**	**19.11.04-I**	**19.11.04-II**	**12.02.04**	**08.12.05**
location	forest S1	forest S1	forest S2	forest S1	forest S1	forest S1	forest S1	forest S1	above tree line	forest S5
mean soil moisture (Vol%)	HH 10 cm: 26 20 cm: 30 30 cm: 30	HH 10 cm: 23 20 cm: 27 30 cm: 28	HH 10 cm: 23 20 cm: 25 30 cm: 27	HH 10 cm: 23 20 cm: 27 30 cm: 30	HH/CL 10 cm: 30/32 20 cm: 35/32 30 cm: 32/25	CL 10 cm: 31 20 cm: 31 30 cm: 25	CL 10 cm: 31 20 cm: 30 30 cm: 25	CL 10 cm: 31 20 cm: 30 30 cm: 25	unknown	unknown
amount of application	25 mm	25 mm	25 mm	25+45.6 mm	16,7 mm	25 mm	25 mm	50 mm	24 mm	25 mm
intensity of application	6,25 mm/h	8,3 mm/h	7,1 mm/h	6,25 mm/h	4,2 mm/h	8,3 mm/h	8,3 mm/h	20 mm/h	9,1 mm/h	7.9 mm/h
flow pattern	„comb"	„frying pan„	„frying pan„	„frying pan„	„comb"	„comb"	„comb"	„comb"	front	„comb"
max. depth of infiltration	50 cm	80 cm	50 cm	113 cm	35 cm	50 cm	50 cm	100 cm	7 cm	46 cm
max. distance down-slope	ca. 20 cm (no cover)	30 cm (no cover)	20 cm (no cover)	20 cm (no cover)	0 cm (covered)	0 cm (covered)	25 cm (covered)	55 cm (covered)	0 cm (no cover)	0 (covered)

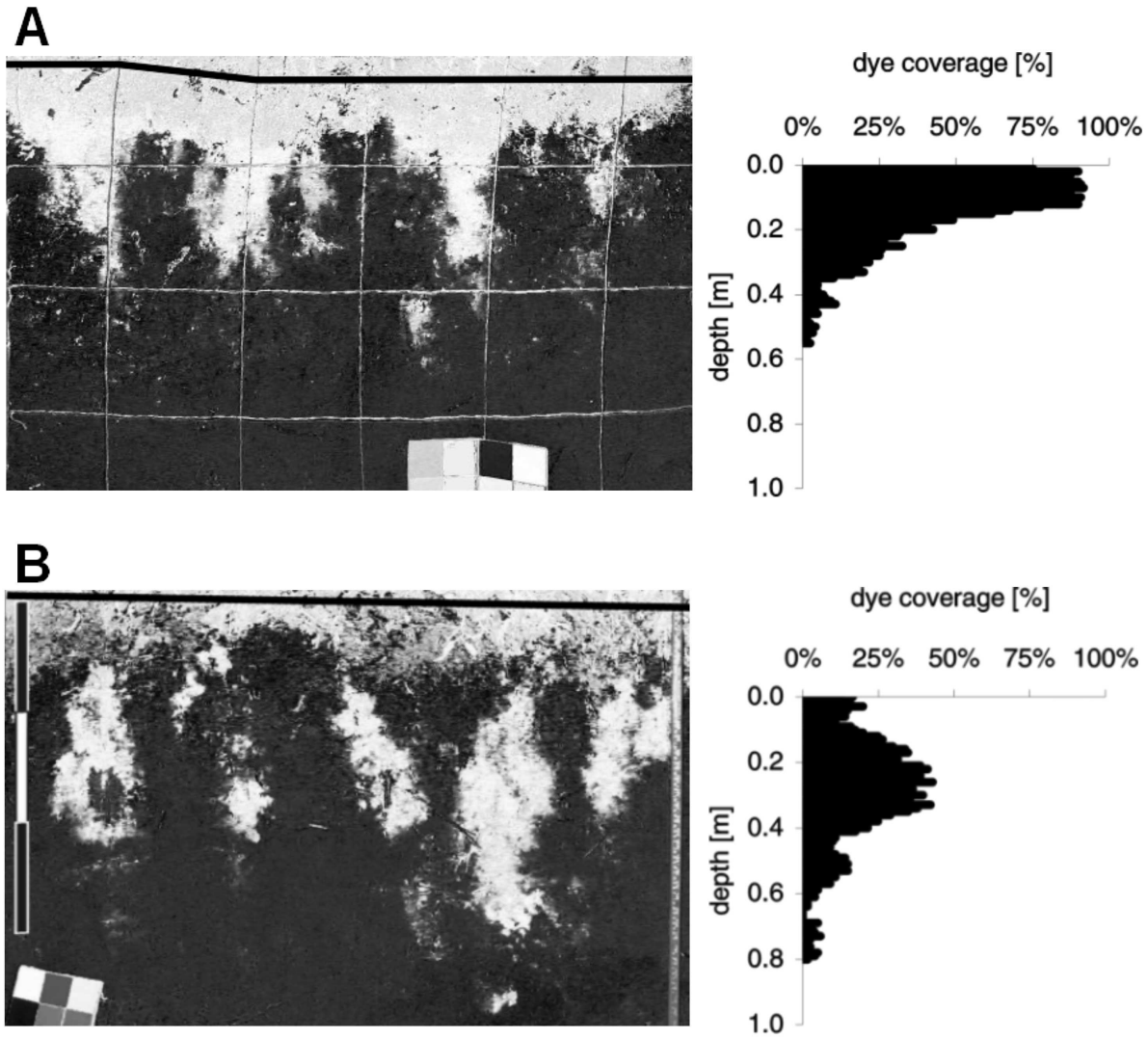

Figure 4.10: Flow patterns and dye coverages for two experiments on forest plots. A) Typical flow pattern of a dye tracer experiment in spring (17.11.04). The grid consists of 20 cm by 20 cm squares. The black line indicates the soil surface. B) Typical flow pattern of a dye tracer experiment in late summer (10.02.04). One unit on the scale bar corresponds to 20 cm.

tensity experiment: 100 cm compared to 50 cm (Table 4.1). This experiment was carried out in late winter 2004 and also exhibits the late winter/spring pattern. Interestingly, it was also found that lateral down-slope transport occurred in the duff layer (layer of decomposing litter) during the high intensity experiment. This was found after removing the litter layer. Maximum downhill transport length was 55 cm from the lower border of the experimental plot. The area down-slope of the plot had been covered with a plastic sheet during the experiment to avoid contamination, due to wind blown dispersal of the dye during spraying.

The experiment carried out on bare volcanic ashes at the catchment rim (for location see Figure 4.1) showed a very different flow pattern. Here, the dye infiltrated as a straight front, no preferential flow occurred (Figure 4.11). The maximum infiltration depth of the dye was only 7 cm.

Fingering in bare sands is possible, either due to air entrapment, increasing conductivity with depth (de Rooij, 2000), or even non ponding rainfall (Selker et al., 1992). However, preferential flow as fingering is often initialised by redistribution of water in the top soil layer due to microtopograpy or small scale difference in degree of water repellency (redistribution flow) (Ritsema & Dekker, 1995). It can also be the result of prior redistribution of rainfall by canopy or litter, leading to preferential flow in places receiving more water (Ritsema & Dekker, 1995). Furthermore, hydrophobicity increases with organic matter content (Dekker & Ritsema, 1994). As organic matter content of the bare ash soil is low, soils are likely to be less water repellent than under forest. In conjunction with the fact that there is no considerable microtopograpy or redistribution of dye/rainfall by canopy or litter on the bare soil this might explain the absence of finger flow at this site and the difference in flow patterns when compared to the forested locations.

4.6 Summary and Conclusions

Tracer experiments were carried out at three different spatial scales in order to investigate runoff generation processes. Hydrograph separation was used to study runoff generation at the catchment scale. Stream and groundwater temperatures were used to investigate groundwater-surface water interactions at the local stream reach scale. Dye tracer experiments were carried out to investigate infiltration and percolation processes at the plot scale.

The results are summarized moving top down in scales:

Hydrograph separation for the December event shows that pre-event water is dominating runoff generation. Throughout the event the fraction of pre-event water remains $> 85\%$.The different response of the tracers (especially of SiO_2 and deuterium), and the fact that fractions of pre-event water of more than 100% occur during the February event, suggest a shift in processes from late summer to early spring (or dry to wet season). Processes not captured by this simple approach are likely to be of importance during the dry season (Figure 4.2), where probably one or more additional flow components are influencing stream chemistry during the event. The strong response of silicate in February suggests fast flow paths, which were not activated during the December event.

The analysis of stream and groundwater temperatures shows that stream water normally exfiltrates to the groundwater in the vicinity of the main stream gauging station (S1). Travel times from the stream to the observation well (W1), a distance of 12 m, are estimated to be 55 hours. On three occasions at high water levels groundwater is no longer dominated by exfiltrating stream water but by lateral groundwater influx. Rising groundwater table at well W5, further upslope, coincided with rising groundwater temperatures at well W1, thus also suggesting a connection between slope groundwater and groundwater close to the stream during large events (Figure 4.9).

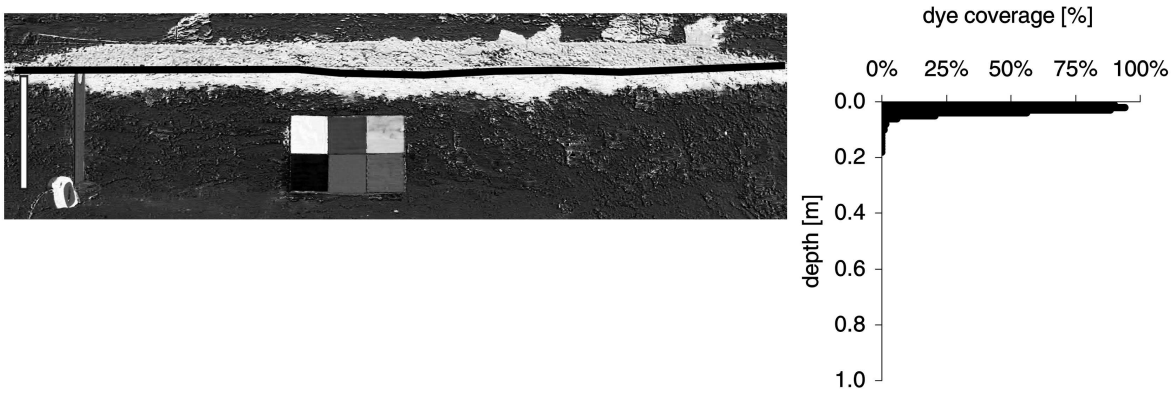

Figure 4.11: Infiltration experiment on unvegetated volcanic ashes: flow patterns and dye coverage. The white scale bar on the left has a length of 20 cm and the black line indicates the soil surface.

However, groundwater-surface water interactions are likely to be highly variable in space and might be different from one stream reach to the next, depending on the geology and topography of the stream bed. Furthermore, annual runoff coefficients are high with around 70% and the remaining 30% are in range of potential evaporation measured with an evaporation pan (chapter 3). The nearly closed water balance suggests that losses to deep groundwater and losses due to groundwater outflow out of the catchment are of minor importance. A survey of stream and stream bed sediment temperatures at times of high temperature gradients between surface and groundwater could provide information on the spatial distribution and relative importance of losing and gaining stream reaches.

Nevertheless, the results of hydrograph separation (high fraction of old water) and the lag times of at least several hours between surface water and groundwater response (chapter 3 and chapter 5) appear contradictory. This is along the same lines as the „old water paradox" described by Kirchner (2003). A possible explanation is the replacement and resulting rapid down-slope transport of old water (having a similar chemical signature as groundwater) in zones of lateral preferential flow along layer interfaces. This would correspond to piston flow within a perched saturated zone. Torres et al. (1998); Williams et al. (2002) and Rasmussen et al. (2000) describe the phenomenon of kinematic wave response in the unsaturated zone leading to response velocities much faster than pore water velocities.

Flow pathways studied with dye tracer experiments at the plot scale differ significantly between forested areas (preferential flow) and the barely vegetated volcanic ashes (no preferential flow). While preferential flow occurs at all plots under forest, water infiltrates as horizontal front at the plot on bare volcanic ashes. Flow patterns of preferential flow at the forest plots change significantly from summer to winter. Water infiltrates as a front which later breaks up into several pathways during winter. During summer water infiltrates along narrow pathways in the top 15 cm and forms separate bulb like plumes at greater depth. As the top layer was very dry during the three summer experiments, this pattern can be explained by hydrophobicity in the upper horizon (chapter 5). The narrow flow paths observed during the summer experiments are likely to transport rainwater faster to greater depths than the flow patterns observed during the wet season. This could explain the shorter response times observed in soil-, ground- and streamwater during summer (chapter 5). The high spatial variability of

throughfall observed in the Malalcahuello Catchment (chapter 3) is likely to increase preferential flow as areas of higher moisture content will have higher unsaturated conductivities. The spatial heterogeneity of throughfall will furthermore also increase the spatial heterogeneity of hydrophobicity. When dye was applied with higher application rates, lateral flow down-slope was observed, mainly within the duff layer. This observation was made during a late winter experiment. It is thus likely that this effect will be further increased by hydrophobicity of the top soil layer in dry summer periods. Interflow along this layer interface might have been an important flow path/flow component with a distinct chemical signature during the event in February 2004 when the 2 component hydrograph separation yielded inconclusive results. In case of clear-cutting the forest hydrophobicity of the top layer is likely to increase, due to lack of shade and therefore increased drying of this layer. Clear-cutting could thus further enhance fast lateral processes or even cause surface runoff. However, in case of surface runoff erosion of the hydrophobic layer would soon again increase infiltrabilities.

With respect to the whole catchment, observations made at the plot scale yield valuable information for a better understanding of observations made at the catchment scale, i.e. the hydrograph separation. It seems a viable assumption that preferential flow patterns found in all 9 dye tracer experiments under forest are typical for these forest soils in general. The importance of these flow patterns for catchment runoff generation, however, depends on the connectivity of lateral preferential flow paths. Lateral flow, probably at layer interfaces, might thus be causing the fast response of stream flow during events, while the catchment is dominated by deeper groundwater flow systems the rest of the time. At the local stream reach scale, flow reversal observed in groundwater-surface water interactions and increased contribution of groundwater from the slope only occurred in the midst of winter, when weather conditions make additional field investigation impossible. It is therefore not possible to investigate if flow reversal is only of local importance or if it is also influencing runoff generation at the catchment scale. Both, groundwater flow reversal/temporary groundwater contribution by the slopes at the main stream gauging station as well as the development of hydrophobicity with drying are likely to be threshold processes controlled by antecedent conditions in the catchment, i.e. soil moisture or groundwater levels (Zehe et al., 2007).

All three approaches used in this study suggest an important shift in dominant processes from dry to wet season: a) a large fraction of pre-event flow during the late winter event and the failure of the two component hydrograph separation in summer, suggesting the importance of additional, so far not included components, b) stream water exfiltration in the lower reaches under normal conditions and flow reversal during periods of high groundwater levels, c) vertical preferential flow in the forested areas (80% of the catchment) and hydrophobicity during the dry months in summer and autumn, which further reinforces preferential flow. However, some details of catchment functioning are still not clearly understood (e.g. what produces the fast reaction of pre-event water during rainfall events and how „old" is this pre-event water) and will need to be investigated further. In a next step, the perception of runoff generation gained in the experimental study will be tested with a physically based model.

Acknowledgements

The authors would like to thank Andreas Bauer, Dominik Reusser (Potsdam University) and Hardin Palacios, Luis Opazo (Universidad Austral de Chile) for help in the field, Prof. Andrés Iroumé and Prof. Anton Huber (Universidad Austral de Chile) for logistic and technical assistance. We are also thankful to Hanno Meyer from the Isotope Laboratory of the Alfred Wegener Institute,

Potsdam, for his help with the isotope analysis. Thanks also to two anonimous reviewers, whose comments and suggestions significantly improved an earlier version of this manuscript. This work was partially funded by the International Office of the BMBF (German Ministry for Education and Research) and Conicyt (Comisión Nacional de Investigación Científica y Tecnológica de Chile) and the „Potsdam Graduate School of Earth Surface Processes", funded by the State of Brandenburg.

Chapter 5

Use of soil moisture dynamics and patterns for the investigation of runoff generation processes with emphasis on preferential flow *

Abstract

Spatial patterns as well as temporal dynamics of soil moisture have a major influence on runoff generation. The investigation of these dynamics and patterns can thus yield valuable information on hydrological processes, especially in data scarce or previously ungauged catchments. The combination of spatially scarce but temporally high resolution soil moisture profiles with episodic and thus temporally scarce moisture profiles at additional locations provides information on spatial as well as temporal patterns of soil moisture at the hillslope transect scale. This approach is better suited to difficult terrain (dense forest, steep slopes) than geophysical techniques and at the same time less cost-intensive than a high resolution grid of continuously measuring sensors. Rainfall simulation experiments with dye tracers while continuously monitoring soil moisture response allows for visualization of flow processes in the unsaturated zone at these locations. Data was analyzed at different spacio-temporal scales using various graphical methods, such as space-time colour maps (for the event and plot scale) and indicator maps (for the long-term and hillslope scale). Annual dynamics of soil moisture and decimeter-scale variability were also investigated. The proposed approach proved to be successful in the investigation of flow processes in the unsaturated zone and showed the importance of preferential flow in the Malalcahuello Catchment, a data-scarce catchment in the Andes of Southern Chile. Fast response times of stream flow indicate that preferential flow observed at the plot scale might also be of importance at the hillslope or catchment scale. Flow patterns were highly variable in space but persistent in time. The most likely explanation for preferential flow in this catchment is a combination of hydrophobicity, small scale heterogeneity in rainfall due to redistribution in the canopy and strong gradients in unsaturated conductivities leading to self-reinforcing flow paths.

*Theresa Blume, Erwin Zehe, Axel Bronstert (2007), *Hydrology and Earth System Sciences - Discussions*, 4, 2587-2624

5.1 Introduction

Identification of patterns of soil moisture response to rainfall and especially the vertical dynamics of soil moisture at the hillslope or plot scale can be useful for the investigation of runoff generation processes in a previously ungauged or data scarce catchment. When investigating runoff generation processes in a previously ungauged catchment it becomes obvious from the start that the equipment we are about to install is insufficient. There will be neither enough data points in time nor in space to characterize these processes in their temporal and spatial variability. A possible way to overcome this problem is the approach where a multitude of experimental methods is applied within a relatively short time frame, producing a data set that highlights a multitude of angles and aspects of catchment functioning. This type of study was carried out in the Malalcahuello Catchment in the Chilean Andes and is described in chapter 3.

One important aspect of the Malalcahuello study was the question wether a combination of spatially scarce soil moisture profiles with high temporal resolution, additional episodic measurements of soil moisture along two hillslope transects and continuously monitored dye tracer irrigation experiments can provide useful insights into the processes of runoff generation in young volcanic ash soils. The young volcanic ash soils of Chile are little understood in their hydrological characteristics and no studies of high temporal resolution soil moisture dynamics were found in our literature search. However, in other parts of the world such as New Zealand or Japan the soil moisture dynamics of volcanic ash soils has been investigated to some extent: Hasegawa (1997) used hourly TDR data to investigate soil water conditions and movement, Musiake et al. (1988) used tensiometric observations and a numerical model to study infiltration and drying behaviour of these soils and Van't Woudt (1954) used 19 small lysimeters to investigate subsurface stormflow.

Soil moisture data has been used as a means to understand runoff generation in other parts of the world (e.g. Kienzler & Naef (in press); Meyles et al. (2003); McNamara et al. (2005); Frisbee et al. (in press); Germann & Zimmermann (2005); Zhou et al. (2002); Hino et al. (1988)) or for the investigation of the effects of changes in land use or management on hydrological processes (Williams et al., 2003; Starr & Timlin, 2004). In most studies soil moisture was measured either with high spatial or with high temporal resolution, thus producing either spatial soil moisture patterns (Bardossy & Lehmann, 1998; Brocca et al., 2007; Meyles et al., 2003; Williams et al., 2003; Western et al., 2004; Rezzoug et al., 2005; Nyberg, 1996) or information on the dynamics (e.g.McNamara et al. (2005); Starr & Timlin (2004); Frisbee et al. (in press)). A combination of both can only be achieved with either a large number of probes measuring continuously such as in Starr & Timlin (2004) and Taumer et al. (2006) or with geophysical methods such as described for example in Zhou et al. (2001), were electric resistivity tomography was used to investigate soil moisture dynamics on a $3.5 \times 3.5m$ plot at hourly resolution. However, the first of these two options is cost-intensive while the second is predominantly carried out on grassland, fields or bare soils with little topography and is not feasible in complex terrain. Combining high temporal resolution soil moisture profiles at few points in space with episodic manual measurements at additional locations thus might be a viable cost-efficient alternative for difficult terrain.

At the Malalcahuello Catchment soil moisture was measured on two steep hillslope transects. Data was collected with a data logger at high temporal resolution at three points and manually at irregular intervals at 11 additional points. Each measurement produces soil moisture data for 6 different depths along a vertical profile. While this is still a pitiful number of data points it is nevertheless possible to get a general understanding of the major processes occurring within the unsaturated zone of this catchment. Data was analyzed using different graphical methods allowing for data ex-

ploration at different spatio-temporal scales. By carrying out rainfall simulation experiments using a dye tracer over each of the continuously measuring probes it was possible to corroborate our perception of flow in the unsaturated zone at these locations. This combination of high temporal resolution soil moisture measurements, rainfall simulation experiments and the use of dye tracers to corroborate the conclusions gained from the soil moisture time series is noteworthy and only one other study (Weiler & Naef, 2003) using a slightly different layout was found in our literature search. The study at the Malalcahuello catchment furthermore included the analysis of response times at the event scale, yearly soil moisture dynamics, spatial patterns and their long-term dynamics for 14 locations and 6 depths and the investigation of small scale soil moisture variability at the decimeter scale.

The four main questions of the study in the Malalcahuello Catchment were:

1) Can soil moisture data be used to investigate the dynamic patterns of unsaturated flow and can these patterns be attributed to runoff generation processes?

2) Are moisture patterns persistent in time and space?

3) What are the causes for the observed moisture/flow patterns?

4) How important are these patterns for the entire system/catchment response?

5.2 Research area

The Malalcahuello Catchment

The research area is situated in the Reserva Forestal Malalcahuello, in the Precordillera of the Andes, IX. Region, Chile. The catchment is located on the southern slope of Volcán Lonquimay (38°25.5'-38°27'S; 71°32.5'-71°35'E). The catchment covers an area of 6.26 km^2. Elevations range from 1120 m to 1856 m above sea level, with average slopes of 51%. 80% of the catchment is covered with forest of the type Araucaria (*Araucaria araucana*) (with Lenga (*Nothofagus pumilio*) and Coigüe (*Nothofagus dombeyi*)) at higher elevations and Roble (*Nothofagus obliqua*)-Raulí (*Nothofagus alpina*)-Coigüe (*Nothofagus dombeyi*) at lower elevations. These types of native forest have a dense understorey of bamboo (*Chusquea culeou*). There is no anthropogenic intervention. Due to this dense vegetation interception losses become significant: on average only 80% of total precipitation reaches the forest floor as throughfall (measured with a raster of throughfall collectors with a diameter of 10.5 cm). However, throughfall amounts are highly variable and can in places also exceed total precipitation (measured outside the forest) by a factor of 2 or even 3 (chapter 3). Above the tree line (20% of the catchment area) there is no significant vegetation cover.

The soils are young, little developed and strongly layered volcanic ash soils (Andosols, in Chile known as Trumaos) (Iroumé, 2003, and chapter 3) High permeabilities (saturated and unsaturated), high porosities (60-80%) and low bulk densities (0.4-0.8 g/cm^3) are typical for volcanic ash soils. They also usually show a strong hysteresis and irreversible changes (e.g. in water retention) with air-drying (Shoji et al., 1993). Soil hydraulic conductivities for the soils in the Malalcahuello catchment were determined in the lab with the constant head method and range from $1.22 * 10^{-5}$ to $5.53 * 10^{-3} m/s$ for the top 45 cm, with an average of $5.63 * 10^{-4} m/s$ (42 samples). The mean conductivity for the fine gravel and pumice layers is $1.88 * 10^{-3} m/s$ (9 samples). Porosities for all horizons sampled range from 56.8% to 82.1%. The mean porosity for the top 45 cm is 71.7% with a standard deviation of 6.6% (16 samples). Layer thickness is also highly heterogeneous, and can range from 2-4 cm to several meters. Depth to bedrock is unknown, however manual augering to depths of 2-3 m, at one occasion even 7 m was possible (chapter 3). At the locations of the 4 wells at

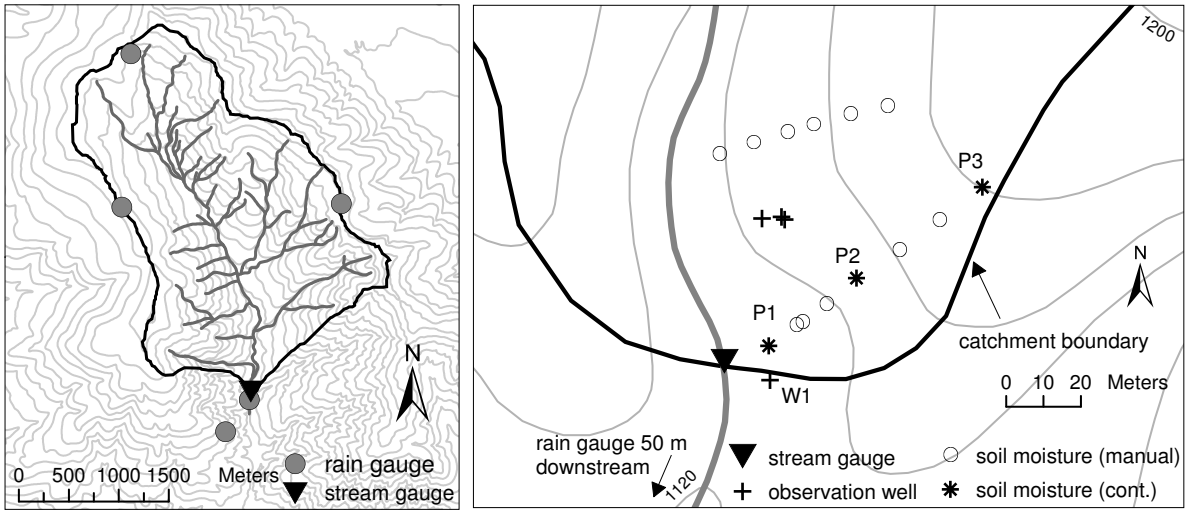

Figure 5.1: Left: The Malalcahuello Catchment including the positions of rain gauges and the gauging station. The vertical resolution of the isolines is 50 m. Right: The slope close to the catchment outlet. Shown are the positions of the continuously measuring soil moisture probes (P1-P3) as well as the locations of the manual soil moisture measurements. The position of the groundwater observation wells is also included. The vertical resolution of the isolines is 20 m.

the lower end of this slope (Figure 5.1) groundwater was found in depths of 1.8-3.2 m below the surface. However, at many other locations on this slope no groundwater was found in auger holes of similar depths. Grain size distributions for the upper horizons resulted in an average of 66.5% sand, 30.4% silt and 3% clay. In the coarse layers the grain size fraction $\geq$2 mm ranges from 38-86% (chapter 3). For a more detailed description of the Malalcahuello Catchment see chapter 3.

The climate of this area can be described as temperate/humid with altitudinal effects. There is snow at higher elevations during winter and little precipitation during the summer months January and February. Annual rainfall amounts range from 2000 to over 3000 $\mathrm{mm/a}$, depending on elevation. Event runoff coefficients are low, with 1 - 10% for 17 events analyzed in 2004/2005, of which a third are smaller than 2% (chapter 2). (The method of baseflow separation used in this analysis is described in chapter 2.) On the other hand, yearly runoff coefficients ($>$ 60%) as well as the baseflow index ($>$ 75%) calculated for the years 2004 and 2005 are high (chapter 3).

An overview of catchment layout and topography as well as instrumentation is given in Figure 5.1.

5.3 Approach and methodology

5.3.1 Approach

The approach of this study is based on the measurement of spatially scarce but high temporal resolution soil moisture profiles on the one hand and additional episodic and therefore temporally scarce soil moisture profiles on the other hand. These two datasets combined with additional experiments described below were used to investigate different aspects of soil moisture response patterns and thus flow in the unsaturated zone. These aspects included the analysis of event response patterns resulting in the deduction of flow processes, the use of rainfall simulation experiments with dye tracers

to corroborate these deductions, but also the analysis of response times at the event scale as well as yearly soil moisture dynamics. The episodic measurements along the hillslope transects allow for the analysis of spatial patterns and their long-term dynamics for 14 locations and 6 depths and for the investigation of small scale soil moisture variability at the decimeter scale.

5.3.2 Soil moisture profiles

Soil Moisture was measured at two transects with FDR (frequency domain reflectometry) profile probes (Delta-T) in 10, 20, 30, 40, 60 and 100 cm depth. Both transects are located on the eastern slope close to the main stream gauging station S1 (Figure 5.1). These profile probes do not measure within a purely circular field as the sensor only extends about two thirds around the probe. By taking three measurements, turning the probe by 120°each time, the full circle is covered. At each depth soil moisture is measured in a soil volume of about 2.5 L, a cylinder with a radius of 10 cm. The absolute measurement error of about 3% (manual of the profile probe) is for the measurement of the dynamics of soil moisture of less importance. The error of the measured dynamics, i.e. the error of the values relative to each other is likely to be smaller than the absolute error. As a result of the special characteristics of the volcanic ash soil, such as the extremely high porosities and the fact that volcanic glass is a primary constituent, the built-in standard calibrations were not applicable. It was thus necessary to calibrate the probe specifically for this type of soil with gravimetrically determined water contents of 19 soil samples of the upper horizons.

Three profile probes were connected to a datalogger and were measuring continuously with a temporal resolution of 10 minutes. The data set extends from March 2003 to May 2006 for the lowest probe and from December 2004 to May 2006 for the two upper probes. For easier reference the three probes are numbered: probe 1 is located at the lower end and probe 3 at the upper end of the hillslope transect. A fourth probe was used for manual measurements at 11 points along the transects. 5 of these measurement locations supplement the transect of the continuously measuring probes, while the remaining 6 form the second transect located to the north of the first (Figure 5.1). The points on the transects were evenly spaced. These manual measurements were carried out at 41 occasions at irregular time intervals during field campaigns (December 2003 - February 2004, October 2004 - December 2004, November 2005 - December 2005 and April - May 2006).

5.3.3 Rainfall simulation experiments

By carrying out rainfall simulation experiments using a dye tracer over each of the continuously measuring probes it was possible to test our perception of flow in the unsaturated zone at these locations. The dye tracer experiments were carried out in May 2007. The plot size was 1.2 m^2 with the probe situated in the center. For all experiments the dye tracer Brilliant Blue with a concentration of 4 $\mathrm{g/l}$ was used. The dye was applied with a hand pressurized pesticide sprayer in order to simulate rainfall. 30 liters of the dye were sprayed over a period of 3 hours. This corresponds to a total of 25 mm at application rates of 8.3 $\mathrm{mm/h}$ on average. Profiles of the plots were excavated the following day and photos of the dye patterns were taken with a digital camera.

5.3.4 Streamflow, groundwater levels and rainfall

Water levels in stream and groundwater were measured with capacitive water level sensors (WT-HR Trutrack®) at 5-10 minute time intervals. Stream water levels were converted to discharge with the help of a rating curve. Rainfall was measured with a tipping bucket rain gauge with a resolution of 0.27 mm. A climate station maintained by the Universidad Austral de Chile is located in a nearby forest plantation at 1270 m elevation. This climate

station has been logging the parameters rainfall, temperature, relative humidity, wind direction and velocity as well as global radiation at hourly intervals since 1999. During the winter of 2005 an ultra-sonic snow height sensor was also installed at this climate station. For more details on the experimental methods applied in the Malalcahuello Catchment see chapter 3.

5.3.5 Response times

Response times were calculated from the time series of rainfall, soil moisture, groundwater levels at well W1 (Figure 5.1) and streamflow (all with 10 minute resolution). Response time in this case was defined as the time period between begin of precipitation and first response of soil, ground- and stream water. The following threshold values were used to identify the point of first response in the time series: an increase of 0.2 $\mathrm{Vol}\%$ in soil moisture, an increase of 0.005 m in groundwater level and an increase of 0.01 m^3/s in stream flow.

5.3.6 Data analysis

Data was analyzed at different space-time scales using various graphical methods. The space-time scales analyzed included event and longterm scale, point and hillslope scale. Event scale datasets with high temporal resolution were analyzed with the help of colour maps which included temporal dynamics similar to those used by Weiler & Naef (2003). Here, time is plotted on the x-axis while depth is plotted on the y-axis. Soil water content at each depth and point in time is visualized by color, changing from blue to red with increasing wetness. For additional information the response of streamflow and groundwater, as well as the rainfall intensity at each point in time were also included. Color scales were adapted from one event to the next in order to get the best "color resolution"possible, producing clearer patterns of response. It thus becomes possible to explore and identify patterns in moisture response, patterns in space and time that are much more difficult to identify in the classical line plots of soil moisture dynamics. In a next step flow processes were deduced from these patterns.

Soil moisture patterns at the hillslope scale are investigated with the help of indicator maps for each depth. These maps show locations where soil moisture is above/below a certain threshold, here the median value for that depth or the 75% quantile, respectively. Additionally, the temporal aspect of these patterns is also included by plotting location on the slope on the y-axis and time on the x-axis, thus giving an idea of pattern persistency.

Simple line plots were used to analyze annual dynamics as well as small scale variability of soil moisture.

5.3.7 Unsaturated conductivities

In order to obtain unsaturated conductivities for the top horizons it was necessary to estimate the Van Genuchten parameters by fitting the Van Genuchten equation to the soil moisture characteristic curves. Soil moisture characteristic curves were deterimend with a pressure chamber for the first two horizons below the humus layer (3 samples each). The Van Genuchten parameters were then used to determine the unsaturated conductivities for a chosen matric potential.

5.3.8 Hydrophobicity

Potential hydrophobicity was measured with the Water Drop Penetration Time (WDPT) test as described in Dekker & Ritsema (1994) for 12 air dried soil samples from 4 different locations and depths from 5 to 80 cm. The WDPT test is a simple test for water repellency where a water drop is applied to a soil sample and the time between application of the water drop and its penetration into the soil is measured. Water drop penetration times for air dried soil have been classified by Dekker & Ritsema (1994) into 5 classes of water repellency: wettable (<5 s), slightly water repellent (5-60 s), strongly water repellent (60-600 s), severely

water repellent (600-3600 s) and extremely water repellent (>3600 s). After testing if a soil sample was wettable soil samples showing water repellency were submitted to 12 repetitions of the WDPT, each test carried out with a different subsample.

5.4 Results and discussion

5.4.1 Soil moisture dynamics on event basis

The soil moisture response was analyzed with the help of space-time maps for 34 rainfall events during the period from December 2004 to December 2005. The temporal resolution of these plots is 10 minutes. The analysis included some events influenced by snow, either directly by snowfall or by rain on snow events. While snowfall will reduce the amount of water infiltrating at the time of the event, rain on snow events will have the effects of flow on or within the snowcover as well as infiltration of meltwater. However, as snow water equivalent was not measured, these effects could not be measured directly.

Three typical events are shown in Fig 5.2. Probe 1 is located at the lower end and probe 3 at the upper end of the hillslope transect. Details of event response and antecedent conditions are listed in Table 5.1.

For the first event, the event on March 3^{rd} 2005 (Figure 5.2a), total precipitation amounted to 52 mm with a highest intensity of 8.6 mm/10 min. The maximum change in soil moisture was high with 8.6 Vol%, which is due to the fact that this event was the rainfall event with the lowest antecedent moisture content of all events studied. The most prominent patterns found for this event are a) extremely fast vertical water transport (arrow 1 in Figure 5.2a), due to high rainfall intensities and high hydraulic conductivities, and b) very little reaction at the 10 cm depth for probes 1 and 3 (arrow 2 in Figure 5.2a). This is probably due to hydrophobicity resulting from the dry antecedent moisture conditions. This pattern was observed only for the 3 driest occasions. Soil moisture increase below the hydrophobic layer must be due to lateral inputs, either at the the decimeter scale or at the hillslope scale. Potential hydrophobicity of soil samples from 5 to 80 cm depth was tested with the Water Drop Penetration Time test. It was found that while the top horizons show strong to extreme water repellency, samples from greater depths are wettable (Table 5.2). However, this test determines only potential hydrophobicity, measured in air dried soil. Water repellency under field conditions is likely to be less pronounced.

The rainfall event on April 6^{th} 2005 (Figure 5.2b) has a total precipitation of 28 mm and only low rainfall intensities. The maximum increase in soil moisture, as well as streamflow and groundwater levels are low with 3.8 Vol%, 0.06 m^3/s and 3 cm, respectively (Table 5.1). The major patterns found here are: a) fast vertical water transport, due to high hydraulic conductivities (arrow 3 in Figure 5.2b), and b) late but persistent response at 100 cm depth for probes 2 and 3, while no such reaction can be seen at the 60 cm sensor (arrow 4 in Figure 5.2b). As water is apparently not transported to this point vertically, this seems to be the result of lateral water input, causing a slow trailing „wave" at this depth.

The event on May 27^{th} 2005 (Figure 5.2c) has a very high total precipitation of 124 mm with a highest intensity of 3.2 mm/10 min. However, as this event is probably a rain on snow event, it is difficult to estimate the actual amount of water entering the soil. While the response of discharge (3.22 m^3/s increase), and ground water levels (120 cm increase) is extremely strong, soil moisture shows a much less pronounced reaction. This is explained by the fact that this is not only an event with high rainfall amounts, but that snow was also present in the catchment at this time (30 cm of snow were measured at the climate station just outside of the research catchment at 1270 m elevation, while the soil moisture transect is located at about 1140 m elevation.). Therefore some of the runoff

Table 5.1: Response characteristics and antecedent conditions for the three events shown in Figure 5.2 (P_{tot}= rainfall amount, P_{Int}= maximum rainfall intensity, $antec.\theta$= antecedent mean soil moisture content for the top 30 cm, $max.\Delta\theta$= max. increase in soil moisture of all sensors, $antec.$Q= antecedent streamflow, $max.\Delta$Q= max. increase in streamflow, $antec.$GW= antecedent groundwater level at well W1, $max.\Delta$GW = max. increase in groundwater levels)

Date	P_{tot} (mm)	P_{Int} (mm/10 min)	$antec.\theta$ (Vol%)	$max.\Delta\theta$ (Vol%)	$antec.$Q (m^3/s)	$max.\Delta$Q (m^3/s)	$antec.$GW (m)	$max.\Delta$GW (m)
03/03/2005	52	8.6	21.6	8.6	0.13	0.45	0.08	0.11
06/04/2004	28	1.6	26.8	3.8	0.13	0.06	0.01	0.03
27/05/2004	124	3.2	29.1	5.5	0.29	3.22	0.42	1.20

Table 5.2: Results of the Water Drop Penetration Time (WDPT) test. If a sample showed water repellency the WDPT test was carried out with 12 repetitions, i.e. with 12 sub-samples. Shown are the number of tests per sample falling in the different classes of water repellency. Samples "forest 1-3"were taken at the slope of the soil moisture transect, while samples named "pine"were taken in a pine plantation downstream of the catchment outlet.

location	depth (cm)	wettable	slightly water repellent	strongly water repellent	severely water repellent	extremely water repellent
forest 1	5-10	no	-	-	5	7
forest 1	10-15	no	-	2	3	7
forest 2	10-20	no	-	12	-	-
forest 2	20-60	yes	-	-	-	-
forest 2	60-80	yes	-	-	-	-
forest 3	10-20	no	3	9	-	-
forest 3	20-60	yes	-	-	-	-
forest 3	60-80	yes	-	-	-	-
pine	0-5	no	-	-	-	12
pine	5-20	no	12	-	-	-
pine	20-60	yes	-	-	-	-
pine	60-80	yes	-	-	-	-

might be generated at the snow surface or within the snow layer. Furthermore, as all water in excess of field capacity is likely to be transported quickly to greater depths, soil moisture increases most for dry antecedent conditions and less in conditions of high antecedent wetness, which was the case during this event. The most prominent patterns for this event are: a) slow vertical water transport, probably due to lower rainfall intensities (arrow 5 in Figure 5.2c) and b) strong response at 40 cm depth for probe 1, very local and short-term (arrow 6 in Figure 5.2c). This reaction might be due to an underlying capillary barrier, causing the water to pond above it until breakthrough. This pattern was observed at this location quite frequently (for 15 events out of 34).

5.4.2 Dye tracer rainfall simulation

In May 2006 rainfall simulation experiments with blue dye were carried out at the locations of the three continuously measuring probes. The soil moisture dynamics of these three experiments are shown in Figure 5.3. As the same amount of dye was applied over the same amount of time during each of these experiments, the three experiments were plotted in one single figure as if corresponding to a single rainfall event. The time period and intensity of dye application is plotted in the top bar. The same colour scale was applied for the intensity of application as for the rainfall intensities in Figure 5.2. Neither streamflow nor groundwater level dynamics are plotted as there was no reaction to these small scale experiments (small in comparison to the size of the hillslope). The mean antecedent moisture content for the top 30 cm was 27.7 Vol%. The dynamic moisture patterns show fast/preferential vertical flow for probes 1 and 2 and slow vertical water transfer for probe 3 (Figure 5.3). One day after the beginning of the sprinkling experiment, crossections of the infiltration plots were excavated and the dye stain patterns marking the flow paths of the dye in the unsaturated zone were photographed. The three photos of the crossections at the locations of the soil moisture probes are shown in Figure 5.4. Preferential flow is found at all three plots. Flow occurred in plumes, which are separated by distinct areas of little or no flow and thus are not marked by blue dye.

Figure 5.4a shows the flow paths of probe 1 (located at the bottom of the slope). While blue dye can be seen in the top 5 cm, hardly any dye stains could be found in depths of 5-ca.30 cm (arrow 1 in Figure 5.4a). This is most likely the suspected zone of hydrophobicity which was also found in the analysis of the time-space maps of soil moisture response to rainfall events. This zone of hydrophobicity or water repellency is most pronounced after summer dry periods but is still visible at the time of the sprinkling experiment where only little reaction was seen at the 10 cm sensor of probe 1 (Figure 5.3). Distinct plumes of dye can be found at depths of ca.30-60 cm (arrow 2 in Figure 5.4a) (also at the location of the soil moisture probe), just above a very prounced layer interface between the silty sand layer above and the gravelly layer below (arrow 3 in Figure 5.4a). This confirms the hypothesis that a capillary barrier could be the cause of the ponding at the 40 cm sensor which was seen in the event response analysis (Figure 5.3 (arrow A)). The dye stains also indicated the locations were water leached into the capillary barrier (arrow 3 in Figure 5.4a). The maximum depth of dye infiltration was about 1 m. Probe 1 is thus intersecting a preferential flow path, which is in part due to roots and in part probably due to flow patterns caused by water repellency of the soil. In late summer the 10 cm and sometimes also the 20 cm sensor are surrounded by hydrophobic soil (Figs 5.2a and 5.2b).

The crosssection at probe 2 (Figure 5.4b) shows as most distinct feature the saprolite layer (weathered bedrock) starting at the location of the 60 cm sensor (arrow 1 in Figure 5.4b). The 100 cm sensor is thus located within the saprolite. It was also found that the probe is located within a preferential flow path coinciding with a concentration of

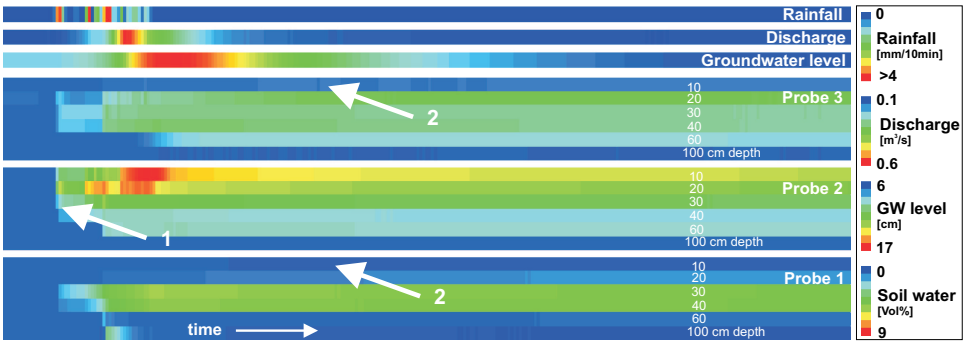

(a) Rainfall event March 3^{rd} 2005.

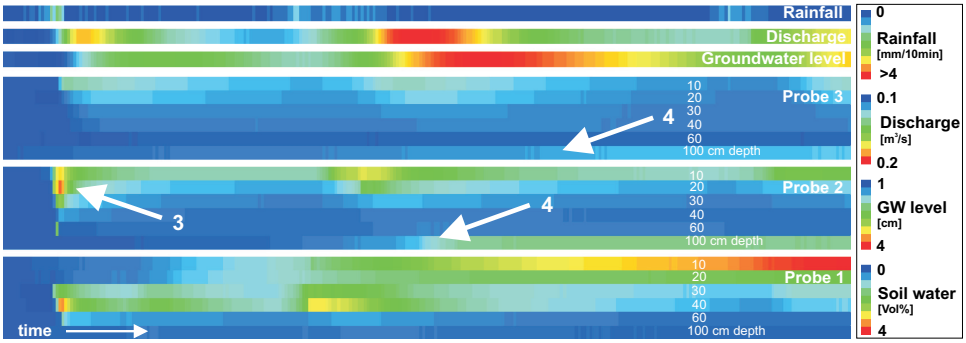

(b) Rainfall event April 6^{th} 2005.

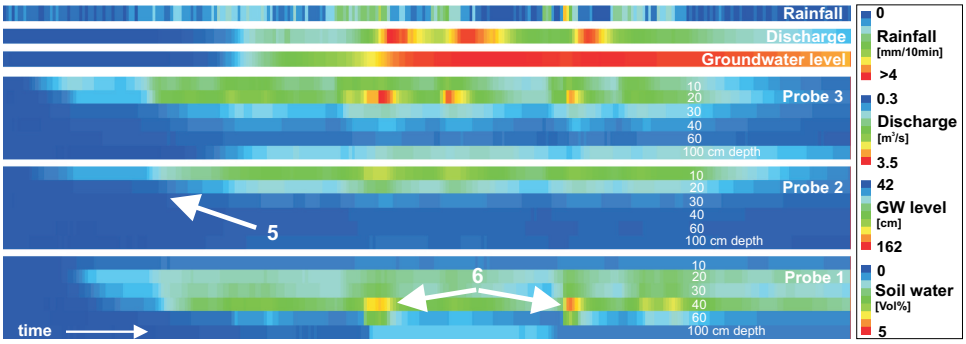

(c) Rainfall event May 27^{th} 2005.

Figure 5.2: Event response patterns of soil moisture for three rainfall events. Time is plotted on the x-axis. All plots show a two day period. Explanation of color bars from top to bottom: The uppermost bar shows 10-minute rainfall intensity: dark blue is equivalent to 0 $\mathrm{mm}/10\ \mathrm{min}$, dark red is equivalent to $\geq 6\ \mathrm{mm}/10\ \mathrm{min}$. The two following bars show the increase of discharge and of groundwater level (at well W1), respectively. The color scale is stretched from minimum to maximum values. Down below follow the three wide bars representing the soil moisture response at the hillslope transect. The upper bar corresponds to the profile probe at the upper end of the slope (P3), the middle bar to the mid-slope probe (P2) and the lowest bar to the profile probe at the lower end of the slope (P1). Within these three wide colour bars, each stripe corresponds to a certain depth: 10, 20, 30, 40, 60 and 100 cm. 0 on the soil water color scale corresponds to antecedent moisture content. The arrows indicate the most prominent features and are numbered for easier reference.

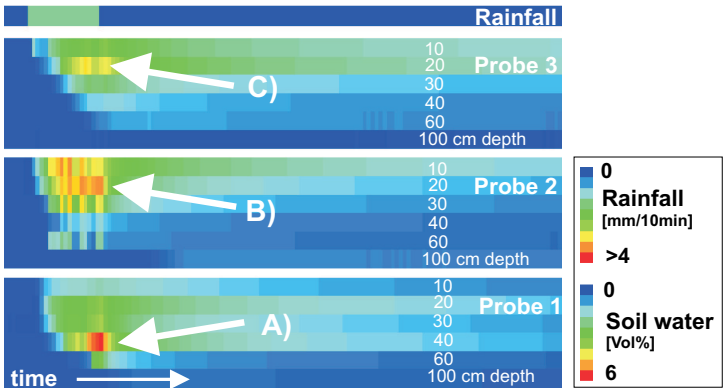

Figure 5.3: Rainfall simulation with dye tracer at the locations of the soil moisture probes: amount of dye applied: 25 mm, intensity of application: 8.3 mm/h. The arrows A, B and C mark the most prominent patterns observed during this simulated rainfall event. The time scale of this plot has a length of one day.

fine roots (arrow 2 in Figure 5.4b). Maximum infiltration depth is about 80 cm in the three major plumes. A hydrophobic layer with very little staining can be seen in the crossection (arrow 1 in Figure 5.4b). However, this layer was not identified in the soil moisture data, as the probe is located within the preferential flow path and not in a hydrophobic patch. The high velocity of flow and the strong response in this preferential flow path is also visible in Figure 5.3 (arrow B) and was also a feature of the soil moisture response space-time maps at this location.

The soil at probe 3 (Figure 5.4c) differed compared to the two others as the vegetation at this plot included a thicket of low shrubs, causing a higher density of roots in the top 20 cm (arrow 1 in Figure 5.4c). The probe was here located in between dye stained preferential flow paths. While blue dye is found in the vicinity of the probe at depths 10-20 cm, very little of it is found close to the probe at greater depths. The 60 cm sensor is located just at the interface between the silty sand and layer of fine gravel (arrow 2 in Figure 5.4c), thus probably measuring in both layers, while the 100 cm sensor is situated in a layer of more compacted silty sand starting at a depth of approx. 75 cm. Maximum depth of infiltration is 80 cm. The fact that the layer at the 100 cm sensor is more compacted might explain why reaction at this sensor occurs delayed and prolongued. This would correspond to lower hydraulic conductivities in the compacted layer causing a delay in response and a prolongued peak. However, as the response at the 60 cm sensor is often very weak, the water causing the peak at 100 cm depths is most likely transported to this point not vertically but laterally. The dense root zone in the top 20 cm explains the strong reaction at the 20 cm sensor (Figure 5.3, arrow C). Probe 3 shows a slower reaction to rainfall compared to the other two probes (Figure 5.3 and also Figure 5.2), which is explained by the fact that this probe is not situated within a preferential flow path.

5.4.3 Response times

A comparison of response lags for 27 rainfall events between December 2004 and April 2006 is shown in Figure 5.5. S20, S30, S40 are the response lags of the soil moisture sensors at 20, 30 and 40 cm depth, GW is the response lag of ground water level at well W1 (Figure 5.1) and Q is the response lag of stream flow. Response lags of all parameters show similar behavior over time: response times are short from January to

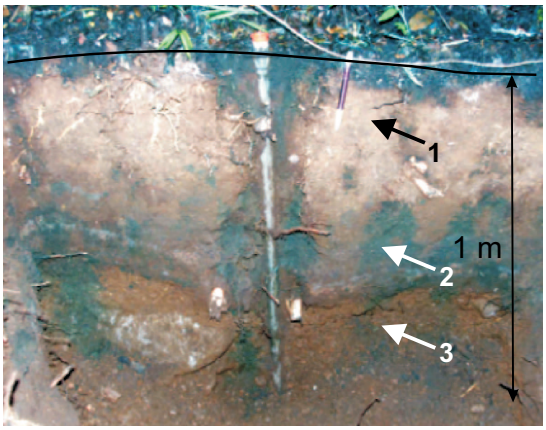

(a) Flow paths at profile probe 1

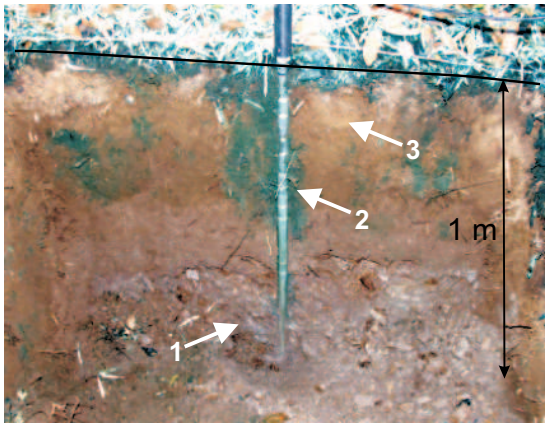

(b) Flow paths at profile probe 2

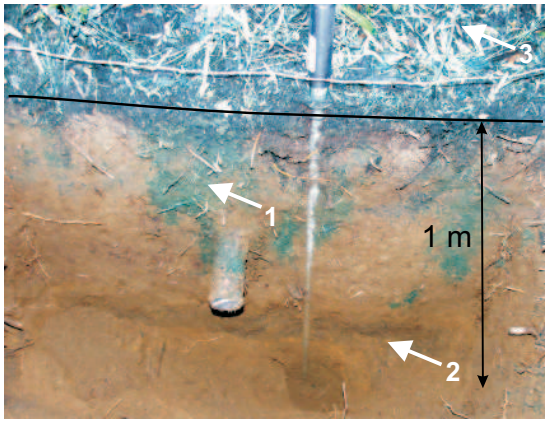

(c) Flow paths at profile probe 3

Figure 5.4: Flow path visualization at the locations of the three continuously logging profile probes. The probes have a length of 1.2 m. The black line indicates the soil surface and the arrows the most important features in each photo. They are numbered for easier reference.

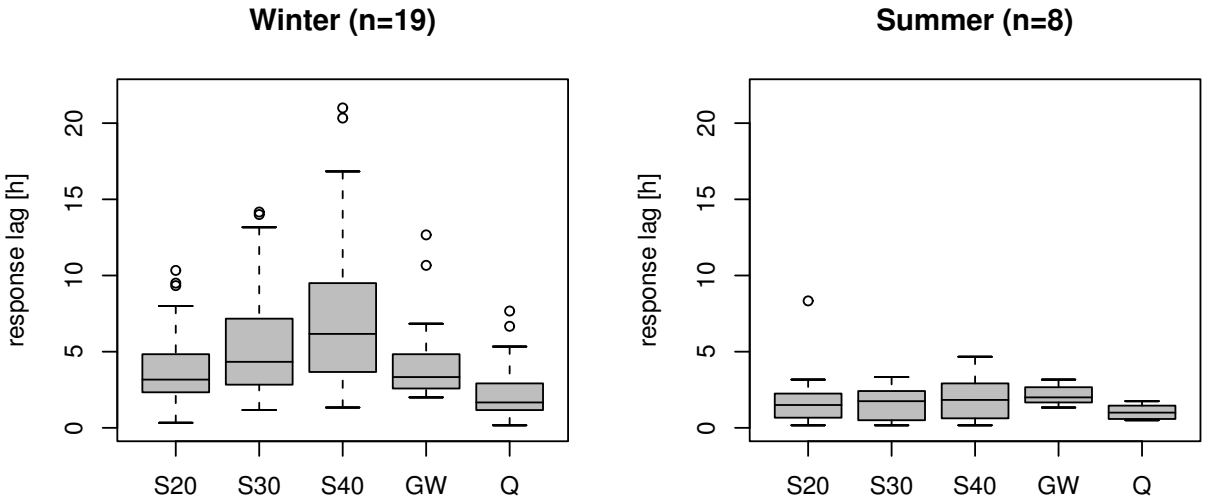

Figure 5.5: Lag times of response in soil moisture, discharge (Q) and groundwater levels (GW) for 19 events in winter and 8 events in summer. Soil moisture response times are shown for 20, 30 and 40 cm depth (S20, S30, S40).

April (summer and early fall) when compared to the winter months. This is probably the result of a) enhanced preferential flow due to hydrophobicity and b) higher rainfall intensities. Groundwater response is generally slower than stream flow response. (At this hillslope the groundwater surface at well W1 in the vicinity of the stream is generally about 60 cm below the stream bed.) Surprisingly, the soil moisture sensors often react slower than stream flow. This could either mean that rainfall is not uniformly distributed over the catchment or that these sensors are bypassed by preferential flow paths. Surface runoff is unlikely, due to high infiltration rates and porosities and has not been observed during field campaigns.

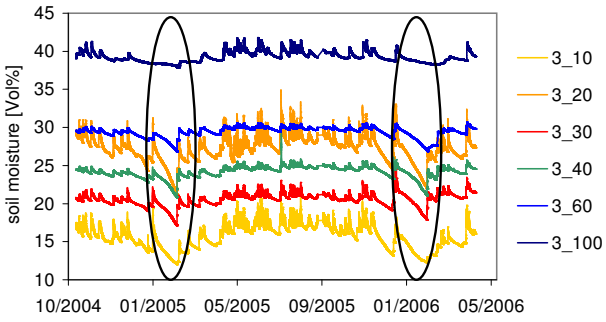

Figure 5.6: Time series of soil moisture dynamics of probe 3. The short summer drying period is circled.

5.4.4 Annual dynamics of soil moisture

The annual dynamics of soil moisture, in Figure 5.6 shown exemplary for probe 3 (Oct 2004-May 2006), are little pronounced in comparison to the event dynamics. Only during the summer months (January and February) a short drying period can be observed (circled in Figure 5.6). However, as soon as the first rainfalls start in autumn, soil moisture values rebound to their previous level. The fact that soil moisture values for the 20 cm depth are high compared to the 10 and 30 cm depths is either due to textural differences or to a root found close to this sensor during the excavation of this profile (Figure 5.4c).

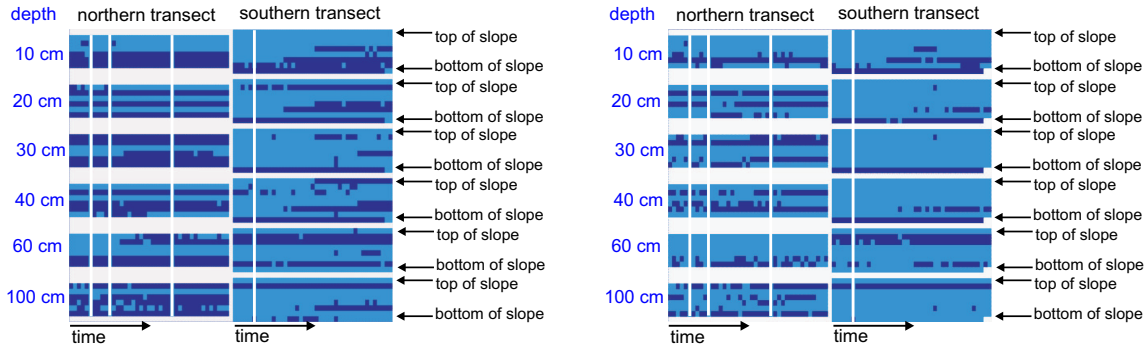

(a) Soil moisture pattern with threshold=median

(b) Soil moisture pattern with threshold=75% quantile

Figure 5.7: Manual soil moisture measurements at irregular intervals at 41 occasions during the field campaigns (December 2003 - February 2004, October 2004 - December 2004, November 2005 - December 2005 and April - May 2006). The northern transect is shown on the left, the southern transect is shown on the right. Each block corresponds to one depth on that particular slope. Sensors are ordered as follows: lowest sensor on the slope is plotted on the lowest line of a single block. On the left transect there are 6 sensors, on the right transect there are 8 sensors. y axis is position on the slope (within bars) and depth (from one bar to the next), x axis is time (i.e. the 41 temporally irregularly spaced data points). Dark blue indicates measurements of soil moisture above the median (a) or the 75% quantile (b) of that depth, light blue are values below these thresholds. Missing data is indicated with white fields.

5.4.5 Soil moisture spatial patterns at the hillslope scale

Soil moisture patterns at the two transects are depicted in Figure 5.7. It was found that patterns are quite persistent over time. There seems to be a correlation with position on the slope for the 10 cm sensor, but not for the sensors at greater depths. At 10 cm depth the lower part of the slope is generally wetter than the upper part of the slope. This is probably due to shading effects: the deeper in the steep valley the fewer hours of direct sunshine. The northern transect is wetter than the southern transect, which is probably due to denser vegetation.

5.4.6 Variability of soil moisture at the decimeter scale

Profile probes measure predominantly in a certain direction. By taking three measurements, turning the probe by 120°each time, the full circle is covered. Figure 5.8 shows the small scale variability in soil moisture measured by twisting the probes at the manual measurement points H4 and H5. Differences in soil moisture around the probe can be very pronounced, e.g. it is wetter/drier in one direction than in the others. These patterns of small scale variability are quite persistent over time while the temporal variability of soil moisture at this time resolution (irregular time intervals during field campaigns) is generally low. It can be seen that while for measurement point H4 only the 20 and the 40 cm sensor show a stronger directional variability of 2.3 Vol% and 4.3 Vol%, respectively, this phenomenon is found for all depths but the 100 cm level at location H5. Overall 68% of the sensors show directional variability (median variability$\geq$1.8 Vol%) when counting each sensor along the probes separately (i.e. 6 depths times 11 locations). 29% of all sensors have a variability $\geq$ 3 Vol%, 18% have a variability $\geq$ 4 Vol% and 6% show a variability of more than 5 Vol%. As the profile probes have a range of only 10 cm, this

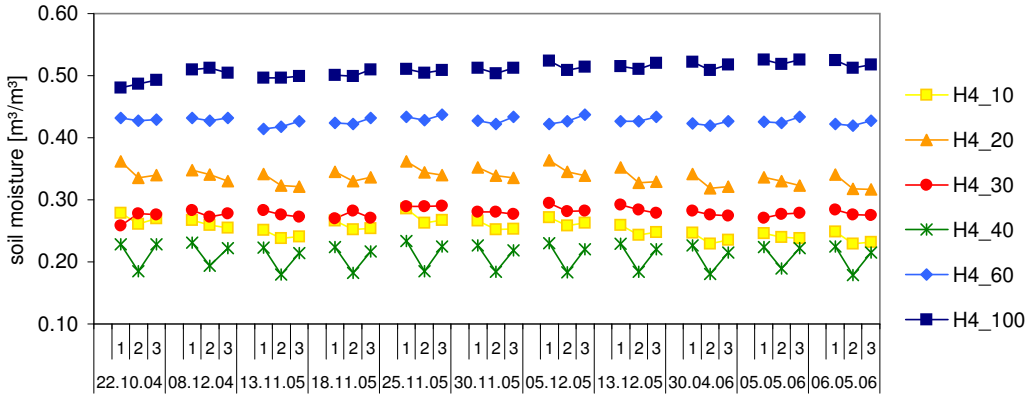

(a) H4

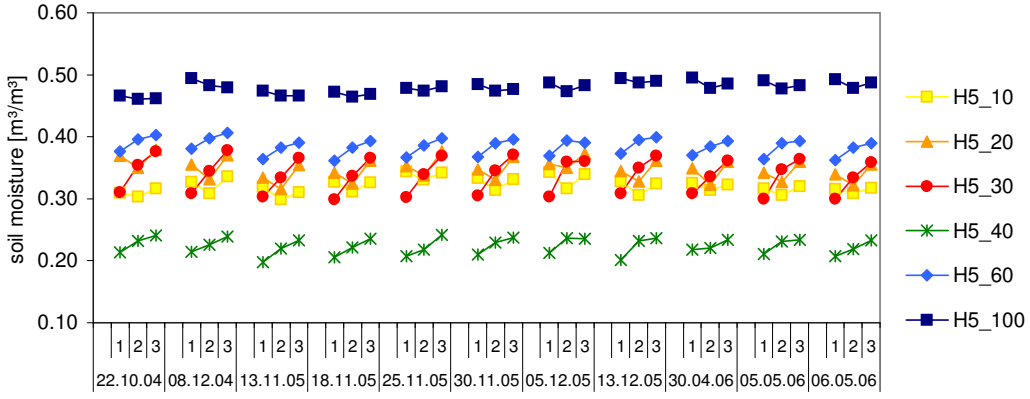

(b) H5

Figure 5.8: Directional or small scale variability at manual measurement points H4 and H5. Measurements 1,2,3 at each date are repetitions within the same access tube, while rotating the probe by 120°. Note that the measurements are taken at irregular time intervals.

observed variability of soil moisture occurs on a very small scale, the scale of decimeters. A possible explanation for these strong gradients in water content over such a small distance is the presence of preferential flow patterns which were found during the dye tracer experiments (see Figure 5.4), as well as during a more extended dye tracer study in this catchment (chapter 4). If a sensor is located near the interface of such a preferential flow path, soil moisture will differ considerably depending on the direction of the measurement. The scale or width of these flow paths is in the order of <3 decimeters, thus matching the scale of the measurement. A sensor showing no directional variation must therefore be located either in the center of a flow path or in the center of the matrix with no flow path within reach of the measurement. Ritsema & Dekker (1996) also used small scale (5-10 cm) variability of soil moisture as a measure for preferential or finger flow. In their study moisture gradients between flow paths and non-flow areas ranged between 3 and 6 Vol%. Assuming small scale soil moisture variability does indeed indicate the presence of a preferential flow path, the fact that in Malalcahuello 68% of all sensors show this type of variability also gives us a measure of the importance of preferential flow in this catchment. There are five possible explanations for the surprising persistency of these soil moisture patterns (or preferential flow patterns) over the course of more than one and a half years (Figure 5.8).

1) These patterns might be caused by air gaps between access tube and the surrounding soil due to faulty installation. However, special care was taken to avoid this problem, by using the auger supplied by the manufacturer of the probes. Furthermore no noticeable air gaps were found during excavation of the probes at the end of the field study, on the contrary, probes were sitting tightly in the soil.

2) They might also be due to textural differences. However, as the sensors have only a range of 10 cm the measured volume is likely to be located within a single layer.

3) These patterns might also be induced by roots, which are not likely to change position on this time scale. However, roots were only found in some instances were these preferential flow patterns were observed during dye tracer experiments.

4) They might be due to hydrophobicity in some parts of the soil, which would produce self reinforcing patterns likely to persist if not subjected to long periods of saturation.

5) These patterns could also be self reinforcing due to the strong gradient in soil moisture itself, leading to faster vertical transport within the wetter area (the flow path) than lateral flow into the drier area as a result of the strong gradient in matric potential.

This last possibility was investigated by calculating the unsaturated conductivities for a number of gradients in soil moisture and thus matric potential: from 20 to 25 Vol%, from 25 to 30 Vol% and from 30 to 35 Vol%, thus covering the range from 20 to 35 Vol% of soil moisture, where most of the variability was observed. The gradient of 5 Vol% chosen to investigate this phenomenon was in the upper range of gradients observed in the field (as the profile probes are not measuring unilaterally in one direction, the gradients perpendicular to a flow path interface are likely to be even higher than the gradients obtained from these measurements). In order to compare flow within the flow path with flow perpendicular to the flow path interface a three step calculation was carried out: First, the Van Genuchten parameters were obtained through fitting the Van Genuchten equation to the soil moisture characteristic curves. Then the gradient in matric potential was determined for the above gradients in soil moisture from the soil moisture characteristic curves. The Van Genuchten equation can then be used to determine the unsaturated conduc-

tivities for the chosen matric potential. As the longitudinal distance a length of 10 cm was chosen, as this is the range of the instrument. The ratio of the gradients in potential (across interface/within flow path) was then compared with the ratio of the unsaturated hydraulic conductivities (within the flow path/ across the interface). The effective unsaturated hydraulic conductivity across the flow path interface was calculated by treating the interface as two layers of differing conductivity (due to the differences in water content) and therefore using the harmonic mean for its calculation. The gradient in potential within the flow path is assumed to be equal to 1 $[cmH_2O/cm]$. In case the ratio of the of the unsaturated hydraulic conductivities is much larger than the gradient in matric potential across the interface (Eq. 5.1), these flow paths are likely to persist over time.

$$\frac{K_\theta(flowpath)\,[m/s]}{K_\theta(interface)\,[m/s]} \gg \frac{\Delta\psi(interface)\,[cmH_2O/cm]}{1\,[cmH_2O/cm]} \quad (5.1)$$

It was found that this would indeed be the case for a pure sand (with a ratio of K_θ up to 11 times larger than the ratio of $\Delta\psi$), however, in these soils, which have a fraction of at least 20% silt, it is very difficult to achieve these conditions (the ratio of K_θ is less than half that of the ratio of $\Delta\psi$). It is thus unlikely that solely the gradient in soil moisture causes the flow paths to persist in time. Nevertheless, if the unsaturated conductivity across the interface is further diminished by the effects of hydrophobicity a persistant pattern becomes more probable. Furthermore this type of soil is known to be hysteretic (Shoji et al., 1993; Musiake et al., 1988) thus causing a shift in the wetting curve compared to the here used draining curve, which could also change the outcome of this rough estimation. Persistent fingers as a result of hysteresis of the soil moisture characteristic curves were described by Selker et al. (1996) and Nieber (1996). Nieber (1996) explains that fingers will persist if the water entry pressure on the main wetting curve is smaller then the air entry pressure on the main drainage curve. However, due to lack of information on the main wetting curve, this effect cannot be assessed for the soils in the Malalcahuello Catchment.

5.5 Conclusions

The soil moisture data obtained in this study provided diverse insights covering different aspects of runoff generation processes in this catchment. It was shown that high resolution time series in combination with manual measurements at irregular time intervals can be a valuable addition to time series of precipitation and discharge when investigating runoff generation processes. This is especially true for catchments where only short time series of data are available, as in the Malalcahuello Catchment. The approach of combining high temporal but spatially scarce data with episodic additional measurements allowed for the investigation of soil moisture dynamics as well as patterns and proved to be less expensive than high density installation of continuously logging sensors while also being applicable to difficult terrain, i.e. densely forested and steep hillslopes.

By analyzing the dynamics of soil moisture response to rainfall events with the help of space-time maps it was possible to identify a number of patterns which can be attributed to different phenomena of flow in the unsaturated zone. The very subdued response of soil moisture in the upper soil horizon at two locations during the driest period (late summer) was attributed to the formation or reinforcement of hydrophobicity in this layer. The accumulation/ponding of water at certain depths was assumed to be due to the effect of capillary barriers. This was confirmed by the dye tracer experiment carried out at this location. Strong response at certain depths while the layers just above show little reaction indicate the importance of lateral flow processes.

It was furthermore found that infiltration dynamics differed from summer to winter, which could be due to differences in rainfall intensities as well as the amplification of preferential flow due to hydrophobicity in the top layer. Potential water repellency was tested with "Water Drop Penetration Time"- method (e.g. Dekker & Ritsema (1994)) and was found to be strong to extreme for the upper horizon. Hydrophobicity has been observed in these Chilean young volcanic ash soils by other researchers (Bachmann et al., 2000; Ellies, 1975) and is also of importance in volcanic ash soils of Ecuador (Poulenard et al., 2004). Differences in flow patterns from dry to wet period were also found in the Malalcahuello Catchment during a more extensive study involving a total of 10 dye tracer experiments (chapter 4). The change in flow pattern observed in this study further supports the theory that preferential flow in this catchment is reinforced by hydrophobicity. Similar flow patterns also attributed to hydrophobicity were observed in other studies (Ritsema & Dekker, 2000; Ritsema et al., 1998; Ritsema & Dekker, 1994; Dekker & Ritsema, 2000; de Rooij, 2000). The fact that throughfall amounts are highly heterogenous in this catchment (chapter 3) is likely to be the reason why some locations (probably on the decimeter scale) are drier than others and thus more likely to develop water repellency. Spots of high water input are therefore likely to become preferential flow paths. These observed patterns in dynamics were found to be spatially and temporally persistent insofar as the event pattern dynamics of soil moisture observed in Fall 2005 (Figure 5.2) matched well with the flow patterns found during the dye tracer experiments one year later. The persistency of the spatial patterns of soil moisture for 14 locations and 6 depths (Figure 5.7) shows that spatial variability is much higher than temporal variability and that wetter locations are likely to remain wet. Furthermore the patterns of soil moisture variability at the decimeter scale, which were also attributed to the presence/absence of preferential flow paths, were found to be persistent over a period of more than one and a half years. While in the case of the larger scale soil moisture patterns the spatial differences in water content could also be attributed to differences in soil texture, the small scale variability is most likely located within a single soil layer and thus not caused by textural differences.

Other possible causes for the observed flow patterns/finger flow apart from hydrophobicity are: flow along roots or preferential flow paths maintained purely by the strong gradient in soil moisture and thus also in unsaturated conductivity. However, roots were found only in some cases of preferential flow patterns. Furthermore, a simple back-of-the-envelope calculation of unsaturated conductivities within and in between flow paths and their corresponding gradients in matric potential showed that these flow paths might be self-reinforcing in pure sand but not in this type of soil. Hydrophobicity is therefore still the most likely explanation for the flow patterns found here. However, the effects of hydrophobicity are likely to be aggravated by root channels, strong gradients in matric potential and the hysteresis of the soil moisture characteristic curves of volcanic ash soils as described by Shoji et al. (1993).

The last and maybe the most important question is the question of how important this locally observed preferential flow is for the system as a whole, i.e. runoff response/runoff generation at the catchment scale. Several findings indicate that while preferential flow was only observed at the plot scale it might indeed be important factor of runoff generation at the catchment scale. That preferential flow occurs throughout the catchment is indicated by the fact that additionally to the three tracer experiments shown in this study all 9 dye tracer experiments carried out under forest at various locations in the catchment showed preferential flow patterns (chapter 4). The fact that 68% of the sensors at the 11 manual measurement points showed small scale soil moisture variability is another indicator for the importance of these preferential flow paths. Last but not least the analy-

sis of response times for soil moisture, groundwater and streamflow reveiled that response lags are generally much shorter during the summer months were preferential flow is also likely to be further enforced by stronger hydrophobicity. Interestingly streamflow often shows faster response than both groundwater and soil water. This might be due to non-uniform rainfall distribution (i.e. earlier onset of rainfall further up in the catchment causing stream levels to respond while soil moisture at the slope close to the catchment outlet remained unchanged). However, as our data points in space are restricted to only three locations it is also likely that there are other preferential flow paths with even faster response than the ones measured by our instruments. In this case preferential flow in the vertical and then a fast reaction along a horizontal layer interface might be the reason for the short response lags of streamflow found in this catchment. (Finger flow is known to cause faster breakthrough as investigated by de Rooij & deVries (1996) in a modelling study.) The question whether or not these preferential flow processes are important for catchment response could be investigated further by application of a physically based hydrological model either on the hillslope or on the catchment scale.

To summarize the main conclusions in short:

1) the combination of high temporal resolution but spatially scarce soil moisture data with episodic additional measurements proved to be useful for the investigation of runoff generation processes, especially with respect to preferential flow. While being less expensive than measuring at higher spatial resolution with a high number of continuously logging probes it is also suitable for difficult terrain (i.e. very steep slopes) where geophysical techniques are problematic. The use of continuously monitored rainfall experiments with subsequent excavation of soil profiles adds additional insights into the flow processes in the unsaturated zone.

2) soil moisture/flow patterns were shown to be persistent in time and highly variable in space

3) the most likely explanation for the observed flow patterns is a combination of hydrophobicity with strong gradients in unsaturated conductivities, were flow paths are caused either by the presence of roots or the highly heterogeneous distribution of throughfall and thus water input

4) the flow patterns observed at the local scale are likely to be important for runoff response at the catchment scale.

Acknowledgements

The authors would like to thank Andreas Bauer, Dominik Reusser (Potsdam University) and Hardin Palacios, Luis Opazo (Universidad Austral de Chile) for help in the field,and Prof.Andrés Iroumé and Prof.Anton Huber (Universidad Austral de Chile) for logistic and technical assistance. This work was partially funded by the International Office of the BMBF (German Ministry for Education and Research) and Conicyt (Comisión Nacional de Investigación Científica y Tecnológica de Chile) and the "Potsdam Graduate School of Earth Surface Processes", funded by the State of Brandenburg.

Chapter 6

Different models for different purposes - testing process hypotheses on hillslope scale and investigating influence of land use on catchment scale *

Two types of models were used to simulate the hydrology of a small catchment in the Chilean Andes. The physically based model Catflow was used as a tool for the testing of process hypotheses, which were developed during field campaigns. Hypotheses concerning lateral and vertical preferential flow as well as the importance of rainfall redistribution in the forest canopy were tested on the hillslope scale. Additionally, the influence of land use on runoff response was investigated with the process oriented model Wasim-ETH by simulating different scenarios of deforestation. It was found that while peak runoff generally increased with deforested area, the location of these areas within the catchment also had an effect.

*Theresa Blume, Erwin Zehe, Axel Bronstert (in preparation), *Water Resources Research*

6.1 Introduction

Computer models can be a useful tool in the investigation of runoff generation processes because the experimental investigation of these processes is restricted: it is impossible to measure all the data necessary to characterize the full heterogeneity, variability and dynamics of runoff generation processes active in any one catchment. Therefore most experimental investigations stop at a certain level of data availability or process knowledge, either because time or finances have run out, the current level of process understanding has already developed so far that additional research scores badly on cost-benefit calculations or because the equipment necessary for a more detailed or more exact investigation simply does not exist. Furthermore most processes, their interactions and their resulting integral response are too complex to allow us to make simple and adequate quantitative statements about cause and effect in catchment functioning.

Computer models of catchment or hillslope hydrology seem to be a feasible way out of this dilemma. These models can serve as a tool for

- a) the testing of our hypotheses on catchment functioning, which we have developed from observations in the field,
- b) the investigation of spatial structures and their importance on rainfall runoff response,
- c) the spatial and temporal interpolation of processes observed at plot or point scale along the hillslope in order to determine their importance for the integral response of the system (catchment or hillslope),
- d) the spatial extrapolation of data from the experimental scale (plot or hillslope) to the catchment scale,
- e) the temporal extrapolation of data and response understanding, e.g. for flood prediction and
- f) extrapolation of process response to different boundary conditions, such as climate or land use change scenarios.

However, not all of these possible uses of hydrological models require the same level of complexity in simulation: If these computer models are physically based in their representation of the dominant processes and their parameters (including their spatial variability) as well as the state variables can be measured in the field, they can serve for most purposes, given sufficient data (and computer speed). Physically based in this context also means that these models are spatially explicit in all process components and account for mass, momentum and energy balance. As data availability is often limited, less complex but nevertheless spatially distributed models (allowing for spatial variability of parameters and responses) can be a viable alternative for purposes d), e) and f), especially for larger spatial scales. These less complex models usually contain some conceptual approaches (e.g. the linear storage concept), are often not spatially explicit in all process components and often cannot account for the momentum balance. While in physically based models the implemented different subsurface structures result in different process ensembles and thus different responses, process-based models often account for different processes explicitly, e.g. with interacting storage components for direct flow, macropore flow, interflow and baseflow. It is then necessary to calibrate the model to measured streamflow data. While this is a relatively easy way to determine model parameters (compared to measuring data in the field) it does contain certain risks: a model calibrated to the status quo might not be able to simulate catchment response to conditions outside the range it was calibrated for, i.e. especially in case of different boundary conditions such as a change in climate or landuse or even just extreme rainfall events. Simple extrapolation of status quo responses might therefore cause severe errors in prediction. The highly non-linear or threshold re-

sponse of natural systems thus increases the need for process understanding and the incorporation of this understanding into hydrological models.

The focus of the presented study lies on a small, anthropogenically undisturbed catchment in the Andes of Southern Chile. However, while Southern Chile still offers undisturbed landscape, many areas of the region also undergo substantial and rapid land use change. During the last decades this lead to conversion of vast areas of farm land and native forest to forest plantations of exotic species such as Eucalyptus and Pinus radiata (Monterey Pine). Governmental subsidies resulted in an increase in area under plantation from 330000 ha in 1974 to 1.5 million ha in 1992 (Donoso & Lara, 1995) to 2.1 million ha in 2006 (CORMA, 2007). Land use changes at this extent are likely to affect biodiversity, water and nutrient budgets as well as sediment transport. In recent years tourism and recreational land use (such as hiking and winter sports) are gaining more importance and thus a new kind of pressure is exerted especially on protected areas such as national parks.

The study area, the Malalcahuello Catchment, is characterized by high rainfall amounts, old-growth forest, steep topography and young volcanic ash soils. The high porosities and permeabilities typical for these soils make surface runoff unlikely - subsurface flow dominates runoff response. Fast response times and fast event recessions as well as the results of soil moisture and tracer studies suggest that rapid vertical and lateral flow processes are of importance. The fact that annual runoff coefficients (and annual rainfall amounts) are high indicates that this is an energy limited system. The experimental investigation of runoff generation processes in the Malalcahuello Catchment is described in chapter 3- 5.

In this study the physically based model CATFLOW (Zehe et al., 2001; Maurer, 1997) is used for the investigation of runoff generation processes at the hillslope scale. Special focus is given to the importance of subsurface structures, the importance of macropores and the importance of variable rainfall input as a result of redistribution processes in the forest canopy.

Additionally, the process oriented model WASIM-ETH (Schulla, 1997; Schulla & Jasper, 1999) is used to investigate the importance of land use for runoff response on the catchment scale.

6.2 Approach

The purpose of this study is twofold: a) the investigation of runoff generation processes and here especially the importance of physical structures and rainfall variability on the hillslope scale and b) the investigation of the importance of land use on runoff response on the catchment scale. Two different models with different levels of complexity were used for these purposes. While the process investigation relies on a strongly physically based model (Catflow), the effect of land use change was studied with the process-based Wasim-ETH, a model that is in part physically based but also contains some conceptual approaches. While the simulation with Catflow uses parameters obtained from field data and different hypothetical subsurface structures to test hypotheses of runoff generation (section 6.3.2), the simulation with Wasim required a prior calibration of the model with measured discharge time series. Automatic calibration was carried out with PEST (after manual precalibration) (see section 6.3.3). We are thus using a bottom up approach for the hillslope and the classical top-down approach for the catchment scale study. Due to the difference in scale and approach the two models also contain different inherent assumptions:

Wasim-ETH: The system is controlled by bedrock topography and vertical preferential flow.

Catflow: The system is controlled by rapid vertical and lateral flow paths, i.e. finger flow/macropore flow and flow along layer interfaces, as well as by the groundwater dynamics close to the stream. As hillslope out-

flow is compared with catchment discharge it is further assumed that catchment response can be modeled with a representative hillslope and that the 2D characterisation of this hillslope is a viable simplification (see section 6.3.2).

The data base for this study is the result of the multi-method experimental investigation described in detail in chapter 3- 5.

6.3 Methods

6.3.1 Research area

6.3.1.1 Location and topography

The research area is situated in the Precordillera of the Andes, IX. Region, Chile. The catchment is located on the southern slope of Volcán Lonquimay (38°25.5'-38°27'S; 71°32.5'-71°35'E) and is part of the Reserva Forestal Malalcahuello. The catchment has a size of 6.26 km^2, and the elevation ranges from 1120 m to 1856 m above sea level, with average slopes of 51%.

6.3.1.2 Vegetation and interception

80% of the catchment is covered with old growth native forest, which usually has a dense understorey of bamboo (*Chusquea culeou*). There is no anthropogenic intervention. Due to the dense vegetation interception losses are quite high: on average only 80% of total precipitation reaches the forest floor as throughfall (determined with a raster of throughfall collectors with a diameter of 10.5 cm). Additionally, throughfall amounts are highly variable and can in places also exceed total precipitation (measured outside the forest) by a factor of 2 or even 3 (chapter 3). There is no significant vegetation cover above the tree line. This unvegetated area covers about 20% of the catchment area.

6.3.1.3 Climate and runoff characteristics

The climate of this area can be described as temperate/humid with altitudinal effects. There is snow at higher elevations during winter and generally little precipitation during the summer months January and February. Annual rainfall amounts range from 2000 to over 3000 mm/a, depending on elevation. Event runoff coefficients are low, with 1 - 10 % for 17 events analyzed in 2004/2005. A third of these events have runoff coefficients smaller than 2% (chapter 2). (The method of baseflow separation used in this analysis is described in chapter 2.) However, yearly runoff coefficients ($> 60\%$) as well as the baseflow index ($> 75\%$) calculated for the years 2004 and 2005 are high chapter 3 . The climate station close to the research catchment (Figure 6.1) provided the climatic input data for both models used in this study. The unheated rain gauges at higher elevations were unable to measure snow water equivalents and thus were inactive during the winter months. As furthermore no clear correlation of rainfall amounts with altitude could be established only rainfall data from the climate station as well as the lowest rain gauge (G1 - see Figure 6.1) were used for the simulations.

6.3.1.4 Soils

Soil hydraulic conductivities for the young volcanic ash soils in the Malalcahuello catchment were determined in the lab with the constant head method and range from $1.22 * 10^{-5}$ to $5.53 * 10^{-3} m/s$ for the top 45 cm, with an average of $5.63 * 10^{-4} m/s$ (42 samples). The mean conductivity for the fine gravel and pumice layers is $1.88 * 10^{-3} m/s$ (9 samples). Porosities for all sampled horizons range from 56.8% to 82.1%. The mean porosity for the top 45 cm is 71.7% with a standard deviation of 6.6% (16 samples) (chapter 3) . These high conductivities and high porosities are typical for volcanic ash soils, which also usually show a strong hysteresis and irreversible changes in water retention with air-drying (Shoji

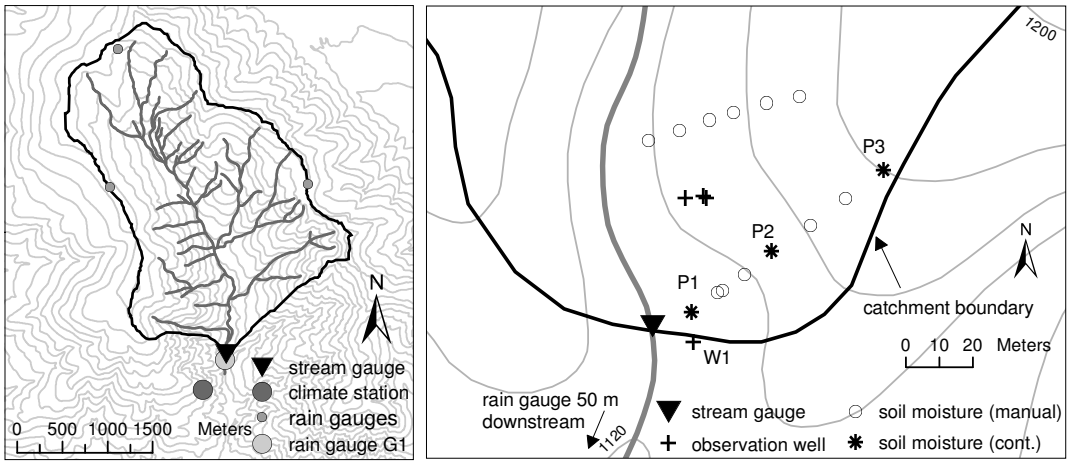

Figure 6.1: Map of the research area and the experimental set-up at the hillslope close to the main stream gauging station. (The vertical resolution of the contour lines is 50 m for the catchment and 20 m for the hillslope scale.)

et al., 1993). Grain size distributions for the upper horizons resulted in an average of 66.5 % sand, 30.4% silt and 3% clay. In the coarse layers the grain size fraction $\geq$2 mm ranges from 38-86% (chapter 3) . Soil layer thickness is highly variable, and ranges from 2-4 cm to several meters. The depth to bedrock is unknown, but manual augering to depths of 2-3 m, at one occasion even 7 m was possible (chapter 3) . At the 4 wells at the lower end of this slope (see Figure 6.1) groundwater was found in depths of 1.8-3.2 m below the surface. However, at many other locations on this slope no groundwater was found in auger holes of similar depths. For a more detailed description of the Malalcahuello Catchment see chapter 3 .

An overview of catchment layout and topography as well as instrumentation is given in Figure 6.1.

6.3.2 Catflow

The importance of physical structures in the subsurface such as macropores and soil layering as well as the effect of non-uniform rainfall distribution caused by redistribution of rainfall in the canopy is investigated with the hillslope module of Catflow.

6.3.2.1 Model description

Catflow (Zehe et al., 2001; Zehe & Bloeschl, 2004; Zehe et al., 2005; Maurer, 1997) is a physically based model as described in section 6.1. It relies on detailed process representation such as soil water dynamics with the Richards equation (mixed form), evapotranspiration with the Penman-Monteith equation, surface runoff with the convection diffusion approximation to the 1D Saint Venant equation. The processes saturation and infiltration excess runoff, reinfiltration of surface runoff, lateral subsurface flow and return flow can be simulated. Macropores can be included with a simplified effective approach by assigning a macroporosity factor F_{macro}. In this approach the hydraulic conductivity of a node is increased rapidly once the degree of saturation reaches a predefined threshold (often taken to be field capacity). Above this threshold the hydraulic conductivity increases linearly with soil moisture content to $F_{macro} * K_s$ at saturation (Maurer, 1997). The

macroporosity factor F_{macro} can be assigned node wise, thus determining depth and location of the macropores. In Zehe et al. (2001) and Zehe & Bloeschl (2004) a threshold value equal to the field capacity of the soils of the study area proved to be suitable. The simulation time step is dynamically adjusted to achieve a fast convergence of the picard iteration. The spatial discretisation of the model is twofold: while a catchment is discretized into a number of hillslopes (linked via the drainage network), each hillslope is discretized as a 2D vertical grid along the main slope line. This grid is defined by curvilinear coordinates (Maurer, 1997). As the hillslope is defined along its main slope line each element extends over the whole width of the hillslope, making the representation quasi-3D. Catflow has proved to be successful for a number of applications: as a virtual landscape for the investigation of the role of initial soil moisture and precipitation on runoff response (Zehe et al., 2005), for the investigation of water flow and bromide transport in a loess catchment (Zehe & Flühler, 2001a), for the process investigation within a slow-moving landslide (Lindenmaier et al., 2005), the investigation of bi-modal runoff response (Graeff et al., submitted) and for the derivation of closure relations for a model based on the "Representative Elementary Watershed"(REW) approach (Lee et al., 2007).

6.3.2.2 Model set-up for the Malalcahuello hillslope

For this investigation the hillslope module was used to simulate a single hillslope. As the outflow at the lower end of the slope is compared with stream hydrographs measured at the main stream gauging station this carries the inherent assumption that the structure and physical characteristics of this single slope are representative of all slopes in the catchment and that a 2D or quasi-3D representation of this slope is a viable simplification. The need to use catchment outflow as a proxy for hillslope runoff generation arises due to the fact that direct measurement of the outflow of the slope

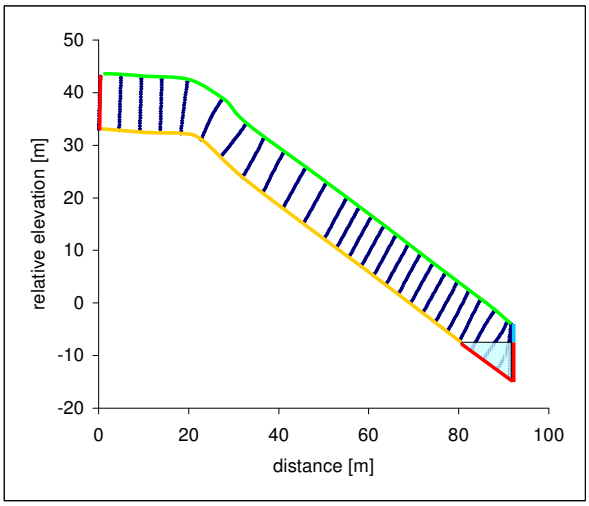

Figure 6.2: Model hillslope geometry. (The boundary conditions are indicated with colored lines: red = no flow, green = atmospheric, blue = seepage, yellow = free drainage.)

was impossible: the soils in this catchment are too deep for hillslope trench investigations. However, as most of the catchment is covered with forest, as soils are assumed to be similar over the catchment area and as steep slopes are indeed characteristic for this catchment, the assumption of a representative slope is not completely unrealistic. The slope chosen for the simulation resembles the slope close to the main gauging station, where additional data sources such as groundwater levels or soil moisture dynamics are available and can also be used for the validation of model structures.

6.3.2.3 Model hillslope geometry

The model slope has a length of 92 m and a change in elevation of 47 m. As no knowledge of depth to bedrock exists the slope was given a depth of 10 m as a first guess. Slope geometry is determined by 27 by 22 nodes (see Figure 6.2). Each node can be given a soil type with the corresponding soil physical characteristics. It is thus technically easy to parametrize subsurface structures such as soil layers.

6.3.2.4 Model parametrization

For soil parametrization values of saturated hydraulic conductivities, porosities, pF curves and fitted Van Genuchten parameters were used (Table 6.1). For the setup used here the 4 most dominant soil horizons found in the field were parametrized. This includes humus and the two soil horizons found in the first meter as well as the gravelly layer which is generally found at depths of more than one meter. In this study the subsurface was parametrized as follows: 5 cm humus layer, 70 cm ash soil horizon 1, 50 cm ash soil horizon 2, 50 cm fine gravel, 50 cm loam or soil horizon 2, 1 m fine gravel, followed by soil horizon 2 (6 m)(see also Table 6.1). Just above the lower boundary another 75 cm of loam are included. Loam was not found in the catchment, however, as the hydraulic conductivity of loam is at least two orders of magnitude below those of the volcanic ash soils, loam was chosen to model the effect of a lower permeability layer. The native forest was parametrized as follows: LAI = 11-14 m^2/m^2, crown coverage = 80%, root depth = 1.5-1.6 m, plant height = 10-35 m, albedo = 0.2 and minimum stomata resistance = 100 s/m (Lusk, 2001; Huber & Iroumé, 2001; Maurer, 1997).

2004 data from the climate station was used as climatic input data. Rainfall time series (6 min temporal resolution), however, stem from rain gauge G1 (see Figure 6.1), as the climate station only provides data with one hour (for some periods half hour) resolution.

6.3.2.5 Boundary conditions

The boundary conditions of the model hillslope are shown in Figure 6.2. The upper boundary has an atmospheric boundary condition (marked as a green line on Figure 6.2), the left boundary is a no flow boundary. 85 % of the lower boundary is a free drainage (as we have no information on depth to bedrock) while the 15 % at the lower end of the slope are parametrized as no flow (indicated in yellow and red on Figure 6.2). The right boundary is a seepage boundary for the upper 2.5 m (light blue on Figure 6.2), where water can leave the domain if field capacity is exceeded. Below 2.5 m the boundary is a no flow boundary, so that a saturated zone is implemented at greater depths.

6.3.2.6 Hypotheses to be tested

As all we know about subsurface structures are that soils are strongly layered and that preferential flow is an important factor, different hypotheses of subsurface structures were tested, such as different soil layering and different representation of macropores.

The effect of macropores was investigated by varying the macroporosity factor F_{macro} between 1 and 40. Macropore depth was estimated as 1 m from dye tracer experiments carried out at this slope (chapter 4) . The threshold for the initiation of macropore flow was 0.5 relative saturation for the top two horizons and 0.8 for the third horizon. These values are at or slightly above field capacity for the first two horizons as suggested in Zehe et al. (2001). For the third horizon the threshold value is above field capacity as less preferential flow was observed in these depths (chapter 4) .

The variability of throughfall amounts found in the field was high (chapter 3). Furthermore, preferential flow also appears to be one of the major processes (chapter 4 and 5) . It was therefore hypothesized that throughfall variability might act reinforcing on preferential flow: higher throughfall amounts will cause higher soil moisture contents which in turn result in higher hydraulic conductivities, all of this being a very local phenomenon. To investigate the influence of the variability of throughfall amounts on runoff generation a simple approach was chosen: Two rainfall time series were created, one with 1.75 and the other with 0.25 times the amount of rainfall per time step of the original time series. As precipitation time series can be assigned node wise for the surface nodes, these two time series were used alternatingly as in-

Table 6.1: Catflow: soil physical parameters of the simulated soil types (K_s = saturated hydraulic conductivity, θ_s, θ_r = saturated and residual water content, α, n = van Genuchten parameters, ρ_b = bulk density, m_t = threshold saturation for initiation of macropore flow, depth = location in the simulated soil profile, SU2 = model set-up 2)

	K_s $[m/s]$	θ_s [-]	θ_r [-]	α $[1/m]$	n [-]	ρ_b $[kg/m^3]$	m_t [-]	depth [cm]
humus	2.7*10^{-3}	0.80	0.01	24.3	1.25	0.48*10^3	0.5	0-5
horizon 1	3.5*10^{-4}	0.72	0.06	18.0	1.20	0.7*10^3	0.5	5-75
horizon 2	4.0*10^{-4}	0.68	0.20	10.7	1.34	0.8*10^3	0.8	75-125
								(SU2:175-225)
								325-925
fine gravel	1.6*10^{-3}	0.66	0.11	18.7	1.21	0.9*10^3	-	125-175
								225-325
loam	2.9*10^{-6}	0.50	0.08	3.6	1.56	1.4*10^3	-	175-225
								925-1000

put, so that two neighboring nodes receive a highly different amount, but the same dynamics of rainfall.

The three specific hypotheses tested in this study are in summary:

1) lateral preferential flow plays an important role in runoff response (in the Malalcahuello Catchment)

2) vertical preferential flow plays an important role in runoff response

3) small scale rainfall variability caused by redistribution processes in the forest canopy acts reinforcing on preferential flow.

The general assumptions of the representative hillslope, the 2D representation of this slope and the importance of groundwater dynamics close to the stream also apply to all model set-ups tested in this study. A short summary of the compared set-ups can be found in Table 6.2.

6.3.3 Wasim-ETH

The importance of land use for catchment response is investigated using the process-oriented, grid based model Wasim-ETH.

6.3.3.1 Model description

The Topmodel-based Wasim-ETH (Schulla, 1997; Schulla & Jasper, 1999) is a deterministic and distributed model for the simulation of catchment water balance. It was originally developed for the investigation of climate change effects on water balance. It was has been extended to include macropore flow, siltation and water retention in the landscape as well as an improved representation of urban areas (Niehoff et al., 2002). It is grid based in the calculation of evapotranspiration, interception, snow melt and snow storage, infiltration and vertical soil water movement. Direct flow, interflow and baseflow are simulated as linear storages; the first two are calculated per grid cell while baseflow is calculated on the basis of the entire subcatchment. For the routing of streamflow the kine-

Table 6.2: Catflow: the compared model set-ups as well as corresponding runoff-coefficients and Nash-Sutcliffe efficiencies. (SU = model set-up)

	SU1 (best run)	SU2	SU3	SU4	data
loam layer	yes	no	yes	yes	-
F_{macro}	32	32	20	32	-
variable precipitation	yes	yes	yes	no	-
runoff coeff.	0.60	0.61	0.33	0.66	0.60
Nash-Sutcliffe	0.46	0.44	0.06	0.29	-

matic wave approach is used (Niehoff, 2002). For the simulation of evapotranspiration the Penman-Monteith equation is implemented. Infiltration is modelled with the Green and Ampt approach, deviding the incident rainfall into infiltration excess water and infiltrating water which is routed to the soil model. The soil model does not model soil water movement but uses a system of storages centering around the saturation deficit. The calculation of the saturation deficit is based on the Topmodel approach of the topographic index. The/most parameters of the different storages need to be calibrated (Niehoff, 2002). Wasim-ETH is a process oriented model, as it models flow components such as infiltration/saturation excess, direct runoff, interflow and baseflow and some of the soil storage characteristics can be connected to soil physical parameters. For matters of conciseness Wasim-ETH will be referred to as "Wasim"throughout this publication.

6.3.3.2 Model parametrization

Necessary input grids are landuse, soils and a number of topographical grids determined from a digital elevation model. The spatial resolution chosen for this study were 25 m grid cells, and one hour time steps were used for the simulation. For the Malalcahuello Catchment 3 different types of forest were parametrized: Mixed broadleaved and evergreen forest, evergreen forest and krummholz. For parameter values see section 6.3.2.4. Data from the climate station served as input data for the entire simulation period. For the period 2004-2005 the model was run first with rainfall data from the climate station and in a second run with data from rain gauge G1 in order to investigate the influence of the input rainfall time series on model results.

6.3.3.3 Calibration and validation

Calibration was carried out with PEST (a freely available software for non-linear parameter estimation using the Gauss-Marquardt-Levenberg algorithm) (Doherty, 2004) after manual pre-calibration for the year 2002 and 2003, while for validation data from 2004 and 2005 was used. For calibration 6 different soil parameters and 4 snow model parameters were estimated. For the parameter descriptions and the ranges used for the calibration see Table 6.3. Streamflow data from the main stream gauging station served as reference.

6.3.3.4 Land use scenarios

To investigate the influence of land use on hydrologic response 4 scenarios were simulated: Scenario 1) deforestation in the lowest subcatchment, close to the main stream gauging station, Scenario 2) deforestation in the two lowest subcatch-

Table 6.3: Parameters of Wasim calibrated with PEST, including their ranges and best values.

parameter	description	unit	range	best value (areal mean)
m	recession parameter for baseflow	m	0.001 - 0.1	0.05
T_{corr}	correction factor for soil transmissivity	-	0.05 - 20.0	2.8
K_{corr}	correction factor for vertical percolation	-	600 - 2000	1052
k_D	single reservoir recession const.-surface runoff	h	10 - 80	50
H_{max}	maximum storage capacity of interflow storage	mm	10 - 200	49
k_H	single reservoir recession const.-interflow	h	50 - 300	98
t_{0r}	temperature limit for rain	C	-2.0 - 2.0	-0.5
t_0	temperature limit for snow melt	C	-2.0 - 2.0	-0.9
c_0	degree-day-factor	mm/d/C	1.0 - 5.0	1.8
c_{melt}	fraction of snowmelt which is suface runoff	-	0.0 - 1.0	0.1

ments, Scenario 3) deforestation in the upper subcatchments and Scenario 4) complete deforestation (Figure 6.3). The land use class "fallow land"as "worst case scenario"of clear cutting with a vegetation cover of only 1% and the macroporosity reduced by 90% compared to the forest was implemented for the deforested sites.

6.3.4 Model evaluation

Simulation runs were evaluated with the Nash-Sutcliffe efficiency (NSE), the mean error (ME) and the root-mean-squared error (RMSE). The equations for these "goodness-of-fit"descriptors are given below.

$$NSE = 1 - \frac{\Sigma(Q_O^t - Q_P^t)^2}{\Sigma(Q_O^t - \overline{Q}_O)^2} \tag{6.1}$$

$$ME = \frac{1}{n}\Sigma(Q_P^t - Q_O^t) \tag{6.2}$$

$$RMSE = \sqrt{\frac{1}{n}\Sigma(Q_P^t - Q_O^t)^2} \tag{6.3}$$

where Q_O^t are the observed values and Q_P^t are the predicted values at a given time step t.

6.4 Results

6.4.1 Catflow

A number of different subsurface structures and macropore parametrisations were modeled with Catflow (Table 6.2) and the results, i.e. the sum of specific outflow out of the right slope, were compared to measured specific discharges. Comparing hillslope outflow with catchment discharge was necessary due to lack of discharge data on the hillslope scale (see section 6.3.2).

The best (in terms of water balance and Nash-Sutcliffe coefficients) set-up included a loam layer at a depth of 1.75 m and a macroporosity factor of 32. The time series of simulated and observed specific discharges are shown in Figure 6.4. The Nash-Sutcliffe coefficient (Eq.1) for this model run was 0.46. Other goodness of fit descriptors are given in Table 6.4. While a Nash-Sutcliffe of 0.46 would be low for a calibrated model it is acceptable for a non-calibrated physically based model

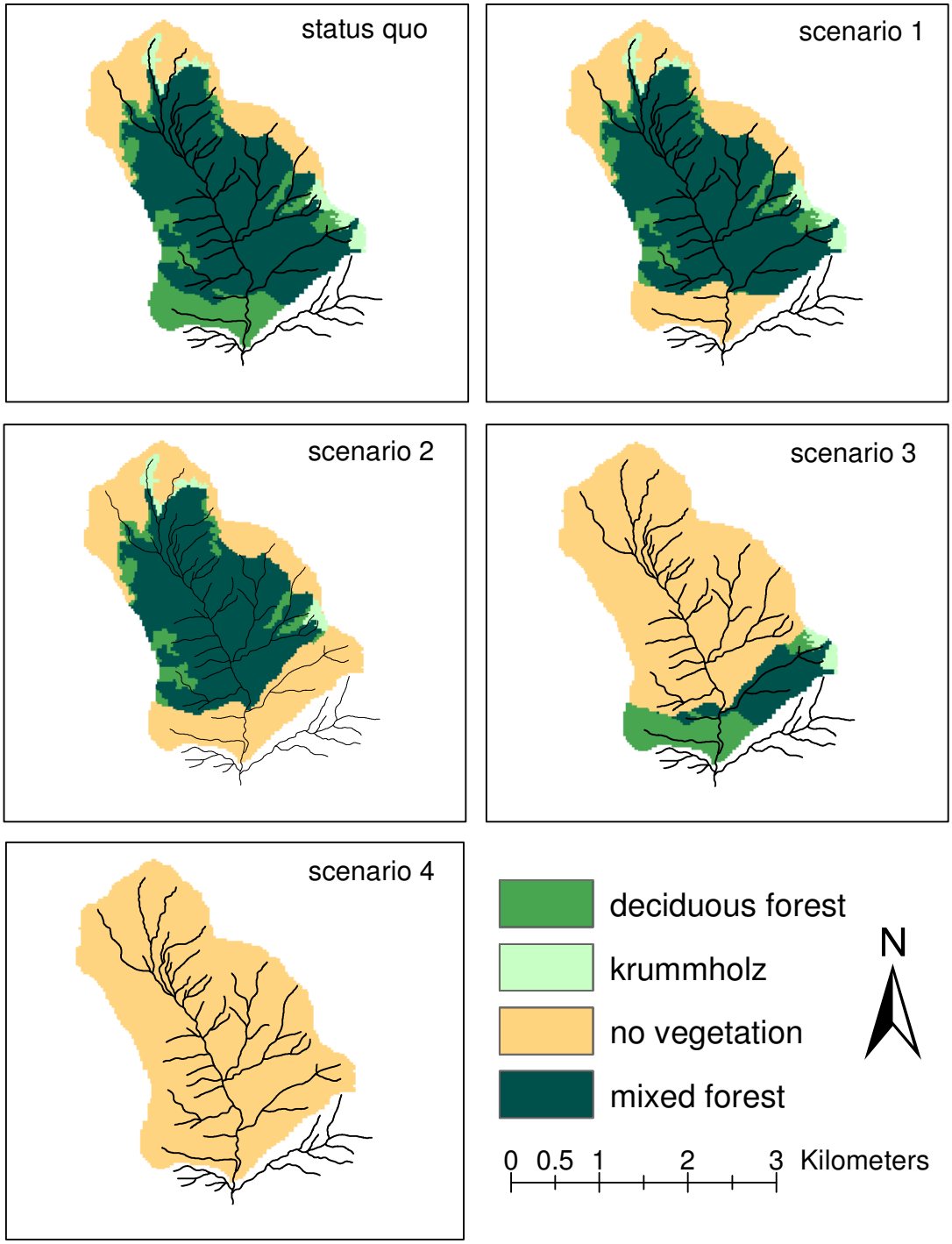

Figure 6.3: Land use scenarios simulated with Wasim

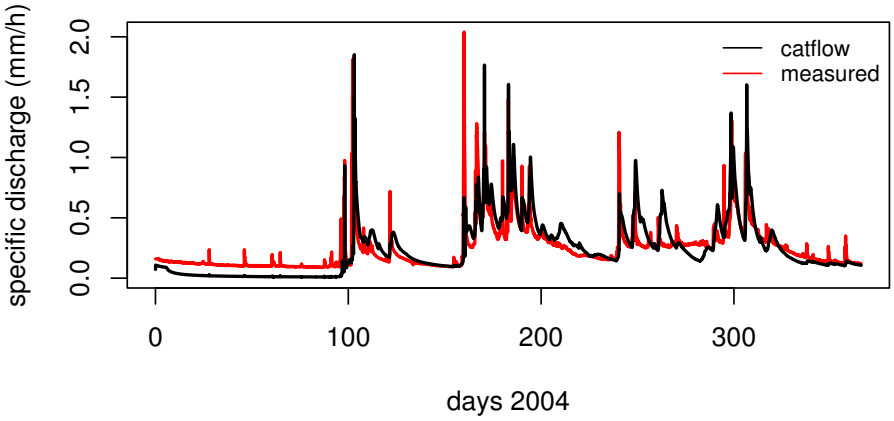

Figure 6.4: Observed and modeled time series for 2004 (Catflow)

considering the lack of detailed knowledge (especially concerning the depth to bedrock) and considering the fact that we are comparing hillslope outflow with the outflow of the entire catchment (thus not accounting for the effects of runoff routing and assuming that the catchment can be represented by a single slope). Additionally, winter flows are likely to be erroneous in the simulation, as snow effects can not be accounted for in Catflow. An example for this type of error can be seen in Figure 6.4: flow peaks were significantly overestimated by the model for the events on day 250 and 262 as a result of snowfall.

Generally must be said, that while long term recessions are simulated quite well, the event recessions of the model are much too slow. Outflow at the lower end of the slope occurs mainly in the layer above the low permeability layer and from the overflow of the saturated zone (nodes 5 and 7) (Figure 6.5a). However, further upslope (shown exemplarily for a crossection at 15 m distance from the right boundary) lateral flow occurs mainly at node 3, the interface of the two volcanic ash horizons (Figure 6.5b)

6.4.1.1 Subsurface structures

Comparing the best simulation run (set-up 1) with a set-up that did not include the lower permeability loam layer (set-up 2) shows that the inclusion of the loam leads to a faster and more pronounced response (Figure 6.6a). While it leads to an overestimation of flow peaks for some events; at other occasions, e.g. at day 160 in Figure 6.6a, little or no response is found in the simulated time series if the loam layer is not included. It thus seems likely that a layer interfaces, such as a layer of lower conductivity or a capillary barrier are causing fast lateral subsurface flow and thus response. This effect could not be achieved with the soil parameters determined from soil samples which were used to parametrized the top 4 horizons.

6.4.1.2 Macroporosity

Varying the macroporosity factor (F_{macro}) between 1 and 40 it was found that only if this factor was above 30 a response as fast and pronounced as was measured in the field could be achieved. However, some peaks are overestimated in this case. In

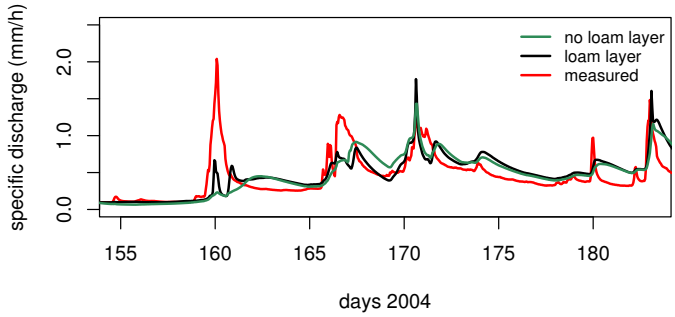

(a) The effects of different subsurface parametrisation. Comparison of SU1 (black) and SU2 (green)

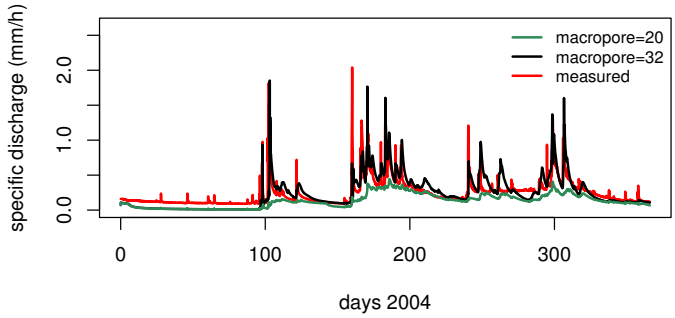

(b) The effects of the macroporosity factor F_{macro}. Comparison of SU1 (black) and SU3 (green)

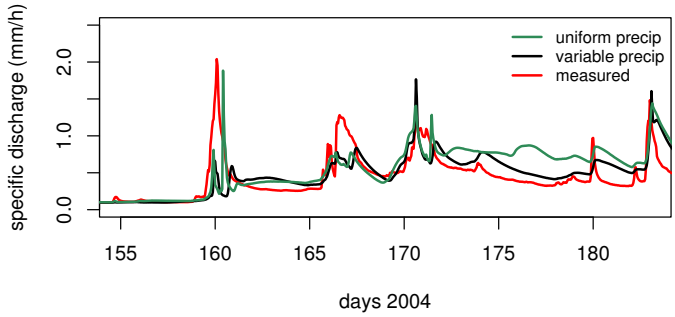

(c) The effects of precipitation characteristics. Comparison of SU1 (black) and SU4 (green)

Figure 6.6: Catflow - influence of subsurface structures, macropores and precipitation characteristics. (SU = model set-up)

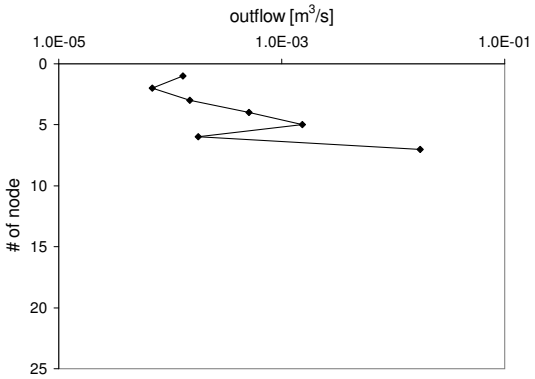

(a) Outflow at the lower end of the slope

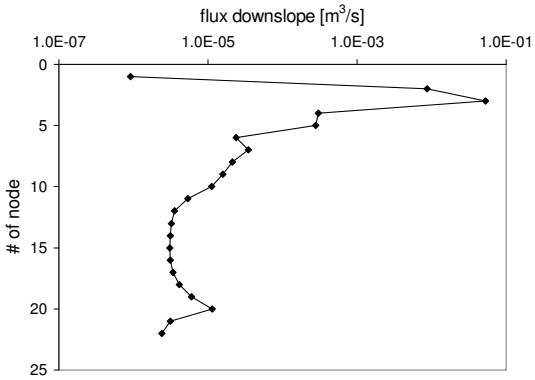

(b) Lateral downslope flow at 15 m distance from the lower end of the slope.

Figure 6.5: Vertical crossections of outflows and lateral flows for day 171 (Catflow)

Figure 6.6b the simulated specific discharge for the case of $F_{macro} = 20$ (set-up 3) and $F_{macro} = 32$ (set-up 1) is shown.

In an earlier set-up of Catflow vertical infiltration without macropores was compared to measured time series of soil moisture profiles (for location of the probes see Figure 6.1): model percolation proved to be much slower than observed soil moisture response (data not shown).

6.4.1.3 Rainfall redistribution

The effect of rainfall redistribution by the forest canopy was investigated by applying two scaled time series of precipitation alternatingly to the surface nodes. In Figure 6.6c variable (set-up 1) and uniform (set-up 4) rainfall input are compared. Uniform precipitation produces a higher peak during the first event (ca. day 160). This high peak is delayed and trailing a smaller first response. Another pronounced trailing peak can be observed at about day 172. Smaller trailing peaks were also observed in case of variable precipitation. For the event at day 174 only a very delayed response could be observed for the case of uniform precipitation. While the pronounced trailing peaks are mainly produced in the layer above the low permeability/loam layer, the delayed response on day 174 is produced by the outflow from the saturated zone. The reasons for these delayed peaks are still not clear and need to be investigated further. The fact that uniform precipitation often causes faster response (e.g. days 160, 165, 169) is most likely due to the fact, that in this case a homogeneous wetting front over the whole hillslope increases lateral flow, while the variable precipitation causes areas of low soil moisture where lateral flow is decelerated. Vertical water transport, however, is increased for variable precipitation input.

The annual runoff coefficients resulting from all model set ups shown in Figure 6.6, as well as the runoff coefficients determined from the measured data and the Nash-Sutcliffe coefficients are given in Table 6.2.

6.4.2 Wasim

6.4.2.1 Calibration

Wasim was calibrated with PEST for the period August 2002 - December 2003. The resulting best parameters are summarized in Table 6.3. For the entire calibration period a Nash-Sutcliffe coefficient of 0.71 was achieved. Considering only the year 2003 the Nash-Sutcliffe coefficient (Eq.1) increased to a value of 0.74. Figure 6.7a shows simulated and measured time series for all of 2003. Most of the peaks are underestimated by the simulation and during periods of low flow modeled discharge shows no response to rainfall events. From October on, flow is generally underestimated by the model, however, part of this apparent underestimation might be due to sedimentation in the stream gauge and thus incorrect measured discharges. The different flow components modeled by Wasim for the period of May-October 2003 are shown in Figure 6.7b. The recessions of direct flow are surprisingly slow, while baseflow only shows a seasonal response. Baseflow during the winter months is underestimated. The response to smaller rainfall events is mainly due to the interflow component, however, event recessions of total flow are much slower than the measured recessions. The events where direct flow (i.e. surface runoff) dominates are likely to be rain on snow events or events influenced by snow melt (10% of snow melt is surface runoff, see Table 6.3). It has to be mentioned that surface runoff has never been observed in the catchment during field campaigns in the months October-May.

6.4.2.2 Validation

Simulated and measured time series for the validation period (2004-2005) are shown in Figure 6.8. The Nash-Sutcliffe coefficient for the validation period is 0.66 (see also Table 6.4). Again, most of the peaks and often also baseflow are underestimated, leading to a mean error of -0.062 (Eq.2). As during the calibration period, smaller rainfall events and rainfall during summer low flow periods do not cause runoff response in the simulation.

6.4.2.3 Rainfall variability and its influence on model results

For the years 2004 and 2005 additional rainfall data from rain gauge G1 which was installed near the catchment outlet at the end of 2003 (see Figure 6.1) was available. Even though the raingauge (G1) and the climate station (CS) are only about 500 m apart, rainfall amounts can differ considerably. In order to investigate the influence of the chosen rainfall time series, the validation period (2004-2005) was simulated with the two time series as input to two separate model runs and the model results were compared. The goodness of fit parameters in Table 6.4 show that using data from G1 as input rainfall results in a lower Nash-Sutcliffe coefficient but also in a smaller mean error. If only 2004 is considered, discharge is even overestimated and the mean error amounts to +0.022. The two modeled time series as well as measured streamflow are plotted in Figure 6.9. Table 6.5 presents the annual amounts of precipitation for both rain gauges, as well as measured and simulated discharges and the resulting runoff coefficients. Annual runoff coefficients are underestimated by both simulations for 2005 and only the rainfall data of G1 in 2004 results in an overestimation.

6.4.2.4 Scenario analysis

4 different scenarios of deforestation were simulated using Wasim. The areas submitted to deforestation were assigned the same land use class (fallow land, only 1% vegetation cover) as the bare volcanic ashes on the catchment rim and amounted to 13% of the entire forest for scenario 1, 26% for scenario 2, 74% for scenario 3 and 100% for scenario 4. However, not only the size of the deforested area but also the location of these areas within the catchment are of importance. For maps

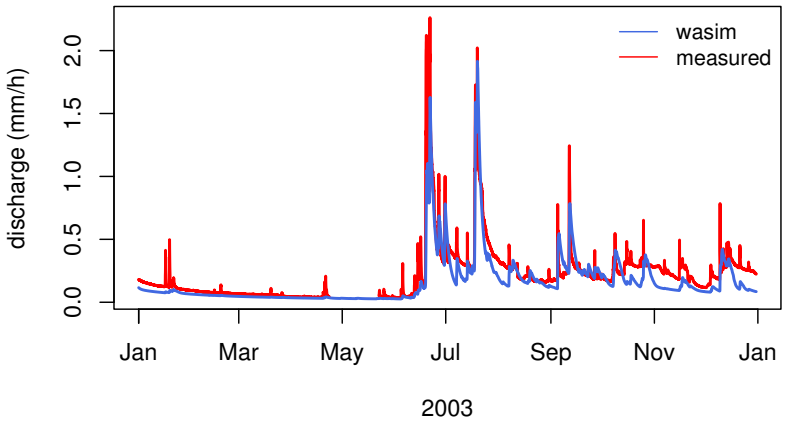

(a) Calibration period.

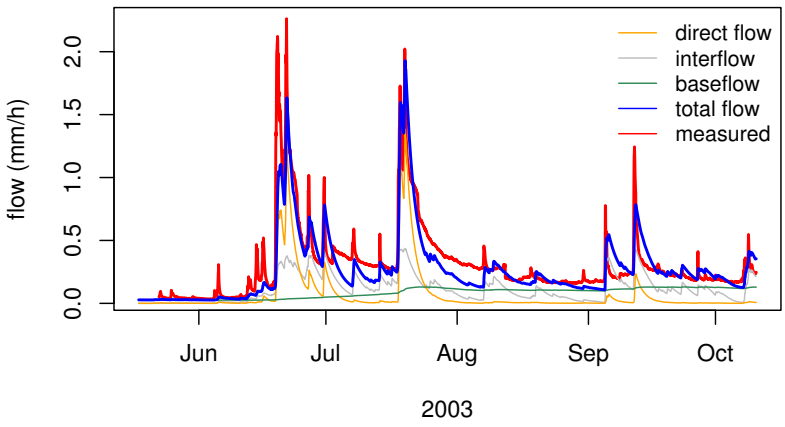

(b) Flow components of the Wasim simulation run.

Figure 6.7: Wasim: calibration period, total flow and flow components.

Table 6.4: Goodness of fit parameters for Wasim and Catflow. (CS stands for input rainfall data from the climate station and G1 for data from rain gauge G1 near the catchment outlet.

	Wasim calibration 03	Wasim validation (CS)	Wasim validation (G1)	Wasim (2004)	Catflow (2004)
Nash-Sutcliffe	0.74	0.66	0.51	0.41	0.46
mean error	-0.049	-0.062	-0.024	0.022	-0.004
RMSE	0.11	0.13	0.16	0.15	0.14

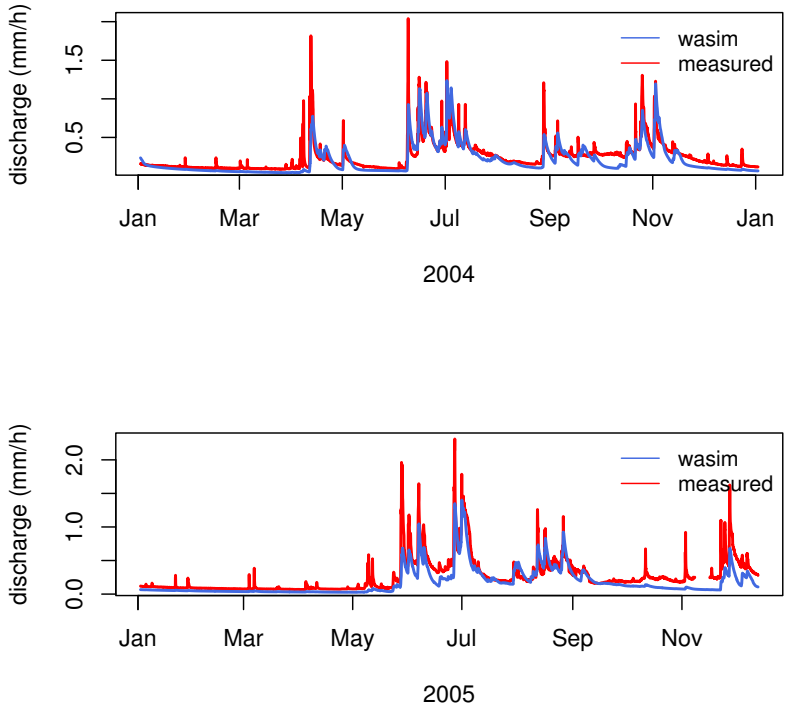

Figure 6.8: Validation of Wasim (using rainfall from the climate station as input)

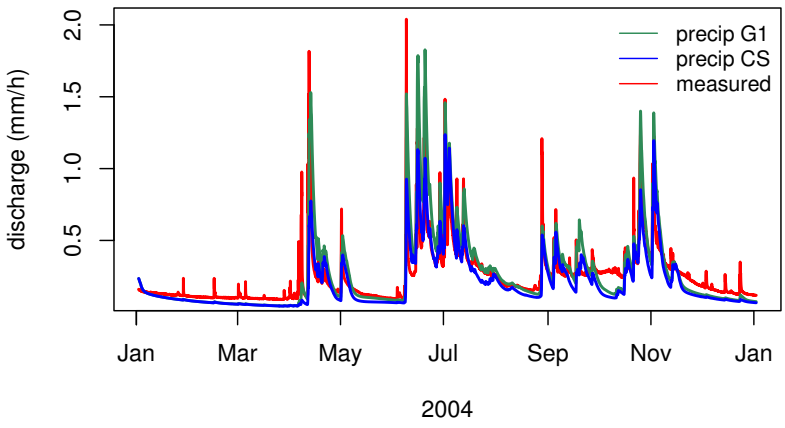

Figure 6.9: The effects of rainfall input time series on modelling results: climate station vs. rain gauge G1. (precip G1/precip CS= simulated time series of specific discharge using rainfall data from rain gauge G1/the climate station as input)

Table 6.5: Comparison of different rainfall input: climate station vs. rain gauge G1.

data source	year	rainfall (mm)	q(data) (mm)	q (Wasim) (mm)	runoff coefficient Wasim (-)	runoff coefficient data (-)
climate station	2004	2934	2128	1795	0.61	0.73
rain gauge G1	2004	3569	2128	2337	0.66	0.60
climate station	2005	2880	2199	1493	0.52	0.76
rain gauge G1	2005	2982	2199	1598	0.54	0.74

of the different scenarios see Figure 6.3.

The results of the scenario analysis are summarized in Table 6.6 and Figure 6.10. Mean discharge, maximum and minimum discharge as well as the annual sum and the standard deviation of flow all increase with increasing deforested area (Table 6.6). The maximum increase in peak flows is 30% (scenario 4) compared to the status quo, while mean flows increased by 21%. The fact that peak flows increase (Figure 6.10) is due to the fact that interception losses, evapotranspiration and macroporosity are lower in areas with no vegetation than in forested areas. Increases in mean flows of 110% and in mean peak flows of 32% after clearcutting were observed in a study by Iroumé et al. (2006), which was investigating the effects of timber harvest in the coastal range of Southern Chile. However, the soils of this area have a much higher clay content than the volcanic ash soils of the Malalcahuello Catchment, making a direct comparison difficult.

The importance of the location of the deforested slopes within the catchment can be seen when comparing the status quo and scenario 2 as well as scenarios 4 and 5. Both times the same area close to the catchment outlet is changed from forested to deforested. However, in the first case the catchment upstream of this area is still forested, while in the second case it is already unvegetated. While the resulting change in mean flows as well as the change in annual discharge is more or less the same, the second case leads to an increase in maximum flow fourteen times higher than in the first case. At the same time the increase in minimum flow is only a third of what it is in the first case (Table 6.6).

6.4.3 Model comparison

The comparison of the time series simulated by Catflow and Wasim shows that both models produce event recessions much slower than observed recessions (Figure 6.11a). The fact that Catflow overestimates winter peaks (6.11b) is most likely due to the fact that snow effects (storage of precipitation and later release during snow melt) are not incorporated. Nevertheless, considering only year 2004, the only year simulated with Catflow, Nash-Sutcliffe efficiencies as well as the mean errors (see Table 6.4) show a better fit for the Catflow simulation (both simulations were run with data from raingauge G1 as input). Furthermore, the annual runoff coefficient is 60% for the Catflow simulation which is equivalent to the runoff coefficient from the observed data (60%) while 66% were simulated with Wasim (Table 6.5).

6.5 Summary and conclusions

6.5.1 Catflow

Catflow was used to simulate runoff generation at the hillslope scale. With current set-up, which is based on field observations, it was possible to achieve Nash-Sutcliffe efficiencies of 0.46. This relatively low value might be due to the fact that we are comparing hillslope outflow with discharge from the entire catchment and could in part also result from the quality of the input rainfall time series (compare section 6.4.2.3 for the effects of the chosen rainfall time series on modelling results from Wasim). However, as event recessions generally tend to be too slow, the subsurface structure of the model hillslope is still likely to be incorrect. Other possible causes for the fast recessions observed in the field are threshold processes of preferential flow (which are not captured by the current simplified approach of macropore flow) or effects of hysteresis (which are not included in the van Genuchten curves used by the model). Long term recessions on the other hand are modeled quite well.

Due to our limited knowledge of the subsurface in the Malalcahullo Catchment and due to the fact that it is impossible to investigate the subsurface flow processes with a hillslope trench study as soils are too deep, the "structural"uncertainty in the model set-up is high. However, if a physi-

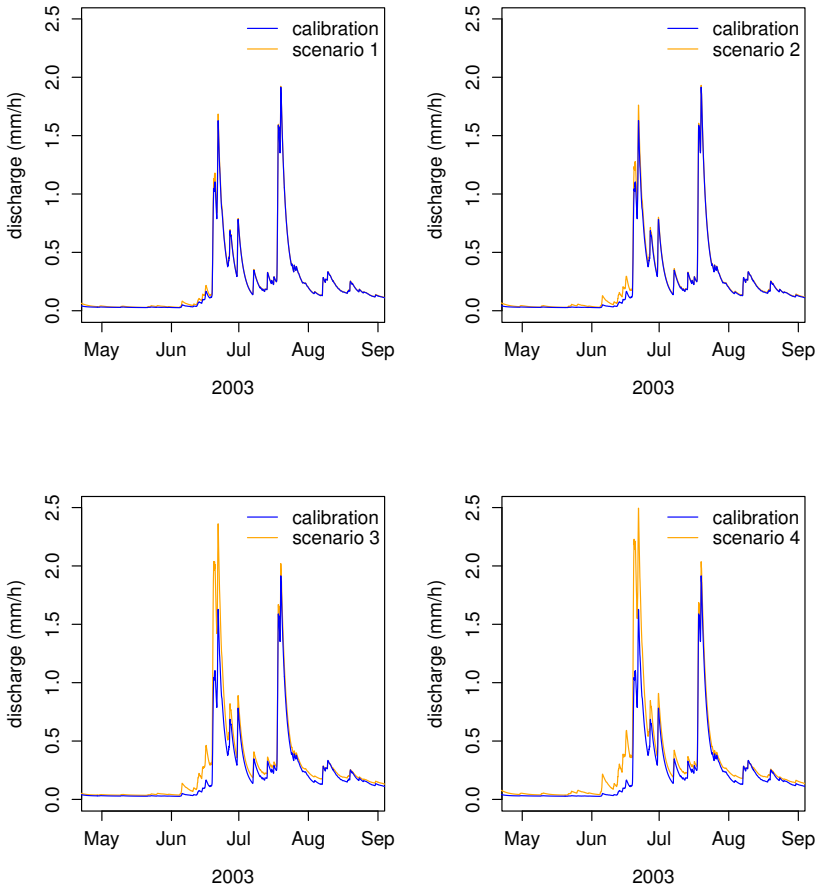

Figure 6.10: Results of the scenario simulations compared to the calibrated time series of the status quo.

Table 6.6: Scenarios of deforestation and resulting discharge characteristics.

scenario	mean q (mm/h)	max q (mm/h)	min q (mm/h)	st.dev.(q) (mm/h)	sum(q) (mm)
status quo	0.163	1.92	0.026	0.206	1424
scenario 1	0.167	1.92	0.028	0.209	1457
scenario 2	0.171	1.93	0.029	0.214	1494
scenario 3	0.188	2.36	0.034	0.259	1646
scenario 4	0.196	2.50	0.035	0.271	1717

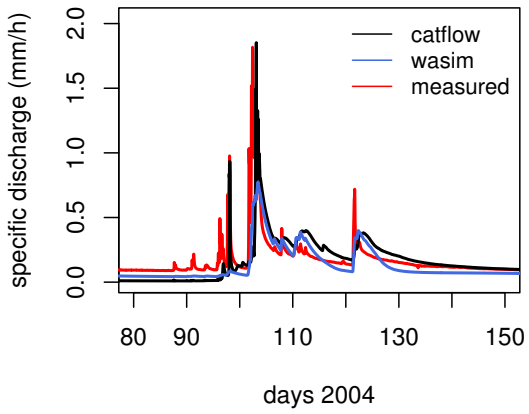

(a) Model comparison for April/May 2004.

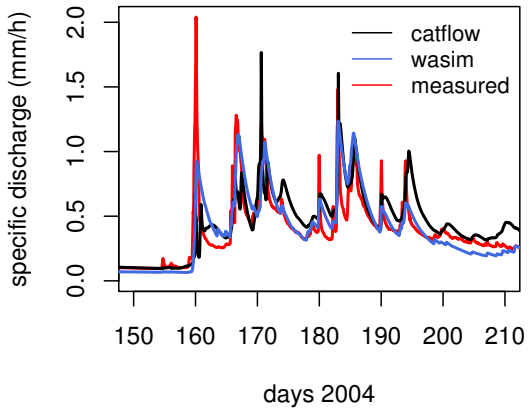

(b) Model comparison for June/Juli 2004.

Figure 6.11: Comparison of model results for Catflow and Wasim

cally plausible subsurface structure can be found that reproduces the response characteristics observed in the field, this will help us to better understand runoff generation processes in the Malalcahuello Catchment. While our hypotheses concerning the importance of vertical and lateral preferential flow as well as the importance of redistribution processes in the forest canopy helped us to improve model performance, the model still does not fully capture runoff response. The model-inherent simplification of the 2D/quasi-3D representation of the hillslope and the simple implementation of macropore flow probably over-simplify structures and processes on this slope.

The different model set-ups tested in this study (low permeability layer, macropores, variable precipitation) all show the big importance of preferential flow for the Malalcahuello Catchment. Despite the high hydraulic conductivities of the volcanic ash soil, the fast runoff response observed in the field can only be achieved with a macroporosity factor > 30. The implementation of a hypothetical loam horizon at 175 cm (which has not been found in the field) only led to slightly better results (Nash-Sutcliffe increased from 0.44 to 0.46). However, including this layer of lower permeability increases lateral preferential flow, while simulating spatially variable precipitation input as a result of redistribution processes in the forest canopy increases vertical preferential flow.

Apart from the "structural uncertainties"described above, other sources of uncertainty, such as the uncertainty of the input rainfall (see section 6.4.2.3), the uncertainty of the measured discharges and also the uncertainty of soil parametrisation from a limited number of soil samples need to be mentioned. While it is difficult to quantify these uncertainties they should be kept in mind when analysing model results.

6.5.2 Wasim

The process-oriented model Wasim-ETH was used to model rainfall-runoff response at the catchment

scale. A Nash-Sutcliffe efficiency of 0.74 was achieved for the calibration period (2003). While this is clearly better than the efficiency achieved with Catflow it is significantly lower than the fits achieved in other studies using Wasim-ETH (Niehoff et al., 2002; Schulla, 1997). However, in the study of Niehoff et al. (2002) it proved to be necessary to calibrate advective and convective events separately because subsurface flow components were underestimated in the first case and overestimated in the second. This separation of event types was not carried out in the Malalcahuello study, where a single parameter set was used over the entire period.

Nash-Sutcliffe efficiencies are also low for the validation period and there are obvious deficiencies in reproducing baseflow (which is underestimated) and event recessions (which are too slow in the simulated time series). Some of the differences between modeled and observed time series are likely due to "imperfect"input rainfall time series. Already the closely neighboring raingauges at the climate station (CS) and at the catchment outlet (G1) produce differing rainfall time series, while in the simulation uniform rainfall over the entire catchment is assumed. However, the incorrect reproduction of baseflow and event recessions cannot be explained by rainfall input and are likely due to wrong process representation and the fact that the hydro-geological conditions of the catchment are incorporated only in the strongly simplified concept of a linear storage.

Comparing Wasim and Catflow for the year 2004 shows that in this case Catflow produces a better fit to the observed time series than Wasim. The overestimation of winter peaks by Catflow is likely due to snow effects. Both models produce unrealistically slow event recessions.

6.5.2.1 Scenario analysis

Even though certain flow characteristics could not be reproduced with Wasim, the current set-up seemed good enough for a first estimate of the influence of land use on hydrological response. The analysis of land use scenarios showed an increase of flows (minimum and maximum) as well as an increase in standard deviation of flow with increasing deforested area. Scenario analysis furthermore revealed the importance of location of the deforested areas. Deforestation of the area close to the catchment outlet had little effect on peak flows (+0.01 mm/h) compared to the status quo while the upstream catchments were still forested. However, in case of deforestation in the upstream catchment, additional deforestation of this area caused a considerable increase in peak flow (+0.14 mm/h).

Other interesting and probably also more realistic changes of land use in this nature reserve would have been the incorporation of hiking trails and forest roads (the scenario of touristic development). In this case the network of hiking trails has the potential to become a second drainage network during rainfall events (as has been observed in the forest plantations just outside of the research catchment). This second drainage network might considerable change the magnitude of flow peaks. However, this type of scenario is difficult to incorporate in the Wasim model set-up and was therefore not included in the current study.

Generally has to be said, that the modelling of land use change scenarios simulated with a model that is calibrated to the status quo produces results that are highly uncertain. Bronstert (2004) states that rainfall-runoff models for this purpose need to incorporate the hydrological processes and their interactions in a way that system changes can also be covered. Multi-process and multi-site calibration is a prerequisite for this task (Bronstert, 2004). Ewen & Parkin (1996) suggested that a model must prove its ability to model catchment output "blindly", i.e. without the use of discharge data for calibration in order to be able to model land use change. If a model is able to "predict"current conditions without prior knowledge of catchment output it is likely able to predict future conditions (where catchment output is also unkown). A model calibrated to a certain status quo is calibrated to a

certain process ensemble. However, it is difficult to identify the effects of land use characteristics on these calibrated parameters (Hundecha & Bardossy, 2004). A shift in process ensemble thus is most likely not captured by the model when simulating a change in land use or even climate. Possible processes caused by deforestation in the Malalcahuello Catchment, which are not incorporated in the model are an increase in hydrophobicity in the top soil layer (chapter 5), followed by surface runoff and subsequent erosion. The incorporation of such process knowledge gained at the plot or hillslope scale into larger scale models is one of the key questions in land use change modelling (Bronstert et al., 2007 (in press).

Acknowledgements

The authors would like to thank Andres Iroumé for the use of the climate station and streamflow data for 2002-2003 and his logistic support during field campaigns, Andreas Bauer, Hardin Palacios and Luis Opazo for their help in the field and Dominik Reusser for help in the field as well as for the use of his computer scripts. This work was partially funded by the International Office of the BMBF (German Ministry for Education and Research) and Conicyt (Comisión Nacional de Investigación Científica y Tecnológica de Chile) and the "Potsdam Graduate School of Earth Surface Processes", funded by the State of Brandenburg.

Chapter 7

Summary and conclusions

The runoff generation processes in a data scarce, undisturbed catchment characterized by volcanic ash soils, steep slopes, old-growth forest and high rainfall amounts were investigated with a "multi-method approach". This approach has the potential to characterize rainfall-runoff response in data scarce catchments by replacing long time series of precipitation and discharge data with a multi-angle data set covering many aspects of runoff generation. The resulting data set can be best visualized as a puzzle which gives us a maybe not complete but nevertheless useful and information-rich picture of the dynamic ensemble of runoff generation processes in this catchment. This picture or perceptual model of runoff generation was tested with the physically based model Catflow on the hillslope scale. Wasim-ETH, a process based model for the meso-scale, was then used to investigate the influence of land use on catchment response.

7.1 Experimental results

Research questions were formulated by using general prior knowledge on soil type, topography and climate of the area. As volcanic ash soils are known for their high porosities and hydraulic conductivities, as the slopes of the catchment are steep and the climate characterized by high rainfall amounts, these first questions were a) how important is subsurface stormflow? b) what type of subsurface flow is dominant and what are the underlying structures? and c) how important are groundwater contributions during events? To answer these questions extensive data collection seemed indispensable. It was necessary to have information on hydraulic conductivities for various depths and layers, to study the flow paths in the unsaturated zone and to explore subsurface structures such as layering and depth to bedrock. To investigate the relative importance of subsurface stormflow and groundwater contributions we needed to know more about the components of the storm hydrograph, the dynamics of soil moisture at different depths and the response of groundwater levels during rainfall events.

Data was collected within a time frame of 2-3 years. While some data was measured continuously over the years (rainfall, water level, ground water level, soil moisture, temperature of stream and groundwater), all other measurements, sampling and experiments (Table 1.1) were carried out during the field campaigns in March 2003, December 2003 – February 2004, October 2004 – December 2004, November 2005 – December 2005 and April – May 2006.

The results of this "multi-method-approach"produced a perceptual model of runoff generation processes in the Malalcahuello catchment (Table 3.4). It was found that two main principles are dominant: *Response to rainfall is generally fast* on the one hand. Short response times and quick recessions are caused by vertical preferential flow (see section 7.1.1) and rapid

lateral flow (section 7.1.2). On the other hand a *large subsurface storage* (section 7.1.3) results in a strong dampening of rainfall signals on the other hand (event runoff coefficients are <10%, often even <2%). Additionally, several findings suggest a *shift in processes from winter (wet) to summer (dry)* causing changes in in flow patterns, changes in groundwater-surface water interactions and changes in the response of stream chemistry during rainfall events (section 7.1.4 and chapter 4).

7.1.1 Vertical preferential flow

Vertical preferential flow (either along roots or due to fingering) is more likely to be the rule than the exception in this catchment. This type of flow has been observed in all dye tracer experiments carried out in the forested part of the catchment while water infiltrated as horizontal front on the bare volcanic ashes up on the catchment rim. Flow patterns of preferential flow at the forest plots change significantly from summer to winter. Water infiltrates as a front which later breaks up into several pathways during winter. During summer water infiltrates along narrow pathways in the top 15 cm and forms separate bulb like plumes at greater depth (chapter 4). As the top layer was very dry during the three summer experiments, this pattern can be explained by hydrophobicity in the upper horizon (chapter 5).

The high spatial variability of throughfall observed in the Malalcahuello Catchment (chapter 3) is further reinforcing preferential flow, as areas of higher moisture content will have higher unsaturated conductivities. The spatial heterogeneity of throughfall will at the same time also increase the spatial heterogeneity of hydrophobicity. Spots of high water input are therefore likely to become preferential flow paths.

Soil moisture event response along the 1 m profiles showed very fast vertical water movement for two of the profile probes, especially during summer events with high rainfall intensities. Dye tracer experiments at these locations and subsequent excavation of the probes showed that these two probes were located within preferential flow paths, while the third probe was located in between flow paths. (chapter 5). The temporally persistent small scale soil moisture patterns found during the manual soil moisture measurements were also attributed to the presence/absence of preferential flow paths. This further supports the conclusion that vertical preferential flow paths are both very common as well as temporally persistent in the Malalcahuello Catchment (chapter 5).

7.1.2 Rapid lateral flow

Vertical preferential flow results in fast transport of water to greater depths. However, rapid lateral flow processes are also necessary to produce the fast event response observed in the catchment. As groundwater response is found to be much slower then streamflow response, this rapid lateral flow is likely to happen either in pipes, the unsaturated zone or in temporary perched saturated zones. Soil moisture dynamics show that lateral flow does indeed happen in the unsaturated zone: during rainfall events an increase in soil moisture was observed in deeper layers while the horizons above showed no response. Wetting of this deeper layer did thus not result from vertical percolation (chapter 5). Lateral flow down-slope was also observed for a dye tracer experiment with higher application rates. In this case lateral flow occurred mainly within the duff layer (chapter 3). The layer interfaces resulting from the textural differences between different layers of volcanic ash (from gravel fraction to silty sand) are other likely flow paths (chapter 3). However, connectivity of these layers along the hillslopes is necessary in order to make them hydrologically relevant on hillslope or catchment scale. Neither pipes nor temporary perched saturated zones could be observed during field campaigns.

7.1.3 The subsurface

The large subsurface storage results in low event runoff coefficients on the one hand (see chapter 2) and in persistent flows even after several weeks of drought on the other hand. The high porosities of the volcanic ash soils (determined in the lab) and the large unsaturated zone (determined by augering and geo-electrical sounding) confirms the capacious volume of this storage. The fact that annual rainfall amounts and annual runoff coefficients are high suggests that evapotranspiration in this system is energy limited (apart from during rare periods of drought). As it is possible to nearly close the water balance using potential evaporation measured at the lower climate station, no significant losses to deep groundwater are expected (chapter 3).

7.1.4 Seasonal shift in processes

The shift in processes from summer to winter was observed in flow patterns, groundwater-surface water interaction, and stream chemistry response (chapter 4). Shorter response times of streamflow, soil moisture and groundwater were found for summer events (chapter 5). One of the likely causes for this shift in processes is increased hydrophobicity in the upper soil horizons after extended dry periods, causing persistent small scale soil moisture patterns and more pronounced fingering (chapter 4 and chapter 5). Futhermore, the lateral flow in the duff layer, which was observed during a high intensity dye tracer experiment in late winter, will be increased by hydrophobicity of the top soil layer in dry summer periods (chapter 4). Hydrograph separation carried out with a number of different tracers for an event in December (late winter - wet season) shows that pre-event water is dominating runoff generation. Throughout the event the fraction of pre-event water remains $>$ 85%. An event in February produced a very different response of tracers (especially of SiO_2 and deuterium), and impossible fractions of pre-event water of more than 100% were calculated for some of the tracers. This also suggests a shift in processes from late summer to early spring (or dry to wet season). Processes not captured by this simple two component separation are likely to be of importance during the dry season, where probably one or more additional flow components are influencing stream chemistry during the event. Interflow along the duff layer interface (see above) might have been an important flow path/flow component with a distinct chemical signature during this event (chapter 4). The strong response of silicate in February, suggesting fast flow paths which were not activated during the December event, might also be explained by flow in the duff layer (or along other near surface layer interfaces) (chapter 4).

The narrow flow paths observed during the dye tracer experiments in summer are likely to transport rainwater faster to greater depths than the flow patterns observed during the wet season (chapter 4). This could also explain the shorter response times observed in soil-, ground- and streamwater during summer (chapter 5).

7.1.5 Open questions

The experimental results provided insight into many of the prevailing processes, however, several open questions remain. We still do not know the exact source of fast response of streamflow, as both soil and groundwater often respond slower than the stream (chapter 3 and chapter 5) . Structures controlling rapid lateral flow could be one of the following: pipes, which have not been observed so far, flow along the bedrock or flow along layer interfaces. Results do not confirm the existence of a deep groundwater system, however, the existence of such a system cannot be ruled out entirely. There also seems to be a contradiction between the results of hydrograph separation (high fraction of old water during events) (chapter 4) and the lag times of at least several hours between surface water and groundwater response at well W3. This might be explained by the replacement of old water

with a similar chemical signature as groundwater in zones of rapid lateral flow along layer interfaces or by the phenomenon of kinematic waves in the unsaturated zone, which leads to response velocities much faster than pore water velocities (Torres et al., 1998; Rasmussen et al., 2000; Williams et al., 2002). And finally, the question of residence time: we do not know how long the water remains in the catchment, how „old" the water is that flows in the stream. It could have entered the system that same year or have been stored for longer than that. These questions could be answered by determining isotope ratios in rainwater and streamflow over a longer period of time.

7.1.6 Evaluation of experimental methods

Most experimental studies in poorly gauged catchments are faced with limited time, financial resources and manpower. The experimental methods used in this study were thus evaluated for a) the gain of process understanding plus the gain of important model input and validation data and b) the expenditures necessary for their application, such as labor and financial cost. This evaluation is summarized in Table 3.5.

In an attempt to further minimize time and financial expenditures while keeping the gain of process understanding as high as possible, the assessment of experimental methods used in this study was used to select the most essential methods. Expensive and time consuming methods were only selected if the gain in process understanding was rated as high. Discharge measurements, for example, are very time consuming but nevertheless crucial. Event hydrograph separation by isotopic tracers is both time consuming and expensive but can deliver high-level integral information about runoff generation in the catchment. Isotopic tracers are preferred over other geo-chemical tracers because of their conservative behaviour. The measurement of water temperatures in wells and in the stream as well as the measurement of electric conductivity have the advantage of producing continuous time series of potential (non-conservative) tracers at relatively low cost. Continuous measurement of soil moisture profile gives valuable insights in flow processes in the unsaturated zone, especially when combined with dye tracers (chapter 5) and are worth the relatively high costs of the sensors. Both, laboratory analysis of soil cores as well as permeability measurements in the field deliver valuable information, however, laboratory analysis of soil cores was preferred. Lab analysis has the advantage that not only hydraulic conductivities can be measured, but also soil moisture characteristic curves. The use of geophysical techniques such as electric resistivity soundings is expensive, time consuming and especially difficult on densely forested steep slopes. Nevertheless, it is the only possible source of information concerning depth to bedrock or groundwater table in this catchment, as soil layer thickness is at least several meters. While highly variable throughfall amounts are likely to influence runoff generation and this fact should be kept in mind, the actual measurement of this variability is probably of less importance in cases of severe time constraint (chapter 3).

7.1.7 Disappointments

While field campaigns in the Malalcahuello Catchment were for the most part very successful (especially given the limited man-power and very difficult accessibility of most of the catchment), there are also a few disappointments to report.

7.1.7.1 Nested catchment approach

The data produced by the nested catchment approach, where 4 subcatchments were instrumented with water level sensors, suffers from high uncertainties as rating curves for these stream gauges only contain 21-24 data points. The low number of data points is due to the difficult accessibility of the stream gauges. During the hydrologically interesting times of peak flows, hiking in the stream - the only way of access - is too dangerous and

stream gauging impossible. A quantitative comparison of the subcatchments on the basis of specific discharges or runoff coefficients is therefore highly uncertain. However, general comparisons of response times and dynamics are possible with the achieved continuous time series of water levels.

7.1.7.2 Measuring snow water equivalent

As runoff generation in the Malalcahuello Catchment during the winter months is clearly influenced by snow, the quantification of snow water equivalents was considered important. However, due to the remoteness and difficult accessibility of the rain gauges at higher elevations it was impossible to equip these gauges with the necessary heating system for the measurement of snow water equivalents. A maintenance-free power supply for such a heating system would have been necessary. The use of snow pillows was also prevented by the difficult accessibility as well as by high financial costs. Snow heights were measured at the climate station during winter 2005, but transfer to the catchment scale proved to be difficult. Because of the dense forest cover, areal photos or satellite images to determine snow limits were not a viable alternative.

7.1.7.3 Comparison with the Piedra Santa Catchment

Data was also collected in the Piedra Santa Catchment, a neighbouring catchment with mixed land use (chapter 3). This included measurements of water level and streamflow (which were mainly carried out by the Universidad Austral de Chile), water quality measurements, permeability measurements with the Guelph permeameter and measurements with a double ring infiltrometer. A comparison of the Piedra Santa and the Malalcahuello Catchment was planned to assess the effect of land use and for the development and parametrization of land use change scenarios. However, direct comparison of the two catchments, as well as clear identification of land use effects proved to be difficult, as slopes in the Piedra Santa Catchment are significantly less steep (average slopes of 18.5° compared to 27°). Furthermore the presence of wetlands upstream of the stream gauge in the Piedra Santa Catchment has likely a significant effect on streamflow response as well as on water quality.

7.2 The Experimental Hydrology Wiki

During several phases of this dissertation, e.g. experimental design, choosing suitable equipment and subsequent installation as well as equipment maintenance, I sometimes found myself in the situation where communication with other hydrologists who had done the same type of measurement or used the same type of equipment and come across the same type of problems would have been very helpful. However, this "experienced field hydrologist"knowledgeable in all types of methods and equipment is not easily found.

I therefore propose a suitable internet platform for the collection of this type knowledge and experiences. This platform has the potential to serve several purposes: it could help us to learn about, recommend, question and discuss new and established, basic and advanced methods of experimental hydrology. It could help us to avoid reinventing the wheel each time we start out measuring something we haven't measured before. It could help us not to make the same mistakes others have made before us. It could help us to share new ideas and concepts. It could help us to find the methodology and the equipment suitable for our investigation. After some thought, research and discussions with other experimental hydrologists, I came to the conclusion that a wiki could be such a suitable platform. The "Experimental Hydrology Wiki", initiated in March 2007, can now be found at **http://www.experimental-hydrology.net**.

A wiki is a collaborative website which can

be directly edited by anyone with access to it. In other words, a very simple, easy-to-use user-maintained database for creating, browsing and searching information (as defined in Wiktionary and Wikipedia). There are thus three main ways to use the wiki: you can read articles and thus obtain information, you can contribute your experiences by writing articles or adding to already existing articles or you can interact with other users through the "Community Portal", the "Help Desk"or simply through the discussion pages to each of the articles. It is also possible to contact other users directly by email or on their personal user pages. The "Experimental Hydrology Wiki"has by now (October 2007) 42 registered users, has been accessed over 1600 times and contains 28 articles on different types of hydrological equipment as well as research catchments. It also contains a section on "Things that went wrong", as these experiences are rarely published in the scientific literature, but can nevertheless be of great value for field hydrologists about to make the same mistake...

However, such a platform can only be successful if enough people take the time to share some of their knowledge and experiences. I therefore want to invite all readers of this dissertation to contribute to the "Experimental Hydrology Wiki", either personally or by advertising it among students and colleagues.

7.3 Modeling event response, runoff generation processes and land use scenarios

Three different types of models have been used for three different purposes in the study of the Malalcahuello Catchment. A linear statistical model for the prediction of event runoff coefficients was developed for an initial assessment of the hydrological response and first catchment characterization. A physically based model (Catflow) was used to test the process hypotheses developed from the experimental results and a process oriented catchment model (Wasim-ETH) was used to investigate the influence of land use on catchment response.

7.3.1 Linear statistical modeling of event based runoff coefficients

Even though the comparison of runoff coefficients of different catchments is a rather simple and standard approach to assess the differences in rainfall-runoff responses, this proves to be difficult due to inconsistencies in terminology as well as a large variability in methodology. The determination of event runoff coefficients is often preceded by hydrograph separation, in order to separate the event response from "background flow", and many different methods for this separation are in use. Event flow in this study was determined with a simple straight line separation method combined with a semi-automatic determination of the endpoint of event flow (see chapter 2). This newly developed method of event-based hydrograph separation has three main advantages in comparison to the other separation methods applied in this study: it is at least partly theoretically based, it does not suffer from a more or less subjective determination the endpoint of event flow and it can also be used with multiple peak events. Furthermore it does not claim to offer information on the progression of baseflow between beginning and end of event flow. The routine could easily be automated allowing for faster data processing in case of larger data sets.

The objective and consistent determination of runoff coefficients might be even more important in data-scarce catchments than elsewhere, as rainfall and runoff are generally the first parameters to be measured in previously ungauged catchments. Having collected data for a few events, the natural question to ask oneself is: „How does the catchment respond to rainfall?" Event runoff coefficients are one of the first parameters to be extracted from these short time series and thus contain the first information on rainfall runoff response of a data-scarce catchment. The method of employing a linear statistical model for runoff coefficients to infer runoff processes and thus using the model as an additional catchment descriptor is es-

pecially useful in these catchments. However, at least several months of higher resolution discharge and precipitation data are needed in order to accumulate a sufficient number of rainfall events. The more additional data (e.g. on soil physics, hydrogeology or soft data such as observations of local residents) is gathered on targeted field campaigns the better the results of the statistical analysis (i.e. the statistical model) can be interpreted.

Overall, event runoff coefficients determined for the Malalcahuello catchment are very low (a third of the events has runoff coefficients $< 2\%$) which is probably due to the extremely high porosities of volcanic ash soil, interception (ca. 80% of the catchment are covered with forest), and the lack of anthropogenic influences resulting in soil compaction (see chapter 2). The linear statistical model developed with data from 17 rainfall events shows that simple interrelationships can be used to predict runoff coefficients with surprisingly good results. Total precipitation and pre-event discharge proved to be the most important predictor variables in our study. Runoff coefficients increase with total precipitation. The more rainfall, the higher the fraction of event flow during the event. This does not necessarily mean that it is the precipitation water itself which is being routed to the stream, as would be the case for overland flow (chapter 4). Possible reasons could be rising groundwater tables, groundwater mounding (increasing hydraulic gradients), pipe flow, but also saturation overland flow. However, due to the extremely high porosities as well as hydraulic conductivities of the volcanic ash soil (chapter 3), overland flow is not likely and has so far not been observed in this catchment. The positive correlation of pre-event discharge indicates that this parameter seems to be a good indicator of catchment state prior to rainfall. Pre-event discharge could be describing groundwater and soil water storage and associated momentarily active runoff processes. It was possible to improve model performance slightly by including the maximum rainfall intensity as additional predictor. However, as the estimated coefficient for this parameter is negative, maximum station rainfall intensity seems to serve as proxy for one or several rainfall characteristics (see chapter 2).

7.3.2 Process modeling on the hillslope scale

Catflow was used to simulate runoff generation at the hillslope scale. With current set-up, which is based on field observations, it was possible to achieve Nash-Sutcliffe efficiencies of 0.46. This relatively low value might be due to the fact that we are comparing hillslope outflow with discharge from the entire catchment. Moreover, the use of a single rainfall time series for the characterization of catchment rainfall is probably inadequate. However, as event recessions generally tend to be too slow, the subsurface structure of the model hillslope is still likely to be incorrect. Possible causes for the discrepancy in modeled and observed recessions are threshold processes of preferential flow (which are not captured by the current simplified approach of macropore flow) and effects of hysteresis (which are not included in the van Genuchten curves used by the model). Long term recessions on the other hand are modeled quite well (see chapter 6).

Due to our limited knowledge of the subsurface in the Malalcahullo Catchment and due to the fact that it is impossible to investigate the subsurface flow processes with a hillslope trench study as soils are too deep, the "structural"uncertainty in the model set-up is high. Nevertheless, if a physically plausible subsurface structure can be found that reproduces the response characteristics observed in the field, this will help us to better understand runoff generation processes in the Malalcahuello Catchment. While our hypotheses concerning the importance of vertical and lateral preferential flow as well as the importance of small scale rainfall variability (resulting from redistribution processes in the forest canopy helped us to improve model performance), the model still does not fully capture runoff response. The model-inherent simplification of the 2D/quasi 3D representation of the hillslope and the simple implementation of macro-

pore flow probably over-simplify structures and processes on this slope.

The different model set-ups tested in this study (low permeability layer, macropores, variable precipitation) all show the big importance of preferential flow for the Malalcahuello Catchment. Despite the high hydraulic conductivities of the volcanic ash soil, the fast runoff response observed in the field can only be achieved with a macroporosity factor > 30. The implementation of a hypothetical loam horizon at 175 cm (which has not been found in the field) only led to slightly better results (Nash-Sutcliffe increased from 0.44 to 0.46). Including this layer of lower permeability increases lateral preferential flow, while spatially variable precipitation input (i.e. throughfall variability) increases vertical preferential flow (see chapter 6).

Apart from the "structural uncertainties"described above, other sources of uncertainty, such as the uncertainty of the input rainfall, the uncertainty of the measured discharges and also the uncertainty of soil parametrisation from a limited number of soil samples need to be taken into account. While it is difficult to quantify these uncertainties, they should be kept in mind when analyzing model results.

7.3.3 Modeling land use scenarios on the catchment scale

The process-oriented model Wasim-ETH was used to model rainfall-runoff response at the catchment scale. A Nash-Sutcliffe efficiency of 0.74 was achieved for the calibration period (2003). While this is clearly better than the efficiency achieved with Catflow it is significantly lower than the fits achieved in other studies using Wasim-ETH (Niehoff et al., 2002; Schulla, 1997). However, in the study of Niehoff et al. (2002) it was necessary to calibrate advective and convective events separately because subsurface flow components were underestimated in the first case and overestimated in the second. This separation of event types was not carried out in the Malalcahuello study, where a single parameter set was used over the entire period (see chapter 6).

Nash-Sutcliffe efficiency is slightly lower (0.66) for the validation period. There are deficiencies in reproducing baseflow (which is underestimated) and event recessions (which are too slow in the simulated time series) (see chapter 6). Some of the differences between modeled and observed time series are likely due to "imperfect"input rainfall time series. The importance of rainfall variability was confirmed by comparing the time series measured at two closely neighboring raingauges at the climate station and at the catchment outlet (while in the simulation uniform rainfall is assumed over the entire catchment). However, the incorrect reproduction of baseflow and event recessions cannot be explained by rainfall input and are likely due to wrong process representation and the fact that the hydro-geological conditions of the catchment are incorporated only in the strongly simplified concept of a linear storage.

7.3.3.1 Scenario analysis

Even though certain flow characteristics could not be reproduced with Wasim, the current set-up seemed good enough for a first estimate of the influence of land use on hydrological response. 4 different scenarios of deforestation were simulated. The analysis of these land use scenarios showed an increase of flows (minimum and maximum) as well as an increase in standard deviation of flow with increasing deforested area. Scenario analysis furthermore revealed the importance of location of the deforested areas. Deforestation of the area close to the catchment outlet had little effect on peak flows (+0.01 mm/h) compared to the status quo while the upstream catchments were still forested. However, in case of deforestation in the upstream catchment, additional clear-cutting of this same area near the catchment outlet caused a considerable increase in peak flow (+0.14 mm/h) (see chapter 6).

The modelling of land use change scenarios sim-

ulated with a model that is calibrated to the status quo produces results that are highly uncertain. Bronstert (2004) states that rainfall-runoff models need to incorporate the hydrological processes and their interactions in a way that system changes can also be covered. Multi-process and multi-site calibration is prerequisite for this task (Bronstert, 2004). Ewen & Parkin (1996) suggested that a model must prove its ability to model catchment output "blindly", i.e. without the use of discharge data for calibration in order to be able to model land use change. If a model is able to "predict"current conditions without prior knowledge of catchment output it is likely able to predict future conditions (where catchment output is also unknown). A model calibrated to a certain status quo is calibrated to a certain process ensemble. However, it is difficult to identify the effects of land use characteristics on these calibrated parameters (Hundecha & Bardossy, 2004). A shift in process ensemble thus is most likely not captured by the model when simulating a change in land use or even climate. Possible processes caused by deforestation in the Malalcahuello Catchment, which are not incorporated in the model are for example an increase in hydrophobicity in the top soil layer (chapter 5), followed by surface runoff and subsequent erosion. The incorporation of such process knowledge gained at the plot or hillslope scale into larger scale models is one of the key questions in land use change modelling (Bronstert et al., 2007 (in press).

7.4 Suggestions for future research and general conclusions

7.4.1 Future research suggestions

Future research in the Malalcahuello Catchment should include the investigation of residence times with environmental isotopes. This could answer the question if water is transported through this catchment on an approximately annual scale or if a deep storage with larger residence times exists.

Further investigation of the phenomenon of losing and gaining stream reaches in more detail would help to determine the importance of losing reaches on the catchment scale. This could be achieved with a temperature survey where stream bed sediment temperatures are measured during times of high temperature gradients between stream and groundwater.

More information on subsurface structures and their variability would greatly improve our understanding of subsurface flow processes. Potential methods to this end are geophysical techniques, such as ground penetrating radar and electromagnetic methods, or the use of a manual penetrometer for areas of shallower soil depths (<3 m).

Extending the physically based hillslope model to 3 dimensions and incorporating a different implementation of preferential flow that also allows for a combination of threshold behaviour and hysteresis would improve the model's capability of hypothesis testing.

As tourism and recreational land use are gaining more and more importance in Southern Chile and here especially in national parks and nature reserves such as the Reserva Forestal Malalcahuello, the construction of hiking paths and forest roads is a scenario that should be investigated with a catchment scale model. As considerable flow has been observed on forest roads in the managed areas of the Reserva Forestal Malalcahuello, a network of hiking trails has the potential to become a second drainage network during high intensity rain storms.

7.4.2 Catchment inter-comparison and classification

On more general terms: a consistent determination of event runoff coefficients would be highly advantageous, as event runoff coefficients and also statistical models for their prediction are useful catchment characteristics and could thus be used for catchment inter-comparison as well as classi-

fication (Hewlett & Hibbert, 1967). In the common case of data scarce catchments this possibility of catchment inter-comparison (also with data-rich catchments) will improve our understanding of runoff generation in the catchment at hand (Bonell et al., 2006), as well as our understanding of hydrological similarity as a function of both the rainfall conditions and the bio-physiographic setting of the landscape, such as morphology, soils and vegetation cover.

7.4.3 Final remarks

Overall, the approach of replacing long time series of data with a multitude of experimental methods was successful and delivered important insights into the hydrological functioning of this catchment. The critical evaluation of the applied experimental methods concerning expenditures vs. gain in process understanding will be helpful for future process studies.

List of Figures

List of Tables

Bibliography

Allander, K. (2003): Trout Creek - evaluating ground-water and surface water exchange along an alpine stream, Lake Tahoe, California, in: Stonestrom, D. & Constantz, J. (Eds.) Heat as a tool for studying the movement of ground water near streams. Circular 1260, U.S. Geological Survey.

Alsdorf, D., Rodriguez, E. & Lettenmaier, D. (2007): Measuring surface water from space, *Reviews of Geophysics*, 45.

Anderson, M. (2005): Heat as a ground water tracer, *Ground Water*, 43 (6): 951–968.

Anderson, M. & Burt, T. (1980): Interpretation of recession flow, *Journal of Hydrology*, 46: 89–101.

Andreoli, A., Carliga, G., Comitia, F. & Iroumé, A. (in pressa): Residuos leñosos de gran tamaño en un torrente de la Cordillera de los Andes, Chile: su funcionalidad e importancia., *Bosque*.

Andreoli, A., Comiti, F. & Lenzi, M. (in pressb): Geomorphic role of large woody debris in a basin of the Chilean Andes, *Earth Surface Processes and Landforms*.

Appleby, F. (1970): Recession and the baseflow problem, *Water Resources Research*, 6 (5): 1398–1403.

Arnold, J. & Allen, P. (1999): Automated methods for estimating baseflow and ground water recharge from streamflow records, *Journal of the American Water Resources Association*, 35 (2): 411–424.

Arya, S. (2001): Introduction to micrometeorology, *International geophysics series*, vol. 79, Academic Press, San Diego, 2nd edition edn.

Bachmann, J., Ellies, A. & Hartge, K. (2000): Development and application of a new sessile drop contact angle method to assess soil water repellency, *Journal of Hydrology*, 231: 66–75.

Bardossy, A. & Lehmann, W. (1998): Spatial distribution of soil moisture in a small catchment. Part 1: Geostatistical analysis, *Journal of Hydrology*, 206 (1-2): 1–15.

Barrientos, C. (2001): Valorización del riesgo global de generación de coladas de piedra en la cuenca torrencial estero Tres Arroyos. IX Región. Chile, Master's thesis, Universidad Austral de Chile.

Bates, B. & Davies, P. (1988): Effect of baseflow separation procedures on surface runoff models, *Journal of Hydrology*, 103 (3-4): 309–322.

Bazemore, D., Eshleman, K. & Hollenbeck, K. (1994): The role of soil-water in stormflow generation in a forested headwater catchment - Synthesis of natural tracer and hydrometric evidence, *Journal of Hydrology*, 162 (1-2): 47–75.

Becker, M., Georgian, T., Ambrose, H., Siniscalchi, J. & Fredrick, K. (2004): Estimating flow and flux of ground water discharge using water temperature and velocity, *Journal of Hydrology*, 296 (1-4): 221–233.

Bergström, S. (1995): The HBV model, in: Singh, V. (Ed.) Computer models of watershed hydrol-

ogy, Water Resources Publications, Highland Ranch, Colorado.

Besoain, E. & Gonzalez, S. (1977): Mineralogia, genesis y clasificacion de suelos derivados de cenizas vocanicas de la region centro-sur de Chile, *Ciencia y Investigacion Agraria*, 4 (2): 109–130.

Blume, T., Zehe, E. & Bronstert, A. (2007a): Rainfall runoff response, event-based runoff coefficients and hydrograph separation, *Hydrological Sciences Journal*, 52 (5): 843–862.

Blume, T., Zehe, E. & Bronstert, A. (2007b): Use of soil moisture dynamics and patterns for the investigation of runoff generation processes with emphasis on preferential flow, *Hydrol. Earth Syst. Sci. Discuss.*, 4: 2587–2624.

Blume, T., Zehe, E. & Bronstert, A. (in preparation): Different models for different purposes - testing process hypotheses on hillslope scale and investigating influence of land use on catchment scale, *Water Resources Research*.

Blume, T., Zehe, E. & Bronstert, A. (in press (b)): Investigation of runoff generation in a pristine, poorly gauged catchment in the Chilean Andes. II: Qualitative and quantitative use of tracers at three different spatial scales., *Hydrological Processes*.

Blume, T., Zehe, E., Reusser, D., Bauer, A., Iroumé, A. & Bronstert, A. (in press (a)): Investigation of runoff generation in a pristine, poorly gauged catchment in the Chilean Andes. I: A multi-method experimental study, *Hydrological Processes*.

Bonell, M. (1993): Progress in the Understanding of Runoff Generation Dynamics in Forests, *Journal of Hydrology*, 150 (2-4): 217–275.

Bonell, M., McDonnel, J., Scatena, F., Seibert, J., Uhlenbrook, S. & van Lanen, H. (2006): HELPing FRIENDS in PUBs: charting a course for synergies within international water research programmes in gauged and ungauged basins, *Hydrological Processes*, 20: 1867–1874.

Bowden, W., Fahey, B., Ekanayake, J. & Murray, D. (2001): Hillslope and wetland hydrodynamics in a tussock grassland, South Island, New Zealand, *Hydrological Processes*, 15: 1707–1730.

Bradshaw, E., Nielsen, A. & Anderson, N. (2006): Using diatoms to assess the impacts of prehistoric, pre-industrial and modern land-use on Danish lakes, *Regional Environmental Change*, 6 (1-2): 17–24.

Brocca, L., Morbidelli, R., Melone, F. & Moramarco, T. (2007): Soil moisture spatial variability in experimental areas of central Italy, *Journal of Hydrology*, 333 (2-4): 356–373.

Bronstert, A. (2004): Rainfall-runoff modelling for assessing impacts of climate and land-use change, *Hydrological Processes*, 18 (3): 567–570.

Bronstert, A., Bardossy, A., Bismuth, C., Buiteveld, H., Disse, M., Engel, H., Fritsch, U., Hundecha, Y., Lammersen, R., Niehoff, D. & Ritter, N. (2007 (in press)): Multi-scale modelling of land-use change and river training effects on floods in the Rhine Basin., *River Research and Application*.

Brown, V., McDonnell, J., Burns, D. & Kendall, C. (1999): The role of event water, a rapid shallow flow component, and catchment size in summer stormflow, *Journal of Hydrology*, 217 (3-4): 171–190.

Brutsaert, W. (2005): Hydrology. An introduction., Cambridge University Press, Cambridge.

Burch, G., Bath, R., Moore, I. & O'Loughlin, E. (1987): Comparative hydrological behaviour of forested and cleared catchments in Southeastern Australia, *Journal of Hydrology*, 90: 19–42.

Burns, D., McDonnell, J., Hooper, R., Peters, N., Freer, J., Kendall, C. & Beven, K. (2001): Quantifying contributions to storm runoff through end-member mixing analysis and hydrologic measurements at the Panola Mountain Research Watershed (Georgia, USA), *Hydrological Processes*, 15 (10): 1903–1924.

Buttle, J. & McDonald, D. (2002): Coupled vertical and lateral preferential flow on a forested slope, *Water Resources Research*, 38 (5).

Buytaert, W., Wyseure, G., De Bievre, B. & Deckers, J. (2005): The effect of land-use changes on the hydrological behaviour of histic andosols in south Ecuador, *Hydrological Processes*, 19: 3985–3997.

Ceballos, A., Scipal, K., Wagner, W. & Martinez-Fernandez, J. (2005): Validation of ERS scatterometer-derived soil moisture data in the central part of the Duero Basin, Spain, *Hydrological Processes*, 19 (8): 1549–1566.

Chapman, T. (1999): A comparison of algorithms for stream flow recession and baseflow separation, *Hydrological Processes*, 13 (5): 701–714.

Chirico, G., Grayson, R. & Western, A. (2003): A downward approach to identifying the structure and parameters of a process-based model for a small experimental catchment, *Hydrological Processes*, 17 (11): 2239–2258.

Conant, B. (2004): Delineating and quantifying ground water discharge zones using streambed temperatures, *Ground Water*, 42 (2): 243–257.

Constantz, J. (1998): Interaction between stream temperature, streamflow, and groundwater exchanges in Alpine streams, *Water Resources Research*, 34 (7): 1609–1615.

Constantz, J., Cox, M., Sarma, L. & Mendez, G. (2003a): The Santa Clara River - the last natural river of Los Angeles, in: Stonestrom, D. & Constantz, J. (Eds.) Heat as a tool for studying the movement of ground water near streams. Circular 1260, U.S. Geological Survey.

Constantz, J., Cox, M. & Su, G. (2003b): Comparison of heat and bromide as ground water tracers near streams, *Ground Water*, 41 (5): 647–656.

Constantz, J., Stewart, A., Niswonger, R. & Sarma, L. (2002): Analysis of temperature profiles for investigating stream losses beneath ephemeral channels, *Water Resources Research*, 38 (12).

Constantz, J. & Stonestrom, D. (2003): Heat as a tracer of water movement near streams, in: Stonestrom, D. & Constantz, J. (Eds.) Heat as a tool for studying the movement of ground water near streams. Circular 1260, pages 1–6, U.S. Geological Survey.

CORMA (2007): Corporaciíon Chilena de la Madera, URL: http://www.corma.cl/portal/menu /recurso_forestal/Plantaciones.

Crawley, M. (2005): Statistics. An introduction using R., Wiley, Chichester.

de Rooij, G. (2000): Modeling fingered flow of water in soils owing to wetting front instability: a review, *Journal of Hydrology*, 231: 277–294.

de Rooij, G. & deVries, P. (1996): Solute leaching in a sandy soil with a water-repellent surface layer: A simulation, *GEODERMA*, 70 (2-4): 253–263.

de Rooij GH. (2000): Modeling fingered flow of water in soils owing to wetting front instability: a review, *Journal of Hydrology*, 231: 277–294.

Dekker, L. & Ritsema, C. (1994): How Water Moves in a Water Repellent Sandy Soil .1. Potential and Actual Water Repellency, *Water Resources Research*, 30 (9): 2507–2517.

Dekker, L. & Ritsema, C. (2000): Wetting patterns and moisture variability in water repellent Dutch soils, *Journal of Hydrology*, 231: 148–164.

Dewandel, B., Lachassagne, P., Bakalowicz, M., Weng, P. & Al-Malki, A. (2003): Evaluation of aquifer thickness by analysing recession hydrographs. Application to the Oman ophiolite hard-rock aquifer, *Journal of Hydrology*, 274 (1-4): 248–269.

Dillon, P. & Kirchner, W. (1975): Effects of Geology and Land-Use on Export of Phosphorus from Watersheds, *Water Research*, 9 (2): 135–148.

Dingman, S. (2002): Physical Hydrology, Prentice Hall, Upper Sadle River, New Jersey.

Doherty, J. (2004): PEST - Model-independent parameter estimation.

Donoso, C. & Lara, A. (1995): Utilizacion de los bosques nativos en Chile: pasado, presente y futuro, in: Armesto, J., Villagran, C. & Arroyo, M. (Eds.) Ecologia de los Bosques Nativos de Chile, pages 363–388, Editorial Universitaria, Santiago de Chile.

Dunne, T. (1978): Field Studies of hillslope flow processes, in: Kirkby, M. (Ed.) Hillslope Hydrology, pages 227–293, Wiley and Sons, Ltd.

Eckhart, K. (2005): How to construct recursive digital filters for baseflow separation, *Hydrological Processes*, 19: 507–515.

Ellies, A. (1975): Untersuchungen über einige Aspekte des Wasserhaushaltes vulkanischer Aschenböden aus der gemäsigten Zone Südchiles, Ph.D. thesis, Technical University of Hannover, Germany, Hannover.

Ellies, A. (2000): Soil erosion and its control in Chile - An overview, *Acta Geologica Hispanica*, 35 (3-4): 279–284.

Elrick, D., Reynolds, W. & Tan, K. (1989): Hydraulic conductivity measurements in the unsaturated zone using improved well analyses, *Ground Water Monitoring Review*, 9 (3): 184–193.

ESA (2007): European Space Agency, URL: http://earth.esa.int.

Ewen, J. & Parkin, G. (1996): Validation of catchment models for predicting land-use and climate change impacts. 1. Method, *Journal of Hydrology*, 175: 583–594.

Flury, M., Flühler, H., Jury, W. & Leuenberger, J. (1994): Susceptibility of Soils to Preferential Flow of Water - a Field-Study, *Water Resources Research*, 30 (7): 1945–1954.

Flury, M. & Wai, N. (2003): Dyes as tracers for vadose zone hydrology, *Reviews of Geophysics*, 41 (1).

Frank, D. & Finckh, M. (1997): Impactos de las plantaciones de pino oregon sobre la vegetacion y el suelo en la zona centro-sur de Chile, *Revista Chilena de Historia Natural*, 70: 191–211.

Frappart, F., Seyler, F., Martinez, J.-M., , Leon, J. & Cazenave, A. (2005): Floodplain water storage in the Negro River basin estimated from microwave remote sensing of inundatiton area and water levels, *Remote Sensing of Environment*, 99: 387–399.

Freer, J., McDonnell, J., Beven, K., Peters, N., Burns, D., Hooper, R., Aulenbach, B. & Kendall, C. (2002): The role of bedrock topography on subsurface storm flow, *Water Resources Research*, 38 (12).

Frisbee, M., Allan, C., Thomasson, M. & Mackereth, R. (in press): Hillslope hydrology and wetland response of two small zero-order boreal catchments on the Precambrian Shield, *Hydrological Processes*.

Furey, P. & Gupta, V. (2001): A physically based filter for separating base flow from streamflow time series, *Water Resources Research*, 37 (11): 2709–2722.

Gayoso, J. & Iroumé, A. (1991): Compaction and Soil Disturbances from Logging in Southern Chile, *Annales Des Sciences Forestieres*, 48 (1): 63–71.

Germann, P. & Zimmermann, M. (2005): Water balance approach to the in situ estimation of volume flux densities using slanted TDR wave guides, *Soil Science*, 170 (1): 3–12.

Godoy, R., Oyarzun, C. & Gerding, V. (2001): Precipitation chemistry in deciduous and evergreen Nothofagus forests of southern Chile under a low-deposition climate, *Basic and Applied Ecology*, 2 (1): 65–72.

Graeff, T., Zehe, E. & Bronstert, A. (submitted): Process identification through rejection of model structures in a mid-mountainous rural catchment: model inter-comparison, *Hydrological Processes*.

Guillemette, F., Plamondon, A., Prevost, M. & Levesque, D. (2005): Rainfall generated stormflow response to clearcutting a boreal forest: peak flow comparison with 50 world-wide basin studies, *Journal of Hydrology*, 302 (1-4): 137–153.

Hall, F. (1968): Base-flow recessions - A review, *Water Resources Research*, 4 (5): 973–983.

Hangen, E., Lindenlaub, M., Leibundgut, C. & von Wilpert, K. (2001): Investigating mechanisms of stormflow generation by natural tracers and hydrometric data: a small catchment study in the Black Forest, Germany, *Hydrological Processes*, 15 (2): 183–199.

Hasegawa, S. (1997): Evaluation of rainfall infiltration characteristics in a volcanic ash soil by time domain reflectometry method, *Hydrology and Earth System Sciences*, 1 (2): 303–312.

Hewlett, J., Fortson, J. & Cunningham, G. (1977): Effect of Rainfall Intensity on Storm Flow and Peak Discharge from Forest Land - Reply, *Water Resources Research*, 13 (6): 1027–1028.

Hewlett, J., Fortson, J. & Cunningham, G. (1984): Additional tests on the effect of rainfall intensity on storm flow and peak flow from wild-land basins, *Water Resources Research*, 20 (7): 985–989.

Hewlett, J. & Hibbert, A. (1967): Factors affecting the response of small watersheds to precipitation in humid areas, in: Sopper, W. & Lull, H. (Eds.) International Symposium on Forest Hydrology, pages 275–290, Pergamon Press, New York.

Hillel, D. (1998): Environmental Soil Physics, Academic Press, San Diego.

Hino, M., Odaka, Y., Nadaoka, K. & Sato, A. (1988): Effect of Initial Soil-Moisture Content on the Vertical Infiltration Process - a Guide to the Problem of Runoff-Ratio and Loss, *Journal of Hydrology*, 102 (1-4): 267–284.

Hinton, M., Schiff, S. & English, M. (1994): Examining the Contributions of Glacial Till Water to Storm Runoff Using 2-Component and 3-Component Hydrograph Separations, *Water Resources Research*, 30 (4): 983–993.

Hoeg, S., Uhlenbrook, S. & Leibundgut, C. (2000): Hydrograph separation in a mountainous catchment - combining hydrochemical and isotopic tracers, *Hydrological Processes*, 14 (7): 1199–1216.

Huber, A. & Iroumé, A. (2001): Variability of annual rainfall partitioning for different sites and forest covers in Chile, *Journal of Hydrology*, 248 (1-4): 78–92.

Huber, A. & Trecaman, R. (2000): Effect of a Pinus Radiata plantation on the spatial distribution of soil water content, *Bosque*, 21: 37–44.

Hundecha, Y. & Bardossy, A. (2004): Modeling of the effect of land use changes on the runoff

generation of a river basin through parameter regionalization of a watershed model, *Journal of Hydrology*, 292 (1-4): 281–295.

Institute of Hydrology (1980): Low flow studies, Report No.1, Institute of Hydrology, Wallingford, United Kingdom.

Iroumé, A. (1990): Assessment of Runoff and Suspended Sediment Yield in a Partially Forested Catchment in Southern Chile, *Water Resources Research*, 26 (11): 2637–2642.

Iroumé, A. (2003): Transporte de sedimentos en una cuenca de montańa en la Cordillera de los Andes de la Novena Regíon de Chile, *Bosque*, 24 (1): 125–135.

Iroumé, A. & Huber, A. (2002): Comparison of interception losses in a broadleaved native forest and a Pseudotsuga menziesii (Douglas fir) plantation in the Andes Mountains of southern Chile, *Hydrological Processes*, 16 (12): 2347–2361.

Iroumé, A., Huber, A. & Schulz, K. (2005): Summer flows in experimental catchments with different forest covers, Chile, *Journal of Hydrology*, 300 (1-4): 300–313.

Iroumé, A., Mayen, O. & Huber, A. (2006): Runoff and peak flow responses to timber harvest and forest age in southern Chile, *Hydrological Processes*, 20 (1): 37–50.

Johnson, A., Boer, B., Woessner, W., Stanford, J., Poole, G., Thomas, S. & O'Daniel, S. (2005): Evaluation of an inexpensive small-diameter temperature logger for documenting ground water-river interactions, *Ground Water Monitoring and Remediation*, 25 (4): 68–74.

Kienzler, P. & Naef, F. (in press): Subsurface storm flow formation at different hillslopes and implications fro the 'old water paradox'., *Hydrological Processes*.

Kim, J., Lee, G., Lee, J., Chon, C., Kim, T. & Ha, K. (2006): Infiltration pattern in a regolith-fractured bedrock profile: field observation of a dye stain pattern, *Hydrological Processes*, 20 (2): 241–250.

Kirchner, J. (2003): A double paradox in catchment hydrology and geochemistry, *Hydrological Processes*, 17 (4): 871–874.

Knödel, K., Krummel, H. & Lange, G. (1997): Geophysik, *Handbuch zur Erkundung des Untergrundes von Deponien und Altlasten*, vol. 3, Springer, Berlin Heidelberg.

Ladouche, B., Probst, A., Viville, D., Idir, S., Baque, D., Loubet, M., Probst, J. & Bariac, T. (2001): Hydrograph separation using isotopic, chemical and hydrological approaches (Strengbach catchment, France), *Journal of Hydrology*, 242 (3-4): 255–274.

Lange, J., Leibundgut, C., Greenbaum, N. & Schick, A. (1999): A noncalibrated rainfall-runoff model for large, arid catchments, *Water Resources Research*, 35 (7): 2161–2172.

Leavesley, G. & Stannard, L. (1995): The precipitation-runoff modeling sytem PRMS, in: Singh, V. (Ed.) Computer models of watershed hydrology, pages 281–310, Water Resources Publications, Highland Ranch, Colorado.

Lee, H., Sivapalan, M. & Zehe, E. (2007): Predictions of rainfall-runoff response and soil moisture dynamics in a microscale catchment using the CREW model, *Hydrology and Earth System Sciences*, 11: 819–849.

Lindenmaier, F., Zehe, E., Dittfurth, A. & Ihringer, J. (2005): Process identification at a slow-moving landslide in the Vorarlberg Alps, *Hydrological Processes*, 19 (8): 1635–1651.

Lohmann, D., Raschke, E., Nijssen, B. & Lettenmaier, D. (1998): Regional scale hydrology: I. Formulation of the VIC-2L model coupled to a

routing model, *Hydrological Sciences Journal-Journal Des Sciences Hydrologiques*, 43 (1): 131–141.

Lusk, C. (2001): When is a gap not a gap? Light levels and leaf area index in bamboo-filled gaps in a Chilean rain forest., *Gayana Botanica*, 58: 25–30.

Mao, L., Uyttendaele, G., Iroumé, A. & Lenzi, M. (in press): Field based analysis of sediment entrainment in two high gradient streams located in Alpine and Andine environments, *Geomorphology*.

Maurer, T. (1997): Physikalisch begründetete, zeitkontinuierliche Modellierung des Wassertransports in kleinen ländlichenen Einzugsgebieten., Ph.D. thesis, Universität Karlsruhe.

McGlynn, B., McDonnel, J. & Brammer, D. (2002): A review of the evolving perceptual model of hillslope flowpaths at the Maimai catchments, New Zealand, *Journal of Hydrology*, 257 (1-4): 1–26.

McGuire, K., McDonnell, J., Weiler, M., Kendall, C., McGlynn, B., Welker, J. & Seibert, J. (2005): The role of topography on catchment-scale water residence time, *Water Resources Research*, 41 (5).

McNamara, J., Chandler, D., Seyfried, M. & Achet, S. (2005): Soil moisture states, lateral flow, and streamflow generation in a semi-arid, snowmelt-driven catchment, *Hydrological Processes*, 19 (20): 4023–4038.

McNamara, J., Kane, D. & Hinzman, L. (1997): Hydrograph separations in an Arctic watershed using mixing model and graphical techniques, *Water Resources Research*, 33 (7): 1707–1719.

McNamara, J., Kane, D. & Hinzman, L. (1998): An analysis of streamflow hydrology in the Kuparuk River basin, Arctic Alaska: A nested watershed approach, *Journal of Hydrology*, 206 (1-2): 39–57.

Meyles, E., Williams, A., Ternan, L. & Dowd, J. (2003): Runoff generation in relation to soil moisture patterns in a small Dartmoor catchment, Southwest England, *Hydrological Processes*, 17 (2): 251–264.

Moreno, H. & Gardeweg, M. (1989): La erupcion reciente en el complejo volcanico Lonquimay (dic 1988-), Andes del Sur, *Revista Geologica de Chile*, 16: 93–117.

Munoz-Carpena, R., Regalado, C., Alvarez-Benedi, J. & Bartoli, F. (2002): Field evaluation of the new Philip-Dunne permeameter for measuring saturated hydraulic conductivity, *Soil Science*, 167 (1): 9–24.

Musiake, K., Oka, Y. & Koike, M. (1988): Unsaturated Zone Soil-Moisture Behavior under Temperate Humid Climatic Conditions - Tensiometric Observations and Numerical Simulations, *Journal of Hydrology*, 102 (1-4): 179–200.

Nieber, J. (1996): Modeling finger development and persistence in initially dry porous media, *GEODERMA*, 70 (2-4): 207–229.

Niehoff, D. (2002): Modellierung des Einflusses der Landnutzung auf die Hochwasserentstehung in der Mesoskala, *Brandenburgische Umweltberichte*, vol. 11.

Niehoff, D., Fritsch, U. & Bronstert, A. (2002): Land-use impacts on storm-runoff generation: scenarios of land-use change and simulation of hydrological response in a meso-scale catchment in SW-Germany, *Journal of Hydrology*, 267: 80–93.

Nyberg, L. (1996): Spatial variability of soil water content in the covered catchment at Gardsjon, Sweden., *Hydrological Processes*, 10: 89–103.

Ohrstrom, P., Hamed, Y., Persson, M. & Berndtsson, R. (2004): Characterizing unsaturated solute transport by simultaneous use of dye and bromide, *Journal of Hydrology*, 289 (1-4): 23–35.

Oyarzun, C. (1995): Land-Use, Hydrological Properties, and Soil Erodibilities in the Bio-Bio River Basin, Central Chile, *Mountain Research and Development*, 15 (4): 331–338.

Oyarzun, C., Campos, H. & Huber, A. (1997): Nutrient export from watersheds with different land uses in southern Chile (Lake Rupanco, X Region), *Revista Chilena De Historia Natural*, 70 (4): 507–519.

Oyarzun, C., Godoy, R. & Sepulveda, A. (1998): Water and nutrient fluxes in a cool temperate rainforest at the Cordillera de la Costa in southern Chile, *Hydrological Processes*, 12 (7): 1067–1077.

Peters, D., Buttle, J., Taylor, C. & Lazerte, B. (1995): Runoff Production in a Forested, Shallow Soil, Canadian Shield Basin, *Water Resources Research*, 31 (5): 1291–1304.

Peters, E. & van Lanen, H. (2005): Separation of base flow from streamflow using groundwater levels - illustrated for the Pang catchment (UK), *Hydrological Processes*, 19: 921–936.

Pilgrim, D. & Cordery, I. (1992): Flood runoff, in: Maidment, D. (Ed.) Handbook of Hydrology, pages 9.1–9.42, McGraw-Hill, Inc., New York.

Post, D. & Jones, J. (2001): Hydrologic regimes of forested, mountainous, headwater basins in New Hampshire, North Carolina, Oregon, and Puerto Rico, *Advances in Water Resources*, 24: 1195–1210.

Poulenard, J., Michel, J., Bartoli, F., Portal, J. & Podwojewski, P. (2004): Water repellency of volcanic ash soils from Ecuadorian paramo: effect of water content and characteristics of hydrophobic organic matter, *European Journal of Soil Science*, 55 (3): 487–496.

Ramirez G., C., San Martin P., C., Ellies Sch., A. & Mac Donald H., R. (1994): Cambios floristicos desde el bosque nativo a comunidades antropogenicas sometidas a diferentes manejos agropecuarios en un suelo trumao (Valdivia, Chile), *Agro Sur*, 22 (1): 57–72.

Rasmussen, T., Baldwin, R., Dowd, J. & Williams, A. (2000): Tracer vs. pressure wave velocities through unsaturated saprolite, *Soil Science Society of America Journal*, 64 (1): 75–85.

Reynolds, W. & Elrick, D. (1987): A laboratory and numerical assessment of the Guelph permeameter method, *Soil Science*, 144 (4): 282–299.

Rezzoug, A., Schumann, A., Chifflard, P. & Zepp, H. (2005): Field measurement of soil moisture dynamics and numerical simulation using the kinematic wave approximation, *Advances in Water Resources*, 28 (9): 917–926.

Rice, K. & Hornberger, G. (1998): Comparison of hydrochemical tracers to estimate source contributions to peak flow in a small, forested, headwater catchment, *Water Resources Research*, 34 (7): 1755–1766.

Ritsema, C. & Dekker, L. (1994): How Water Moves in a Water Repellent Sandy Soil .2. Dynamics of Fingered Flow, *Water Resources Research*, 30 (9): 2519–2531.

Ritsema, C. & Dekker, L. (1995): Distribution Flow - a General Process in the Top Layer of Water Repellent Soils, *Water Resources Research*, 31 (5): 1187–1200.

Ritsema, C. & Dekker, L. (1996): Water repellency and its role in forming preferred flow paths in soils, *Australian Journal of Soil Research*, 34 (4): 475–487.

Ritsema, C. & Dekker, L. (2000): Preferential flow in water repellent sandy soils: principles and modeling implications, *Journal of Hydrology*, 231: 308–319.

Ritsema, C., Dekker, L., Hendrickx, J. & Hamminga, W. (1993): Preferential Flow Mechanism in a Water Repellent Sandy Soil, *Water Resources Research*, 29 (7): 2183–2193.

Ritsema, C., Dekker, L., Nieber, J. & Steenhuis, T. (1998): Modeling and field evidence of finger formation and finger recurrence in a water repellent sandy soil, *Water Resources Research*, 34 (4): 555–567.

Salmon, C., Walter, M., Hedin, L. & Brown, M. (2001): Hydrological controls on chemical export from an undisturbed old-growth Chilean forest, *Journal of Hydrology*, 253 (1-4): 69–80.

Savenije, H. (1996): The runoff coefficient as the key to moisture recycling, *Journal of Hydrology*, 176: 219–225.

Schellekens, J., Scatena, F., Bruijnzeel, L., van Dijk, A., Groen, M. & van Hogezand, R. (2004): Stormflow generation in a small rainforest catchment in the luquillo experimental forest, Puerto Rico, *Hydrological Processes*, 18 (3): 505–530.

Schäfer, M. (1999): Estudio de la variabilidad espacial de la infiltraction en la cuenca del estero Tres Arroyos, Malalcahuello, IX Región., Master's thesis, Universidad Catolica de Temuco.

Schulla, J. (1997): Hydrologische Modellierung von Flussgebieten zur Abschätzung von Folgen der Klimaänderung, *Züricher Geographische Schriften*, vol. 69.

Schulla, J. & Jasper, K. (1999): Modellbeschreibung WASIM-ETH (Manual).

Selker, J., Steenhuis, T. & Parlange, J. (1992): Wetting front instability in homogeneous sandy soils under continuous infiltration, *Soil Science Society of America Journal*, 56: 1346–1350.

Selker, J., Steenhuis, T. & Parlange, J. (1996): An engineering approach to fingered vadose pollutant transport, *GEODERMA*, 70 (2-4): 197–206.

Selker, J., van de Giesen, N., Westhoff, M., Luxemburg, W. & Parlange, M. (2006): Fiber optics opens window on stream dynamics, *Geophysical Research Letters*, 33 (24).

Shanley, J., Kendall, C., Smith, T., Wolock, D. & McDonnell, J. (2002): Controls on old and new water contributions to stream flow at some nested catchments in Vermont, USA, *Hydrological Processes*, 16 (3): 589–609.

Shoji, S., Nanzyo, M. & Dahlgren, R. (1993): Volcanic ash soils - genesis, properties and utilization, *Developments in soil science*, vol. 21, Elsevier, Amsterdam.

Sidle, R., Noguchi, S., Tsuboyama, Y. & Laursen, K. (2001): A conceptual model of preferential flow systems in forested hillslopes: evidence of self-organization, *Hydrological Processes*, 15 (10): 1675–1692.

Sidle, R., Tsuboyama, Y., Noguchi, S., Hosoda, I., Fujieda, M. & Shimizu, T. (2000): Stormflow generation in steep forested headwaters: a linked hydrogeomorphic paradigm, *Hydrological Processes*, 14 (3): 369–385.

Silliman, S. & Booth, D. (1993): Analysis of time-series aeasurements of sediment temperature for identification of gaining vs losing portions of Juday-Creek, Indiana, *Journal of Hydrology*, 146 (1-4): 131–148.

Silliman, S., Ramirez, J. & McCabe, R. (1995): Quantifying downflow through creek sediments using temperature time series: one-dimensional solution incorporating measured surface temperature, *Journal of Hydrology*, 167 (1-4): 99–119.

Sivapalan, M., Bloschl, G., Zhang, L. & Vertessy, R. (2003a): Downward approach to hydrological prediction, *Hydrological Processes*, 17 (11): 2101–2111.

Sivapalan, M., Franks, S., Takeuchi, K. & Tachikawa, Y. (2005): International perspectives on PUB and pathways forward: Outcomes of the Perth PUB Workshop, in: Sivapalan, M., Franks, S., Takeuchi, K. & Tachikawa, Y. (Eds.) Predictions in ungauged basins: International perspectives on the state of the art and pathways forward, vol. 301, IAHS Press, Wallingford.

Sivapalan, M., Takeuchi, K., Franks, S., Gupta, V., Karambiri, H., Lakshmi, V., Liang, X., McDonnell, J., Mendiondo, E., O'Connell, P., Oki, T., Pomeroy, J., Schertzer, D., Uhlenbrook, S. & Zehe, E. (2003b): IAHS decade on Predictions in Ungauged Basins (PUB), 2003-2012: Shaping an exciting future for the hydrological sciences, *Hydrological Sciences Journal - Journal Des Sciences Hydrologiques*, 48 (6): 857–880.

Sivapalan, M., Wagner, T., Uhlenbrook, S., Liang, X., Lakshmi, V., Kumar, P., Zehe, E. & Tachikawa, Y. (Eds.) (2006): PUB: Promise and Progress, *IAHS Publication*, vol. 303, IAHS Press, Wallingford, UK.

Sklash, M. & Farvolden, R. (1979): The role of groundwater in storm runoff, *Journal of Hydrology*, 43: 45–65.

Smithsonian-Institution (2007): Global Volcanism Program: Description of the Lonquimay Volcano.

Starr, J. & Timlin, D. (2004): Using high-resolution soil moisture data to assess soil water dynamics in the vadose zone, *Vadose Zone Journal*, 3 (3): 926–935.

Sujono, J., Shikasho, S. & Hiramatsu, K. (2004): A comparison of techniques for hydrograph recession analysis, *Hydrological Processes*, 18 (3): 403–413.

Szilagyi, J. (1999): On the use of semi-logarithmic plots for baseflow separation, *Ground Water*, 37 (5): 660–662.

Szilagyi, J. & Parlange, M. (1998): Baseflow separation based on analytical solutions of the Boussinesq equation, *Journal of Hydrology*, 204 (1-4): 251–260.

Tallaksen, L. (1995): A Review of Baseflow Recession Analysis, *Journal of Hydrology*, 165 (1-4): 349–370.

Taumer, K., Stoffregen, H. & Wessolek, G. (2006): Seasonal dynamics of preferential flow in a water repellent soil, *Vadose Zone Journal*, 5 (1): 405–411.

Terblanche, D., Pegram, G. & Mittermaier, M. (2001): The development of weather radar as a research and operational tool for hydrology in South Africa, *Journal of Hydrology*, 241: 3–25.

Tetzlaff, D. & Uhlenbrook, S. (2005): Significance of spatial variability in precipitation for process-oriented modelling: results from two nested catchments using radar and ground station data, *Hydrology and Earth System Sciences*, 9 (1-2): 29–41.

Torres, R., Dietrich, W., Montgomery, D., Anderson, S. & Loague, K. (1998): Unsaturated zone processes and the hydrologic response of a steep, unchanneled catchment, *Water Resources Research*, 34 (8): 1865–1879.

Tosso, J. (Ed.) (1985): Suelos volcanicos de Chile, INIA, Santiago de Chile.

Tromp-van Meerveld, H. & McDonnell, J. (2006a): Threshold relations in subsurface stormflow: 1. A 147-storm analysis of the Panola hillslope, *Water Resources Research*, 42 (2).

Tromp-van Meerveld, H. & McDonnell, J. (2006b): Threshold relations in subsurface

stormflow: 2. The fill and spill hypothesis, *Water Resources Research*, 42 (2).

Tromp-van Meerveld, H., Peters, N. & McDonnell, J. (2007): Effect of bedrock permeability on subsurface stormflow and the water balance of a trenched hillslope at the Panola Mountain Research Watershed, Georgia, USA, *Hydrological Processes*, 21 (6): 750–769.

Uhlenbrook, S., Frey, M., Leibundgut, C. & Maloszewski, P. (2002): Hydrograph separations in a mesoscale mountainous basin at event and seasonal timescales, *Water Resources Research*, 38 (6).

Uhlenbrook, S., Wenninger, J. & Lorentz, S. (2005): What happens after the catchment caught the storm? Hydrological processes at the small, semi-arid Weatherley catchment, South Africa, *Advances in Geosciences*, 2: 237–241.

Uyttendaele, G. (2006): Procesos de transporte de sedimentos en áreas de montaña, comparación entre la Cuenca del río Cordón (Alpes, Italia) y el estero Tres Arroyos (Andes, Chile), Ph.D. thesis, Universidad Austral de Chile.

Uyttendaele, G. & Iroumé, A. (2002): The solute budget of a forest catchment and solute fluxes within a Pinus radiata and a secondary native forest site, southern Chile, *Hydrological Processes*, 16 (13): 2521–2536.

van Dijk, A., Bruijnzeel, L., Vertessy, R. & Ruijter, J. (2005): Runoff and sediment generation on bench-terraced hillsides: measurements and up-scaling of a field-based model, *Hydrological Processes*, 19: 1667–1685.

van Lanen, H. & Dijksma, R. (1999): Water flow and nitrate transport to a groundwater-fed stream in the Belgian-Dutch chalk region, *Hydrological Processes*, 13 (3): 295–307, ISSN 1099-1085.

Van't Woudt, B. (1954): On factors governing subsurface storm flow in volcanic ash soils, New Zealand, *Transactions-American Geophysical Union*, 35 (1): 136–144.

Wagner, W., Blöschl, G., Pampaloni, P., Calvet, J.-C., Bizzarri, B., Wigneron, J.-P. & Kerr, Y. . (2007): Operational readiness of microwave remote sensing of soil moisture for hydrologic applications, *Nordic Hydrology*, 38 (1): 1–20.

Weiler, M. & Flühler, H. (2004): Inferring flow types from dye patterns in macroporous soils, *Geoderma*, 120 (1-2): 137–153.

Weiler, M., McGlynn, B., McGuire, K. & McDonnell, J. (2003): How does rainfall become runoff? A combined tracer and runoff transfer function approach, *Water Resources Research*, 39 (11).

Weiler, M. & Naef, F. (2003): An experimental tracer study of the role of macropores in infiltration in grassland soils, *Hydrological Processes*, 17 (2): 477–493.

Wenninger, J., Uhlenbrook, S., Tilch, N. & Leibundgut, C. (2004): Experimental evidence of fast groundwater responses in a hillslope/floodplain area in the Black Forest Mountains, Germany, *Hydrological Processes*, 18 (17): 3305–3322.

Western, A., Zhou, S.-L., Grayson, R., McMahon, S., Bloschl, G. & Wilson, D. (2004): Spatial correlation of soil moisture in small catchments and its relationship to dominant spatial hydrological processes, *Journal of Hydrology*, 286 (1-4): 113–134.

Westhoff, M., Savenije, H., Luxemburg, W., Stelling, G., van de Giesen, N., Selker, J., Pfister, L. & Uhlenbrook, S. (2007): A distributed stream temperature model using high resolution temperature observations, *Hydrology and Earth System Sciences*, 11: 1469–1480.

Williams, A., Dowd, J. & Meyles, E. (2002): A new interpretation of kinematic stormflow generation, *Hydrological Processes*, 16 (14): 2791–2803.

Williams, A., Dowd, J., Scholefield, D., Holden, N. & Deeks, L. (2003): Preferential flow variability in a well-structured soil, *Soil Science Society of America Journal*, 67 (4): 1272–1281.

Winsemius, H., Savenije, H., Gerrits, A., Zapreeva, E. & Klees, R. (2006): Comparison of two model approaches in the Zambezi river basin with regard to model reliability and identifiability, *Hydrology and Earth System Sciences*, 10 (3): 339–352.

Wittenberg, H. (1999): Baseflow recession and recharge as nonlinear storage processes, *Hydrological Processes*, 13 (5): 715–726.

Wittenberg, H. (2003): Effects of season and man-made changes on baseflow and flow recession: case studies, *Hydrological Processes*, 17 (11): 2113–2123.

Woodruff, J. & Hewlett, J. (1970): Predicting and mapping the average hydrologic response for the Eastern United States, *Water Resources Research*, 6 (5): 1312–1326.

Zehe, E., Becker, R., Bardossy, A. & Plate, E. (2005): Uncertainty of simulated catchment runoff response in the presence of threshold processes: Role of initial soil moisture and precipitation, *Journal of Hydrology*, 315 (1-4): 183–202.

Zehe, E. & Bloeschl, G. (2004): Predictability of hydrologic response at the plot and catchment scales: Role of initial conditions, *Water Resources Research*, 40 (10).

Zehe, E., Elsenbeer, H., Lindenmaier, F., Schulz, K. & Blöschl, G. (2007): Patterns of predictability in hydrological threshold systems, *Water Resources Research*, 43 (7): W07434.

Zehe, E. & Flühler, H. (2001a): Preferential transport of isoproturon at a plot scale and a field scale tile-drained site, *Journal of Hydrology*, 247 (1-2): 100–115.

Zehe, E. & Flühler, H. (2001b): Slope scale variation of flow patterns in soil profiles, *Journal of Hydrology*, 247 (1-2): 116–132.

Zehe, E., Maurer, T., Ihringer, J. & Plate, E. (2001): Modeling water flow and mass transport in a loess catchment, *Physics and Chemistry of the Earth Part B-Hydrology Oceans and Atmosphere*, 26 (7-8): 487–507.

Zhao, R. (1992): The Xinanjiang Model Applied in China, *Journal of Hydrology*, 135 (1-4): 371–381.

Zhou, Q., Shimada, J. & Sato, A. (2001): Three-dimensional spatial and temporal monitoring of soil water content using electrical resistivity tomography, *Water Resources Research*, 37 (2): 273–285.

Zhou, Q., Shimada, J. & Sato, A. (2002): Temporal variations of the three-dimensional rainfall infiltration process in heterogeneous soil, *Water Resources Research*, 38 (4).

Acknowledgments

I want to thank my advisors Axel Bronstert and Erwin Zehe: Axel for his trust in me and his continuing support and Erwin for long and helpful discussions and his enthusiasm.

For taking the time to read and review my thesis I want to thank Hubert Savenije (Delft University) and Markus Casper (Trier University).

A very big thank you also to Dominik Reusser and Andreas Bauer (Potsdam University) for their patience and hard work during many weeks of field work. Thank you to Hardin Palacios and Luis Opazo (Universidad Austral de Chile) for help in the field, Prof. Andrés Iroumé and Prof. Anton Huber (Universidad Austral de Chile) for their support, logistic and technical assistance, and the use of climate and streamflow data. Thanks also to the CONAF (Cooperación Nacional Forestal) in Malalcahuello for their support during field campaigns.

Chemical and soil physical analyses were carried out by laboratories at the University of Potsdam, the Universidad Austral de Chile and at Benthos, Validvia. Isotope analyses were carried out at CCHEN in Santiago, Chile and at the Alfred Wegener Institute in Potsdam, Germany.

I thank Boris Schröder for introducing me to the R language of statistical computing and Erika Lück (Potsdam University) for assistance with the geoelectrical sounding equipment and the corresponding data analysis. Dominik Reusser again deserves thanks for introducing me to LaTeX and for his role as "Reusser - Data and Computation", supplying very useful computer scripts.

For their love and encouragement, especially during the last tough months I want to thank my family: Oda and Alfred, Johannes and Susan and of course Dominik.

I also want to thank Stefan, Katja, Britta, Kai and my friends and colleagues at the Institute for Geoecology for their friendship and support, and Ilja and David for staying close despite the distance.

This work was partially funded by the International Office of the BMBF (German Ministry for Education and Research) and Conicyt (Comisión Nacional de Investigación Científica y Tecnológica de Chile) and the „Potsdam Graduate School of Earth Surface Processes", funded by the State of Brandenburg.

Author's declaration

I prepared this dissertation without illegal assistance. The work is original except where indicated by special reference in the text and no part of the dissertation has been submitted for any other degree.

This dissertation has not been presented to any other University for examination, neither in Germany nor in another country.

Theresa Blume
Potsdam, October 2007